Small Molecule Modulators of Transcription

By

Caleb A. Bates

A dissertation submitted in partial fulfillment
of the requirements for the degree of
Doctor of Philosophy
(Medicinal Chemistry)
in the University of Michigan
2010

Doctoral Committee:

       Associate Professor Anna K. Mapp, Chair
       Professor David H. Sherman
       Assistant Professor Garry D. Dotson
       Research Professor Hollis D. Showalter

© Caleb A. Bates

_____

2010

To Mom and Dad

Acknowledgements

There are far too many people to thank in a few short pages. I have been incredibly fortunate to have interacted with so many wonderful people and amazing scientists during my undergraduate degree at Minnesota, and while pursuing my doctorate here at Michigan. First, I would like thank my advisor Anna; she was never without helpful suggestions and encouragement, and was always supportive of my alternative career goals. I would also like to thank my undergraduate advisors Dr. Rick Wagner and Dr. Patrick Hanna for providing such excellent mentorship during my first experience in the lab.

During my first year at Michigan, I was fortunate to have Sara Buhrlage, Marcelle Ferguson, and Amelia Fuller as my labmates. They were helpful, supportive and fun to work with. Many discussions over lunch with Brian Brennan and Steve Rowe shaped the way that I think about science, and I am lucky to call them friends. I am also very fortunate to have worked with Jenifer Lum, Chinmay Majmudar, and William Pomerantz; their help and suggestions were invaluable to completing the work in this dissertation. Matt Leathen, Amy Danowitz and Amberlyn Wands made coming to lab fun, even when nothing was working. Jonas Hojfeldt and Aaron Van Dyke were always willing to read manuscripts, suggest experiments, and provide valuable critiques of data and experimental design. Chris Taylor was always helpful, especially this last year, stepping up when HPLCs broke down or when safety inspections were imminent.

Table of Contents

List of Figures

Chapter I

Chapter II

Chapter III

Chapter IV

Appendix

List of Schemes

Chapter II

Chapter III

Appendix

List of Abbreviations

A	alanine
AIBN	azobisisobutyronitrile
CAN	acetonitrile
AEEA	8-amino-3,6-dioxaoctanoic acid
AP-1	activator protein 1
ATF	artificial transcription factor
$BF_3 \cdot OEt_2$	boron trifluoride diethyl etherate
BME	β-mercaptoethanol
BnBr	benzyl bromide
Boc	*tert*-butylmethoxycarbonyl
BP	benzophenone
BpA	*p*-benzoyl-*l*-phenylalanine
BRG	brahma-related gene
tBuOH	*tert*-butanol
cAMP	cyclic adenosine monophosphate
CBP	creb binding protein
CCl_4	carbon tetrachloride
CDK	cyclin dependent kinase
cDNA	complementary DNA
CH_2Cl_2	dichloromethane
ChIP	chromatin immunoprecipitation
CRE	cAMP response element
CREB	cAMP response element binding protein
D	aspartic acid
D-MEM	Dubelco's Modified Eagle Media
DBD	DNA-binding domain
DMAP	N, N-dimethylaminopyridine
DMF	N, N-dimethylformamide
DMSO	dimethylsulfoxide
DNA	deoxyribonucleic acid
DPPA	diphenylphosphoryl azide
DRIP	vitamin D receptor-interacting protein
E	glutamic acid
E1A	early region 1A
ESC	embryonic stem cell
Et_3N	triethylamine
Et_2O	diethyl ether

EtOAc	ethyl acetate
EtOH	ethanol
ESI	electrospray ionization
F	phenylalanine
Fmoc	9-fluorenylmethoxycarbonyl
FP	fluorescence polarization
g	gram
GAPDH	glyceraldehyde-3-phosphate dehydrogenase
GCN4	general control nonderepressible 4
GR	glucocorticoid receptor
GRE	glucocorticoid response element
HAT	histone acetyltransferase
HeLa	Henrietta Lacks cervical cancer cells
HBTU	2-(1H-benzotriazol-1-yl)-1,1,3,3-tetramethyluronium hexafluorophosphate
hMDM2	human double-minute 2
HOBt	N-hydroxybenzotriazole
HPLC	high pressure liquid chromatography
HRMS	high resolution mass spectrometry
HSV	herpes simplex virus
I	isoleucine
JNK	c-Jun N-terminal kinase
K	lysine
K_D	dissociation constant at equilibrium
kDa	kilodalton
HSQC	heteronuclear single quantum coherence
KID	kinase inducible domain
L	leucine
MCF-7	Michigan cancer foundation 7
MDM2	murine double-minute 2
Med	mediator
MeOH	methanol
MES	2-(N-morpholino)-ethanesulfonic acid
MLL	mixed-lineage leukemia
MnO_2	manganese dioxide
MP	masking protein
mRNA	messenger ribonucleic acid
MsCl	methanesulfonyl chloride
MSNT	1-(mesitylene-2-sulfonyl)-3-nitro-1,2,4-triazole
NaH	sodium hydride
$NaBH_4$	sodium borohydride
$NaIO_4$	sodium periodate
NaN_3	sodium azide
NBS	N-bromosuccinimide
NMO	N-methylmorpholine-N-oxide
NMR	nuclear magnetic resonance

NR	nuclear receptor
NUA4	nucleosome acetyltransferase of histone H4
OsO_4	osmium tetroxide
OxDex	oxidized dexamethasone
p21	protein, 21 kilodaltons
P2P	pocket to pocket
p300	protein, 300 kilodaltons
p53	protein, 53 kilodaltons
p97	protein, 97 kilodaltons
PBS	phosphate buffered saline
PEG	polyethylene glycol
PIC	pre-initiation complex
PPh_3	triphenylphosphine
iPr_2NEt	diisopropyl ethyl amine
PVDF	polyvinyl difluoride
PyBOP	benzotriazol-1-yl-oxytripyrrolidinophosphonium hexafluorophosphate
PyBrOP	bromo-tris-pyrrolidino phosphonium hexafluorophosphate
Rb	retinoblastoma
RID	receptor-interacting domain
RNA	ribonucleic acid
S	serine
SAR	structure-activity relationship
SET	suppressor of enhancer of zeste
shRNA	short hairpin ribonucleic acid
Srepb	steroid response element binding protein
SWI/SNF	switch/sucrose nonfermentable
TAD	transcriptional activation domain
TAF	TATA binding protein associated factor
TBAF	tetrabutylammonium fluoride
TBP	TATA binding protein
TBS	*tert*-butyldimethylsilane
TF	transcription factor
TFA	trifluoroacetic acid
TFB	transcription factor B
THF	tetrahydrofuran
TIPS	triisopropylsilane
TPAP	tetrapropylammonium perruthenate
TRE	phorbol-12-myristate-13-acetate response element
VP16	viral protein 16
WT	wild type
ZFP	zinc finger protein

Abstract

Small Molecule Modulators of Transcription

By

Caleb A. Bates

Chair: Anna K. Mapp

Transcriptional activators are key components in the regulation of gene expression, being critical for precise, high fidelity transcription. Misregulation of transcription is a hallmark of many diseases, including diabetes, leukemias, and other cancers. Transcription-targeted therapeutics that reconstitute activator function have been a long sought after goal in the treatment of these diseases and as mechanistic probes; however, progress has been slow as the molecular recognition events that occur during transcriptional activation are not well understood. Transcriptional activators consist minimally of a DNA-binding domain (DBD) responsible for gene specificity, and a transcriptional activation domain (TAD) that recruits the transcriptional machinery through direct binding interactions. Development of artificial DBDs has been demonstrated in several instances, while artificial TADs have been a much more intractable problem. This is likely due to the lack of knowledge regarding the nature of binding and targets of natural TADs.

The Mapp lab has developed a small molecule isoxazolidine, that when tethered to a DBD, reconstitutes activator function both *in vitro* and in cells.

An open question remains, however, in regard to the mechanism of the first small molecule TAD: does it function in a manner similar to natural TADs, or through another mechanism? To address this question, an isoxazolidine TAD (iTAD) was prepared containing benzophenone, a photoactive group, for use in photocrosslinking experiments. The Creb binding protein (CBP) was identified as a target of iTAD **1** through *in vitro* crosslinking experiments. Furthermore, the binding site of iTAD **1** was found to overlap that of the natural activators MLL, Jun, Tat, and Tax within the KIX domain of CBP. Though CBP has been the only target of iTAD **1** identified to date, there are several other proteins apparent in the crosslinking experiments. The relevance of CBP in iTAD **1**-driven transcriptional activation was further explored in a cellular 2-hybrid system, where it was shown that the activity of the small molecule correlated with the availability of CBP, and more specifically, the KIX domain. These data, coupled with the multiprotein binding profile and *in vitro* binding studies suggest that iTAD **1** functions in a manner similar to endogenous activators.

The overlapping binding site of iTAD **1** with natural activators was further explored using a luciferase-based assay to test the ability of iTAD **1** and related isoxazolidines to inhibit the binding of the endogenous activators MLL and Jun. iTAD **1** was found to inhibit the activity of the minimal TADs of both MLL and Jun. Furthermore, it was shown to decrease the expression of cyclin D1, a gene tightly regulated by Jun, in MCF-7 breast cancer cells. Several isoxazolidine analogs were synthesized to achieve further potency or specificity; however, no compound was more potent than iTAD **1**, though several trends in toxicity were observed.

In addition to modulating transcription in a two-hybrid system, iTAD **1** and a cohort of other small molecules were tethered, through varying linker lengths, to an oxidized analogue of the steroid dexamethasone. These conjugates were used to modify the function of the glucocorticoid receptor (GR), a natural transcriptional activator. Thus, we have shown that the isoxazolidine is an excellent starting point for the development of enhancers, inhibitors, and modifiers of transcriptional activity.

Chapter I

Introduction to Small Molecule Modulation of Transcription

A. Project Focus

Transcriptional activator proteins are critical for reliable and accurate gene transcription, seeking out specific genes and regulating their transcription to precise levels.[1] Misregulation of transcription results in a variety of disease states such as cancer and diabetes.[1-3] There has been tremendous interest in the development of small molecule transcription-based therapeutics that can restore transcription to normal levels. Small molecules carry significant advantages, both as therapeutics and as mechanistic probes, due to their generally favorable stability and immunogenic properties relative to their peptidic counterparts. Activators carry out their function through two separate domains, a DNA-binding domain (DBD) and a transcriptional activation domain (TAD); these domains may be covalently or non-covalently linked.[1, 3, 4] Of the two, the DBD has proved considerably more amenable to artificial replacement than the TAD, partly due to the lack of molecular-level details of the recognition events that occur during the activation of transcription.[1, 4] The Mapp lab first reported a small molecule (iTAD **1**) that is able to reconstitute activator function both *in vitro* and in cells.[5, 6] Although function had been reconstituted, the *mechanism* by which this molecule activated transcription was not well understood and this was essential to understand for the development of next-generation small molecules. Thus, my project began as an investigation of the mechanism of the small molecule activation domain, including the identification of an important coactivator target of iTAD **1**.

The insights gained from these experiments enabled the discovery of compounds that block key transcriptional protein-protein interactions, including those between the KIX domain of the CREB-binding protein (CBP) and the endogenous activators MLL and Jun. These mechanistic studies were expanded to endogenous activators through the synthesis of modified glucocorticoid receptor (GR) ligands for the investigation and alteration of GR binding partners during transcriptional activation.

B. Introduction to Transcription

Transcription is the process of converting of DNA into messenger RNA (mRNA) and the first step in converting the information contained in the genome into proteins. RNA polymerase II is the enzyme that directly catalyzes this conversion, but it requires a number of accessory proteins in order to function properly. Transcription begins when transcriptional activator proteins seek out specific genes in response to extra- or intracellular stimuli (Figure I-1a).[1, 7-9]
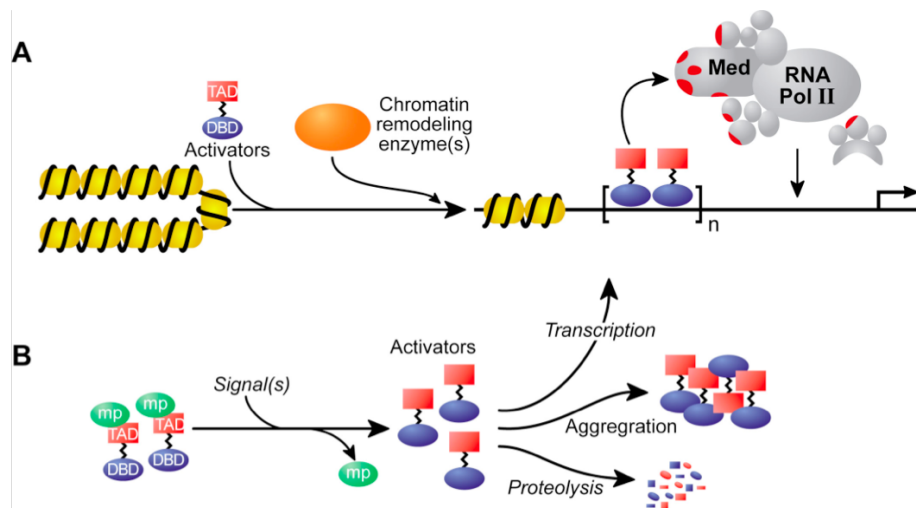
Figure I-1. General schematic of transcription initiation.[1] a) In the nucleus activators bind a specific sequence of genomic DNA and recruit chromatin remodeling enzymes, coactivators such as Mediator, and RNA polymerase II. b) Masking proteins control, in part, the concentration of activators available in the nucleus.

The activators then recruit chromatin-modifying enzymes to alter the DNA architecture of the gene of interest. Subsequently, these activators recruit a class of proteins, known as coactivators, through direct binding interactions, to the gene of interest. Coactivators are responsible for binding and recruiting RNA polymerase II and its associated factors to DNA, resulting in the generation of an mRNA transcript of the target gene.[2, 10-13] The multiprotein complex formed by RNA polymerase II and its associated factors is collectively known as the "transcriptional machinery." The complexity of transcriptional programs necessitates that the availability of transcriptional activators is tightly controlled through regulation of their expression, localization, and their interactions with masking proteins (MPs) (Figure 1-1b).[1, 14, 15] These masking proteins serve to prevent aggregation or degradation of transcriptional activators until an appropriate signal is received indicating the need for increased transcription.

C. Activator Structure and Function

Transcriptional activators play a key role in regulating the precise temporal and spatial control of gene expression through protein·protein and protein·DNA interactions. Transcriptional activators have a modular structure consisting of a DNA-binding domain (DBD) and a transcriptional activation domain (TAD) (Figure I-2a). DBDs are typically well-structured motifs and bind to DNA upstream of a promoter in a sequence-specific fashion. The TAD makes contact with proteins in the transcriptional machinery known as coactivators through direct binding interactions, localizing them to DNA.[1] These coactivators may be chromatin-modifying enzymes, or other proteins necessary for formation of the preinitiation complex (PIC) at the promoter of a target gene. RNA pol II is sufficient for what is termed "basal transcription" (transcription that occurs on naked DNA in the absence of any activating signal). Transcriptional activators, however, are required for promoter recognition and higher levels of transcription.[16-18] The DBD and TAD may be linked covalently or non-covalently and function modularly. This enables the

study of each module individually and the generation of chimeric molecules consisting of the DBD from one activator fused to the TAD of another (Figure I-2b).[1, 19, 20]
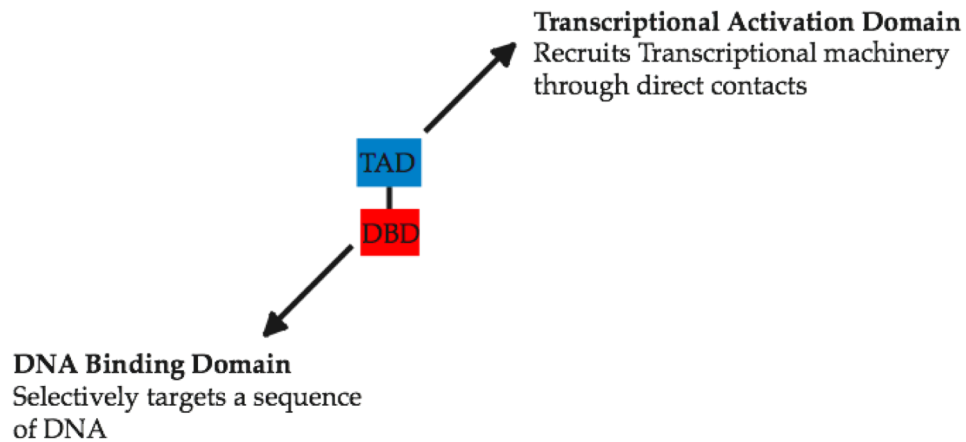
Figure I-2. Transcriptional activators contain two critical modules for function. a) Architecture of a transcriptional activator. b) Domain-swapping experiments demonstrated that the DBD and TAD module function independently.

The most well studied class of activators are the acidic, or amphipathic, activators. These TADs are characterized by alternating regions of hydrophobic and polar amino acid residues, and although typically unstructured in solution, often form amphipathic α-helices upon binding their coactivator targets.[21, 22] These TADs are

thought to function as amphipathic surfaces, rather than highly specific

protein·protein interactions when binding their coactivator targets (Figure I-3a and

b).[23-26]

a)

MLL   2847   DIMDFVLKNT

c-Myb   295   IKELELLL

b)
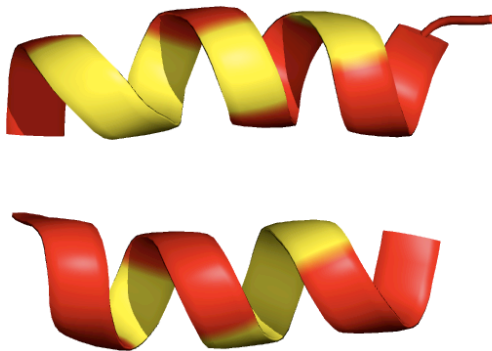
Figure I-3. Natural TADs MLL and c-Myb. a) Sequences are comprised of interspersed hydrophobic and polar residues. b) Amphipathic helices are the most common secondary structures of amphipathic TADs. MLL and Myb are shown here with hydrophobic residues in red and polar residues in yellow. Figure adapted from 2agh.

Several groups have shown that TADs are quite tolerant of mutagenesis, with

specific residues generally being unimportant for activator function.[27, 28] For

example, Triezenberg and coworkers used alanine scanning mutagenesis in the

VP16 TAD and showed that 22/28 mutants tested (without replacing glycine or

existing alanines) retained >60% WT activity.[29] Similar studies have been done with

p53, Gcn4, and GR.[30-33] In addition, many peptides randomly generated from the *E.

coli* genome where shown to activate transcription *in vitro* (Figure I-4). Thus, TADs

function through binding with moderate affinity and specificity to a large number of

coactivator proteins. These multivalent interactions facilitate multiple

configurations of particular coactivators to be recruited under different conditions, allowing for combinatorial control of gene expression across different cell and tissue types.

Name	Residues	β-Gal Units	Sequence
B17	28	794	ILDLQLACEDNSGLPEESQFQTWLNAVI
B3	18	359	IAALEDNDDLFGHGLFLV
B4	21	83	IDITPQRVLEELNALLLQEEV
B41	15	30	IPPSELAVWFSTPGW
No Gal 4	<1	<1	-
WT Gal 4	-	1895	-

Figure I-4. Artificial Peptidic TADs. Sequences from randomly generated TADs and their activity relative to endogenous yeast activator Gal4.[19]

D. Activator·Coactivator Interactions

Although few in number, structural studies of the TAD·coactivator complex in the literature provide a valuable starting point for the development of artificial TADs. The most well characterized TAD·coactivator complexes are that of the KIX domain of CBP and the activators Creb, Myb, and MLL, and the Tfb1 domain of TFIIH bound to the activators VP16 and p53.[22, 34-38] The CBP KIX domain is comprised of 5 helices and interacts with over 10 transcriptional activators; the solution structures have been solved for three of these (MLL, Creb, Myb) in complex with the KIX domain.[22] The Tfb1 domain of TFIIH is composed of an α-helix and 7 β-sheets; the solution structure of Tfb1 in complex with p53 and VP16 have been solved.[22, 34, 35] In each case, the TAD binding region was composed of 9-15 residues that formed an amphipathic helix where the hydrophobic residues make contact with the coactivator binding site (Figure I-5a and I-5b).
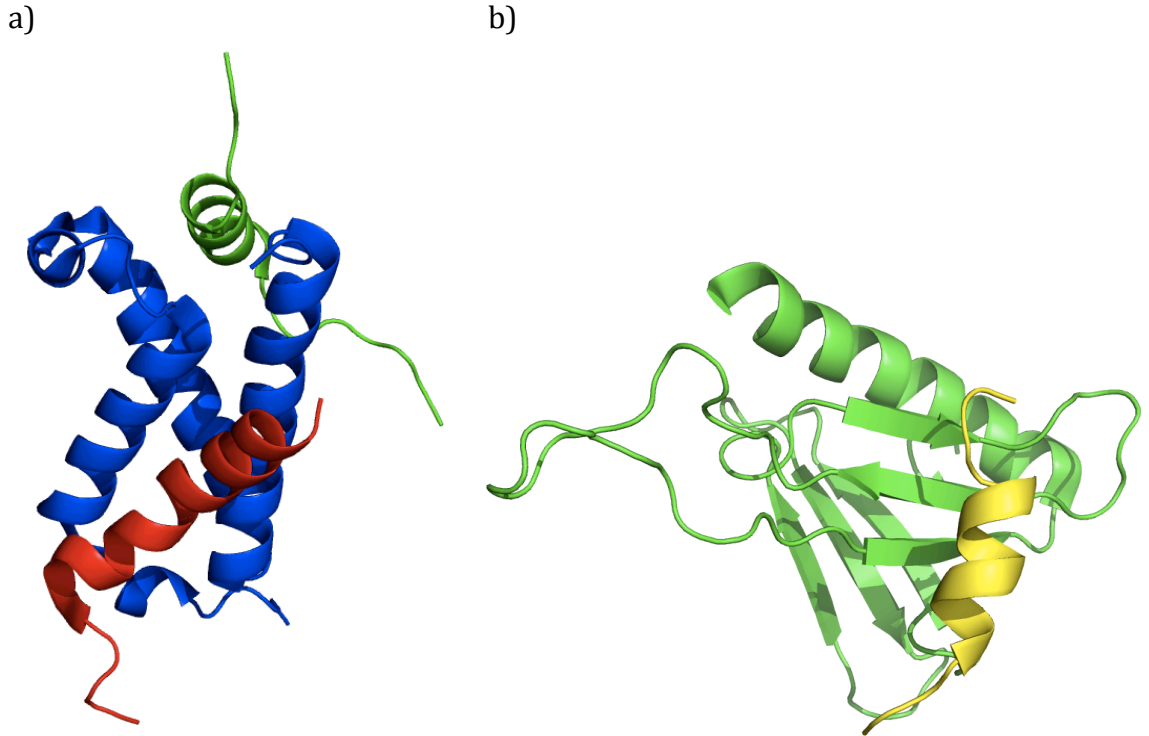
Figure I-5. TAD·coactivator complexes. a) Myb·KIX·MLL, KIX is shown in blue, Myb in red, and MLL in green.[36] Figure adapted from 2agh. b) VP16·Tfb1, Tfb1 is in green and VP16 is in yellow.[34] Figure adapted from 2k2u.

These structures reinforce data from previous experiments by showing that the precise identity and arrangement of hydrophobic residues is not critical for binding. For example, the hydrophobic regions of VP16 and p53 that contact the same binding site on Tfb1 consist of different residues: Ile, Phe, and Trp for p53 and Met, Phe, and Phe for VP16.[34, 35] In addition to the hydrophobic residues inserting into a binding pocket, there is also at least one polar residue (usually Ser or Thr) that contributes an important hydrogen bonding or ionic interaction with the coactivator. The structures of the KIX·MLL·Myb ternary complex and the Tfb1·VP16 complex are shown in Figure I-5.

E. Coactivators

In order to facilitate the initiation of transcription, TADs must recruit coactivator proteins through one or more direct binding interactions. Coactivators can be broadly classified into two groups, those that covalently modify histones and other proteins, (i.e. acetylation, methylation, phosphorylation), and adaptors that direct recruitment of the transcriptional apparatus.[12] Yet, significant debate still revolves around the identity of the coactivators that interact directly with the TAD. The coactivators present at a given promoter can vary significantly between tissue types, at different times during the cell cycle, and can depend on the presence or absence of specific external stimuli.[39-42] Coactivator recruitment thus offers an additional level of combinatorial control over gene expression by modifying transcriptional output in response to a new signal or environmental change.

The ability to covalently modify chromatin is a key enzymatic feature of many coactivators; common modifications include acetylation, methylation, and phosphorylation. For example, histone acetylation leads to increased transcription through loosening of the chromatin structure, increasing accessibility of the promoter.[43] In addition, some coactivators may also covalently modify activators in addition to DNA, fine-tuning their activity in some cases to increase transcription further or to result in the dismissal of activators from the promoter and their degradation.[44] Other coactivators function as a protein scaffold, serving to form noncovalent interactions between activators and components of the transcriptional machinery.

Coactivators are found both as signal entities or part of large (>1 MDa) multi-protein complexes, with several coactivators appearing in different complexes.[10, 12, 45-49] Coactivator complexes allow for the initiation of intricate cell-signaling programs at the transcriptional level. Some complexes that have been implicated in transcriptional regulation include the SAGA complex, Mediator (Med), SWI/SNF, NuA4, CBP, and TBP-associated factors (TAFs) (Figure I-6).[50-59]
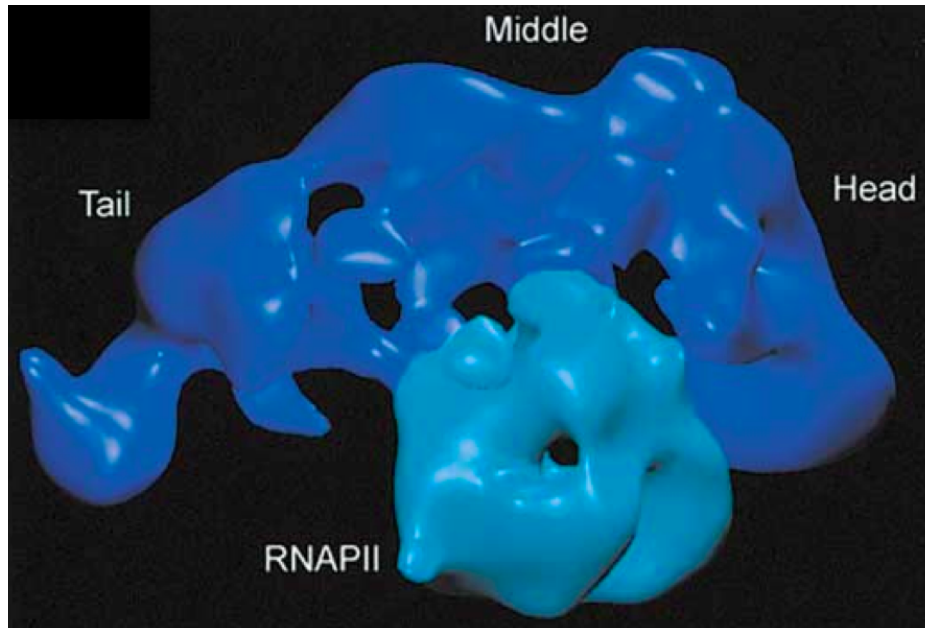
Figure I-6. Mediator·RNA pol II complex.[60] The Mediator complex is composed of ~30 proteins divded into three regions, the head, middle, and tail. This is an EM image of Mediator bound to RNA pol II.

Prevailing evidence suggests that activators bind multiple coactivator targets to exert their effects. This has been notably demonstrated by *in vitro* crosslinking experiments carried out in the Hahn lab, where DNA-bound activators Gal4 and GCN4 (well-characterized yeast amphipathic activators) were exposed to nuclear extracts and found to bind to an overlapping set of targets, including Tra1, Med15, and TAF12.[56, 58] These proteins are components of four different coactivator complexes: SAGA, Mediator, NuA4, and TFIID. TAF12 and Tra1 are components of the chromatin-remodeling SAGA complex, while Med15 is a component of Mediator.[47, 59] In addition, significant *in vitro* binding data has been amassed from a variety of techniques as further evidence that TADs exhibit a multipartner binding profile. For example, more than 6 binding partners have been identified for the glucocorticoid receptor (an endogenous activator) including BRG1, DRIP150, CBP, and several members of the p160 family of coactivators.[61-68] In addition, components of the transcriptional machinery interact with multiple TADs; for example, over 350 proteins have been found to bind to the coactivator CBP.

F. Creb Binding Protein (CBP)

CBP and its paralog p300 are key nodes in many cellular signaling pathways. CBP is a 2400 amino acid, multidomain protein that serves to integrate signals in the nucleus from a variety of stimuli (Figure I-7).[49]

RID   CH1   KIX   Br CH2   CH3   SID
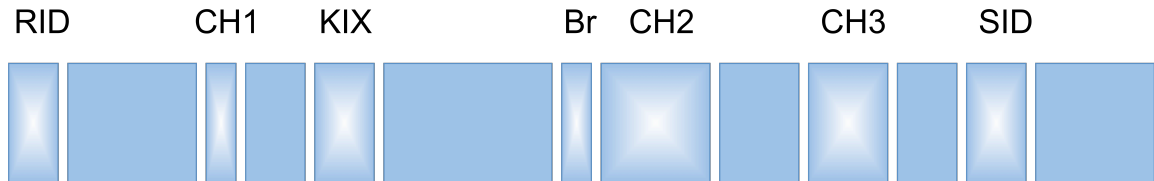
Figure I-7. Creb-binding protein. CBP contains three cysteine-histidine rich domains (CH1-CH3, or TAZ1-3), an N-terminal receptor-interacting domain, a bromodomain, a KIX domain, an SRC-1 interacting domain, and a histone acetyltransferase domain.

CBP has been implicated in long-term memory formation, circadian rhythms, cell growth, differentiation, and development.[69-73] CBP is highly conserved across metazoans, with human and murine CBP cDNA sharing 89% sequence homology. Loss of both CBP alleles is lethal between days 8-10 in embryonic development, and although CBP heterozygotes may survive to adulthood, they possess physical and mental deficits. In humans, CBP heterozygosity results in Rubenstein-Taybi syndrome, characterized by broad fingers and toes, heart defects, and mental retardation.[52, 69, 74-79] The Brindle lab, however, has shown that mutation of three critical residues within the KIX domain of CBP in mice results in essentially normal animals.[80] Over 350 proteins are known to bind to CBP, which contains an N-terminal receptor interacting domain (RID), three cysteine-histidine rich regions (CH1, CH2, and CH3), a bromodomain, and a KIX domain. CBP also possesses a histone acetyltransferase (HAT) domain, as part of the CH1 domain, that can acetylate lysines on both histone and non-histone substrates, such as p53. With its many protein-interacting domains, CBP is thought to serve as a bridge between different activators, facilitating the assembly of a large complex, known as the enhanceosome, at the promoters of target genes.[81] Both of these functions increase

the local concentration of transcription factors, thus facilitating protein·protein and protein·DNA interactions. CBP is found in limiting quantities in the cell, resulting in a competition for CBP between its different binding partners.[76, 82, 83] This enables exquisite tuning of CBP-mediated transcriptional response to a diverse array of stimuli and highlights the central role CBP plays in cell-signaling pathways.

G. Transcription-Based Therapies for the Treatment of Disease

Due to their central function in regulating gene expression, it is not surprising that misregulation of transcriptional activators is correlated with a wide range of disease states including diabetes, leukemia, and cancer.[84-87] Artificial activators, nonnatural replacement of activator proteins, would be valuable commodities for use as transcription-targeted therapeutics.

Currently, the most promising transcription-based therapies are based on designer zinc finger proteins (ZFPs). These proteins are engineered to bind short tracts of DNA (9-18 bp) in the promoter region of a particular gene of interest. These ZFPs are then be fused to other proteins with diverse functionality such as DNA methyltransferases, histone acetyltransferases, hormone receptors, and others.[88, 89] The gene activation or repression function thus arises from the fusion partner of the ZFP (Figure I-8).
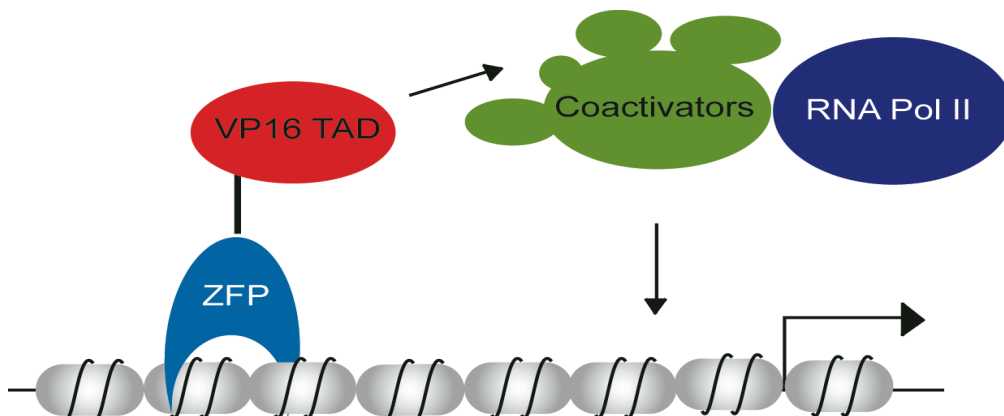
Figure I-8. Schematic of zinc-finger protein therapeutics. ZFP binds a specific tract of DNA where the tethered VP16 TAD recruits coactivators and RNA polymerase II, leading to increased levels of gene expression.

Sangamo Biosciences currently has several designer ZFPs in clinical trials to treat diabetic neuropathy, cancer, and HIV infection.[89-91] While ZFPs are promising drug candidates, they are expensive to develop and are not orally bioavailable. In addition, they must be delivered via adenoviral infection, which poses several problems including delivery of the therapeutic gene to the proper location and the potential of a massive immune response to the vector.

Ideally, artificial activators would completely reconstitute the function of natural activators, upregulating specific target genes to desired levels in a signal and time-responsive fashion. Current challenges to achieving this goal are the delivery of artificial transcription factors to tissues of interest, their cell and nuclear permeability, and finally their ability to interact with the intended DNA and protein targets. This has been especially challenging due to the complex natural of cell-signaling pathways that result in the upregulation of a single gene. The few efficacious artificial activators to date have consisted of minimal TAD and DBD motifs, with peptidic TADs and nucleic acid or peptide-nucleic acid DBDs.[92] These successful examples of artificial activators are outlined below.

H. Artificial Activators

There has been moderate success with artificial activators to date; however, significant challenges remain, including delivery, cellular stability, and immunogenicity. Small molecule artificial transcriptional activators provide an attractive alternative to peptidic activators in all these areas. To generate such a construct one would synthesize two low-molecular-weight halves, one to bind DNA sequence specifically, and the other to bind coactivator targets, and tether the molecules through a linker. Thus, through direct DNA and protein binding interactions, a small molecule could recruit the necessary components of the transcriptional machinery to a specific gene, resulting in the upregulation of transcription.

Stanojevic and Young reported an artificial transcription factor in 2002 that consisted of a triplex-forming oligonucleotide DBD coupled to a synthetic peptide (derived from the HSV VP16 activation domain) through a short linker.[93] This construct was able to activate the transcription of a reporter gene 30 fold in cell culture. Similarly, another peptide from the VP16 TAD tethered to a synthetic polyamide DBD upregulates transcription almost 35 fold *in vitro*.[94] Zinc finger protein DBDs tethered to the VP16 TAD activates 25 fold in cell culture.[88] Finally, the Mapp, Kodadek, and Uesugi groups have all shown examples of non-peptidic molecules that activate transcription when localized to DNA (Figure I-9). While peptide, peptoid, and their hybrids are able to bind larger (therefore more specific) tracts of DNA and form multivalent interactions with target proteins; these molecules are generally not cell permeable and are sensitive to degradation. On the other hand, small molecules are much more cell permeable and insensitive to degradation; however they also must be tethered to some DNA-binding functionality which may present permeability and degradation problems. These different strategies each have merit as mechanistic probes of transcription in different model systems.
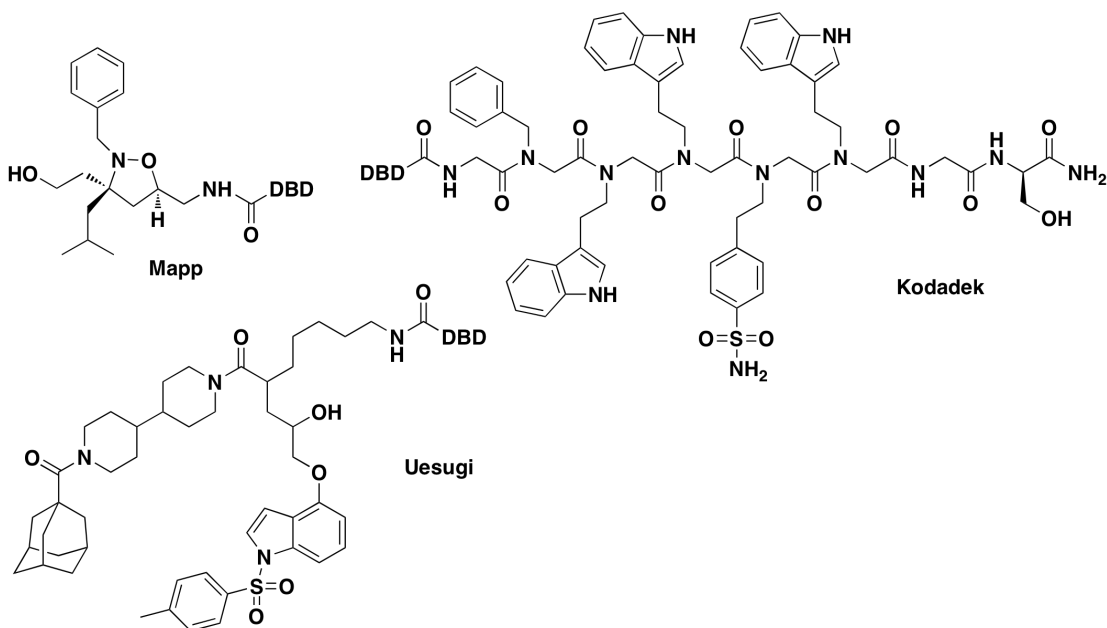
Figure I-9. Artificial non-peptidic TADs. Mapp isoxazolidine[6] 292 Da, Wrenchnolol[95] 801 Da, Kodadek peptoid[96] 1206 Da (molecular weight without DBDs).

13

The development of small molecule DNA binding domains has seen significant progress in the last 10 years with the design and synthesis of polyamide molecules (an example show below, Figure I-10), which bind in a sequence specific manner to DNA. The development of small molecule TADs, however, has proven to be a much more challenging endeavor. This is due to the multiprotein binding profile of TADs and the lack of molecular detail describing these interactions. Developing a small molecule that can emulate endogenous TADs, then, represents a considerable challenge. Developing small molecule activator mimics is further complicated because not all coactivator targets have been elucidated, making high throughput screens problematic to execute. In addition, there is a dearth of structural information for TADs either alone or bound to a coactivator target, making structure-based design impossible.
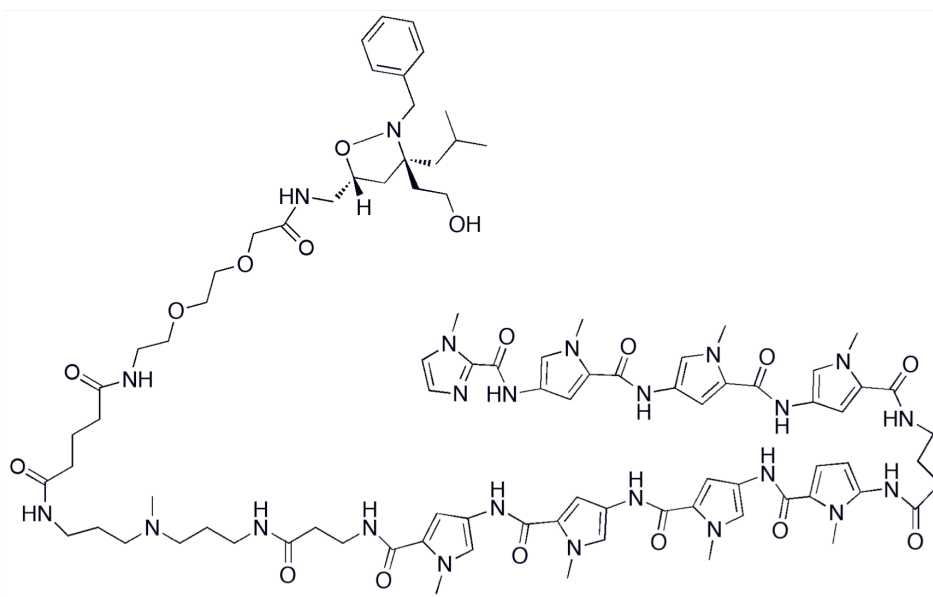
Figure I-10. Fully synthetic small molecule-based activator. Small molecule iTAD **1** tethered to a polyamide DBD (RJC-IV-18).

I. First Small Molecule TAD

Protein·protein interactions have been notoriously difficult to modulate using small molecules, often due to the large surface of the interacting regions and the number of contacts required to achieve specificity.[97-105] In 2004, the Mapp lab reported the

first small molecule able to reconstitute the function of a natural activator *in vitro* and extended the work into cells in 2006 (Figure I-11).[5, 6] This small molecule consists of a five-membered isoxazolidine heterocycle functionalized with hydrophobic (benzyl, isobutyl) and polar (hydroxyethyl) groups. This isoxazolidine transcriptional activation domain (iTAD **1**) contains amphipathic functionality similar to that of natural activators and the rigid scaffold displays the functional groups in fixed positions (Figure I-11). Currently, however, there are still only two examples of small molecule TADs, despite extensive research in this area. Development of a small molecule TAD is further complicated by lack of knowledge of activator binding partners, interactions between TADs and masking protein, and the formation of non-productive interactions. These features are key for the precise, signal-responsive regulation of transcription by endogenous activators, but are extremely difficult to imitate with small molecules. Despite its similarity to endogenous TADs, it remained unclear if the small molecule iTAD **1** functioned via a similar mechanism.
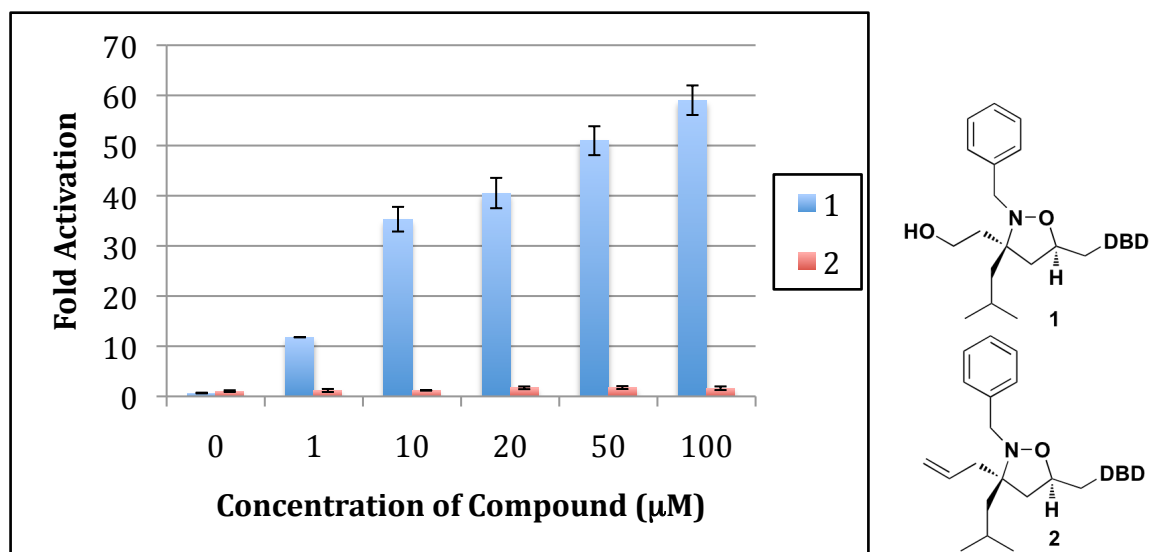
Figure I-11. iTAD **1** function in cell culture. Amphipathic **1** activates transcription in HeLa cells while fully hydrophobic **2** does not.

J. Thesis Outline

Chapter I seeks to further develop our understanding of small molecule-based transcriptional modulators: the questions I sought to answer were whether the hydrophobic and amphipathic iTADs function by a similar mechanism to endogenous TADs, by binding multiple transcription factor targets with low affinity, and to then exploit this information to design modulators of specific protein·protein interactions.

Chapter II focuses on identifying the protein targets of iTAD **1** and specifically the binding sites within those targets. To achieve this, a derivative of iTAD **1** was synthesized containing a photoactive benzophenone group that was used to photocrosslink iTAD targets *in vitro* using nuclear extracts. Through this work it was discovered that iTAD **1** binds multiple proteins, notably, this includes the Creb-binding protein (CBP). A binding site within CBP, the KIX domain, was further characterized by NMR and implicated that the binding site of iTAD **1** overlaps with the binding site for natural TADs MLL, Jun, and viral TADs Tat, and Tax. Further cell-based experiments demonstrated that the KIX·iTAD interaction was critical for iTAD function.

Chapter III describes an investigation into the exploitation of the overlapping binding sites of iTAD **1**, MLL, and Jun. This overlapping binding site may result in competition for binding between iTAD **1** and endogenous TADs. Towards this end, several analogues were synthesized using the isoxazolidine framework to alter specificity and/or potency for inhibiting particular TAD·KIX interactions. iTAD compounds were tested both in a cell-based luciferase assay in endogenous promoter contexts. Most structural modifications resulted in the abrogation of activity or significant toxicity, indicating that iTAD **1** possesses some particular advantage in this molecular recognition event. However, iTAD **1** decreased the production of cyclin D1, whose gene is tightly regulated by Jun, in MCF-7 breast cancer cells.

16

The experiments discussed thus far have presented a powerful strategy for the identification and characterization of binding partners of a small molecule TAD. In the Appendix, I will describe the extension of this methodology towards the identification of binding partners of a natural transcriptional activator, the glucocorticoid receptor (GR). The appendix highlights the design, synthesis, and evaluation of modified glucocorticoid receptor ligands. These ligands were used as crosslinking agents to trap interactions between GR and its coactivator targets during the activation of transcription. In addition, several compounds were synthesized to modify the activity of GR during transcriptional activation; these compounds were shown to alter GR function in different promoter contexts, suggesting a possible mechanism for further small molecule control of gene expression through modulation of endogenous receptor function.

In sum, the evidence suggests that isoxazolidine-based TADs function in a similar mechanism to that as natural TADs: they exhibit a multiprotein binding profile, bind to a site utilized by natural activators, and are able to competitively inhibit natural TAD binding to that site. Furthermore, iTAD **1** has emerged as an inhibitor of Jun function in cells, decreasing the expression of cyclin D1, a gene tightly regulated by Jun. In addition, we have shown that small molecules tethered to nuclear receptor (NR) ligands can alter the function of the native receptor. Both classes of small molecules, iTADs and P2Ps (pocket-to-pocket), serve as excellent starting points for the development of small molecule transcription-based therapeutics.

K. References

1.   Mapp, A. K.; Ansari, A. Z., A TAD further: Exogenous control of gene activation. *Acs Chem Biol* **2007,** *2* (1), 62-75.

2.   Lee, L. W.; Mapp, A. K., Transcriptional Switches: Chemical Approaches to Gene Regulation. *J Biol Chem* **2010,** *285* (15), 11033-11038.

3.   Majmudar, C. Y.; Mapp, A. K., Chemical approaches to transcriptional regulation. *Current Opinion in Chemical Biology* **2005,** *9* (5), 467-474.

4.   Mapp, A. K., Regulating transcription: a chemical perspective. *Organic & Biomolecular Chemistry* **2003,** *1* (13), 2217-2220.

5.   Brennan, B. B.; Buhrlage, S. J.; Minter, A. R.; Mapp, A. K., Functional characterization of a small molecule activation domain. *Abstr Pap Am Chem S* **2006,** *231*, -.

6.   Minter, A. R.; Brennan, B. B.; Mapp, A. K., A small molecule transcriptional activation domain. *J Am Chem Soc* **2004,** *126* (34), 10504-10505.

7.   Farrell, S.; Simkovich, N.; Wu, Y. B.; Barberis, A.; Ptashne, M., Gene activation by recruitment of the RNA polymerase II holoenzyme. *Gene Dev* **1996,** *10* (18), 2359-2367.

8.   Ptashne, M., Regulation of Transcription of Genes. *Philosophical Transactions of the Royal Society of London Series B-Biological Sciences* **1995,** *349* (1329), 255-255.

9.   Barberis, A.; Pearlberg, J.; Simkovich, N.; Farrell, S.; Reinagel, P.; Bamdad, C.; Sigal, G.; Ptashne, M., Contact with a Component of the Polymerase-Ii Holoenzyme Suffices for Gene Activation. *Cell* **1995,** *81* (3), 359-368.

10.   Chadick, J. Z.; Asturias, F. J., Structure of eukaryotic Mediator complexes. *Trends Biochem Sci* **2005,** *30* (5), 264-271.

11.   Spiegelman, B. M.; Heinrich, R., Biological control through regulated transcriptional coactivators. *Cell* **2004,** *119* (2), 157-167.

12.   Naar, A. M.; Lemon, B. D.; Tjian, R., Transcriptional coactivator complexes. *Annu Rev Biochem* **2001,** *70*, 475-501.

13.   Malik, S.; Roeder, R. G., Transcriptional regulation through Mediator-like coactivators in yeast and metazoan cells. *Trends Biochem Sci* **2000,** *25* (6), 277-283.

14.   Isogai, Y.; Tjian, R., Targeting genes and transcription factors to segregated nuclear compartments. *Current Opinion in Cell Biology* **2003,** *15* (3), 296-303.

15.   Ptashne, M.; Gann, A., Imposing specificity by localization: Mechanism and evolvability. *Evolution as Computation* **2002**, 179-200.

16.   Ptashne, M.; Gann, A. A. F., Activators and Targets. *Nature* **1990,** *346* (6282), 329-331.

17.   Mitchell, P. J.; Tjian, R., Transcriptional Regulation in Mammalian-Cells by Sequence-Specific DNA-Binding Proteins. *Science* **1989,** *245* (4916), 371-378.

18.   Ptashne, M., How Eukaryotic Transcriptional Activators Work. *Nature* **1988,** *335* (6192), 683-689.

19.   Ma, J.; Ptashne, M., A New Class of Yeast Transcriptional Activators. *Cell* **1987,** *51* (1), 113-119.

20.   Keegan, L.; Gill, G.; Ptashne, M., Separation of DNA-Binding from the Transcription-Activating Function of a Eukaryotic Regulatory Protein. *Science* **1986,** *231* (4739), 699-704.

21.   Uesugi, M.; Nyanguile, O.; Lu, H.; Levine, A. J.; Verdine, G. L., Induced alpha helix in the VP16 activation domain upon binding to a human TAF. *Science* **1997,** *277* (5330), 1310-1313.

22.   Radhakrishnan, I.; Perez-Alvarado, G. C.; Parker, D.; Dyson, H. J.; Montminy, M. R.; Wright, P. E., Solution structure of the KIX domain of CBP bound to the transactivation domain of CREB: a model for activator:coactivator interactions. *Cell* **1997,** *91* (6), 741-52.

23.   Mapp, A. K.; Ansari, A. Z.; Ptashne, M.; Dervan, P. B., Activation of gene expression by small molecule transcription factors. *P Natl Acad Sci USA* **2000,** *97* (8), 3930-3935.

24.   Lu, X.; Ansari, A. Z.; Ptashne, M., An artificial transcriptional activating region with unusual properties. *Proc Natl Acad Sci U S A* **2000,** *97* (5), 1988-92.

25.   Parker, D.; Jhala, U. S.; Radhakrishnan, I.; Yaffe, M. B.; Reyes, C.; Shulman, A. I.; Cantley, L. C.; Wright, P. E.; Montminy, M., Analysis of an activator:coactivator complex reveals an essential role for secondary structure in transcriptional activation. *Mol Cell* **1998,** *2* (3), 353-9.

26.   Hahn, S., Structure(Questionable) and Function of Acidic Transcription Activators. *Cell* **1993,** *72* (4), 481-483.

27.   Drysdale, C. M.; Duenas, E.; Jackson, B. M.; Reusser, U.; Braus, G. H.; Hinnebusch, A. G., The Transcriptional Activator Gcn4 Contains Multiple Activation Domains That Are Critically Dependent on Hydrophobic Amino-Acids. *Mol Cell Biol* **1995,** *15* (3), 1220-1233.

28.   Cress, W. D.; Triezenberg, S. J., Critical Structural Elements of the Vp16 Transcriptional Activation Domain. *Science* **1991,** *251* (4989), 87-90.

29.   Sullivan, S. M.; Horn, P. J.; Olson, V. A.; Koop, A. H.; Niu, W.; Ebright, R. H.; Triezenberg, S. J., Mutational analysis of a transcriptional activation region of the VP16 protein of herpes simplex virus (vol 26, pg 4487, 1998). *Nucleic Acids Research* **1998,** *26* (23), U9-U10.

30.   Iniguez-Lluhi, J. A.; Lou, D. Y.; Yamamoto, K. R., Three amino acid substitutions selectively disrupt the activation but not the repression function of the glucocorticoid receptor N terminus. *J Biol Chem* **1997,** *272* (7), 4149-4156.

31.   Almlof, T.; Gustafsson, J. A.; Wright, A. P. H., Role of hydrophobic amino acid clusters in the transactivation activity of the human glucocorticoid receptor. *Mol Cell Biol* **1997,** *17* (2), 934-945.

32.   Jackson, B. M.; Drysdale, C. M.; Natarajan, K.; Hinnebusch, A. G., Identification of seven hydrophobic clusters in GCN4 making redundant contributions to transcriptional activation. *Mol Cell Biol* **1996,** *16* (10), 5557-5571.

33.   Lin, J. Y.; Chen, J. D.; Elenbaas, B.; Levine, A. J., Several Hydrophobic Amino-Acids in the P53 Amino-Terminal Domain Are Required for Transcriptional Activation, Binding to Mdm-2 and the Adenovirus-5 E1b 55-Kd Protein. *Gene Dev* **1994,** *8* (10), 1235-1246.

34.   Langlois, C.; Mas, C.; Di Lello, P.; Jenkins, L. M. M.; Legault, P.; Omichinski, J. G., NMR structure of the complex between the Tfb1 subunit of TFIIH and the activation domain of VP16: Structural similarities between VP16 and p53. *J Am Chem Soc* **2008,** *130* (32), 10596-10604.

35.   Di Lello, P.; Jenkins, L. M. M.; Jones, T. N.; Nguyen, B. D.; Hara, T.; Yamaguchi, H.; Dikeakos, J. D.; Appella, E.; Legault, P.; Omichinski, J. G., Structure of the Tfb1/p53 complex: Insights into the interaction between the p62/Tfb1 subunit of TFIIH and the activation domain of p53. *Mol Cell* **2006,** *22* (6), 731-740.

36.   De Guzman, R. N.; Goto, N. K.; Dyson, H. J.; Wright, P. E., Structural basis for cooperative transcription factor binding to the CBP coactivator. *J Mol Biol* **2006,** *355* (5), 1005-13.

37.   Goto, N. K.; Zor, T.; Martinez-Yamout, M.; Dyson, H. J.; Wright, P. E., Cooperativity in transcription factor binding to the coactivator CREB-binding protein (CBP). The mixed lineage leukemia protein (MLL) activation domain binds to an allosteric site on the KIX domain. *J Biol Chem* **2002,** *277* (45), 43168-74.

38.   Radhakrishnan, I.; Perez-Alvarado, G. C.; Parker, D.; Dyson, H. J.; Montminy, M. R.; Wright, P. E., Structural analyses of CREB-CBP transcriptional activator-coactivator complexes by NMR spectroscopy: implications for mapping the boundaries of structural domains. *J Mol Biol* **1999,** *287* (5), 859-65.

39.   Ptashne, M., Regulated recruitment and cooperativity in the design of biological regulatory systems. *Philosophical Transactions of the Royal Society of London Series a-Mathematical Physical and Engineering Sciences* **2003,** *361* (1807), 1223-1234.

40.   Maria Pia Cosma, T. T., Kim Nasmyth, Ordered Recruitment of Transcription and Chromatin Remodeling Factors to a Cell Cycle- and Developmentally Regulated Promoter. *Cell* **1999,** *97*, 13.

41.   Lee, D. K.; Kim, S.; Lis, J. T., Different upstream transcriptional activators have distinct coactivator requirements. *Gene Dev* **1999,** *13* (22), 2934-2939.

42.   Kee, B. L.; Arias, J.; Montminy, M. R., Adaptor-mediated recruitment of RNA polymerase II to a signal-dependent activator. *J Biol Chem* **1996,** *271* (5), 2373-2375.

43.   Kurdistani, S. K.; Tavazoie, S.; Grunstein, M., Mapping global histone acetylation patterns to gene expression. *Cell* **2004,** *117* (6), 721-733.

44.   Luo, J. Y.; Li, M. Y.; Tang, Y.; Laszkowska, M.; Roeder, R. G.; Gu, W., Acetylation of p53 augments its site-specific DNA binding both in vitro and in vivo. *P Natl Acad Sci USA* **2004,** *101* (8), 2259-2264.

45.   Bourbon, H. M.; Aguilera, A.; Ansari, A. Z.; Asturias, F. J.; Berk, A. J.; Bjorklund, S.; Blackwell, T. K.; Borggrefe, T.; Carey, M.; Carlson, M.; Conaway, J. W.; Conaway, R. C.; Emmons, S. W.; Fondell, J. D.; Freedman, L. P.; Fukasawa, T.; Gustafsson, C. M.; Han, M.; He, X.; Herman, P. K.; Hinnebusch, A. G.; Holmberg, S.; Holstege, F. C.; Jaehning, J. A.; Kim, Y. J.; Kuras, L.; Leutz, A.; Lis, J. T.; Meisterernest, M.; Naar, A. M.; Nasmyth, K.; Parvin, J. D.; Ptashne, M.; Reinberg, D.; Ronne, H.; Sadowski, I.; Sakurai, H.; Sipiczki, M.; Sternberg, P. W.; Stillman, D. J.; Strich, R.; Struhl, K.; Svejstrup, J. Q.; Tuck, S.; Winston, F.; Roeder, R. G.; Kornberg, R. D., A unified nomenclature for protein subunits of Mediator complexes linking transcriptional regulators to RNA polymerase II. *Mol Cell* **2004,** *14* (5), 553-557.

46.   Bryant, G. O.; Ptashne, M., Independent recruitment in vivo by Gal4 of two complexes required for transcription. *Mol Cell* **2003,** *11* (5), 1301-1309.

47.   Brown, C. E.; Howe, L.; Sousa, K.; Alley, S. C.; Carrozza, M. J.; Tan, S.; Workman, J. L., Recruitment of HAT complexes by direct activator interactions with the ATM-related tra1 subunit. *Science* **2001,** *292* (5525), 2333-2337.

48.   Dotson, M. R.; Yuan, C. X.; Roeder, R. G.; Myers, L. C.; Gustafsson, C. M.; Jiang, Y. W.; Li, Y.; Kornberg, R. D.; Asturias, F. J., Structural organization of yeast and mammalian mediator complexes. *Proc Natl Acad Sci U S A* **2000,** *97* (26), 14307-10.

49.   Goodman, R. H.; Smolik, S., CBP/p300 in cell growth, transformation, and development. *Genes Dev* **2000,** *14* (13), 1553-77.

50.   Reisman, D.; Glaros, S.; Thompson, E. A., The SWI/SNF complex and cancer. *Oncogene* **2009,** *28* (14), 1653-1668.

51.   Lu, P. Y. T.; Levesque, N.; Kobor, M. S., NuA4 and SWR1-C: two chromatin-modifying complexes with overlapping functions and components. *Biochem Cell Biol* **2009,** *87* (5), 799-815.

52.   Iyer, N. G.; Ozdag, H.; Caldas, C., p300/CBP and cancer. *Oncogene* **2004,** *23* (24), 4225-4231.

53.   Myers, L. C.; Kornberg, R. D., Mediator of transcriptional regulation. *Annu Rev Biochem* **2000,** *69*, 729-49.

54.   Green, M. R., TBP-associated factors (TAF(II)s): multiple, selective transcriptional mediators in common complexes. *Trends Biochem Sci* **2000,** *25* (2), 59-63.

55.   Sterner, D. E.; Grant, P. A.; Roberts, S. M.; Duggan, L. J.; Belotserkovskaya, R.; Pacella, L. A.; Winston, F.; Workman, J. L.; Berger, S. L., Functional organization of the yeast SAGA complex: Distinct components involved in structural integrity, nucleosome acetylation, and TATA-binding protein interaction. *Mol Cell Biol* **1999,** *19* (1), 86-98.

56.   Reeves, W. M.; Hahn, S., Targets of the Gal4 transcription activator in functional transcription complexes. *Mol Cell Biol* **2005,** *25* (20), 9092-102.

57.   Malik, S.; Roeder, R. G., Dynamic regulation of pol II transcription by the mammalian Mediator complex. *Trends Biochem Sci* **2005,** *30* (5), 256-263.

58.   Fishburn, J.; Mohibullah, N.; Hahn, S., Function of a eukaryotic transcription activator during the transcription cycle. *Mol Cell* **2005,** *18* (3), 369-378.

59.   Bhaumik, S. R.; Raha, T.; Aiello, D. P.; Green, M. R., In vivo target of a transcriptional activator revealed by fluorescence resonance energy transfer. *Genes Dev* **2004,** *18* (3), 333-43.

60.   Davis, J. A.; Takagi, Y.; Kornberg, R. D.; Asturias, F. J., Structure of the yeast RNA polymerase II holoenzyme: Mediator conformation and polymerase interaction. *Mol Cell* **2002,** *10* (2), 409-415.

61.   Kobayashi, Y.; Kitamoto, T.; Masuhiro, Y.; Watanabe, M.; Kase, T.; Metzger, D.; Yanagisawa, J.; Kato, S., p300 mediates functional synergism between AF-1 and AF-2 of estrogen receptor alpha and beta by interacting directly with the N-terminal A/B domains. *J Biol Chem* **2000,** *275* (21), 15645-15651.

62.   Glass, C. K.; Rosenfeld, M. G., The coregulator exchange in transcriptional functions of nuclear receptors. *Gene Dev* **2000,** *14* (2), 121-141.

63.	McKenna, N. J.; Xu, J. M.; Nawaz, Z.; Tsai, S. Y.; Tsai, M. J.; O'Malley, B. W., Nuclear receptor coactivators: multiple enzymes, multiple complexes, multiple functions. *J Steroid Biochem* **1999,** *69* (1-6), 3-12.

64.	Almlof, T.; Wallberg, A. E.; Gustafsson, J. A.; Wright, A. P. H., Role of important hydrophobic amino acids in the interaction between the glucocorticoid receptor tau 1-core activation domain and target factors. *Biochemistry-Us* **1998,** *37* (26), 9586-9594.

65.	Henriksson, A.; Almlof, T.; Ford, J.; McEwan, I. J.; Gustafsson, J. A.; Wright, A. P. H., Role of the Ada adaptor complex in gene activation by the glucocorticoid receptor. *Mol Cell Biol* **1997,** *17* (6), 3065-3073.

66.	Chen, H. W.; Lin, R. J.; Schiltz, R. L.; Chakravarti, D.; Nash, A.; Nagy, L.; Privalsky, M. L.; Nakatani, Y.; Evans, R. M., Nuclear receptor coactivator ACTR is a novel histone acetyltransferase and forms a multimeric activation complex with P/CAF and CBP/p300. *Cell* **1997,** *90* (3), 569-580.

67.	Cairns, B. R.; Levinson, R. S.; Yamamoto, K. R.; Kornberg, R. D., Essential role of Swp73p in the function of yeast Swi/Snf complex. *Gene Dev* **1996,** *10* (17), 2131-2144.

68.	Yoshinaga, S. K.; Peterson, C. L.; Herskowitz, I.; Yamamoto, K. R., Roles of Swi1, Swi2, and Swi3 Proteins for Transcriptional Enhancement by Steroid-Receptors. *Science* **1992,** *258* (5088), 1598-1604.

69.	Janknecht, R., The versatile functions of the transcriptional coactivators p300 and CBP and their roles in disease. *Histology and Histopathology* **2002,** *17* (2), 657-668.

70.	Horvai, A. E.; Xu, L.; Korzus, E.; Brard, G.; Kalafus, D.; Mullen, T. M.; Rose, D. W.; Rosenfeld, M. G.; Glass, C. K., Nuclear integration of JAK/STAT and Ras/AP-1 signaling by CBP and p300. *P Natl Acad Sci USA* **1997,** *94* (4), 1074-1079.

71.	Oliner, J. D.; Andresen, J. M.; Hansen, S. K.; Zhou, S. L.; Tjian, R., SREBP transcriptional activity is mediated through an interaction with the CREB-binding protein. *Gene Dev* **1996,** *10* (22), 2903-2911.

72.	Eckner, R., p300 and CBP as Transcriptional Regulators and Targets of Oncogenic Events. *Biological Chemistry* **1996,** *377*, 4.

73.	Arany, Z.; Huang, L. E.; Eckner, R.; Bhattacharya, S.; Jiang, C.; Goldberg, M. A.; Bunn, H. F.; Livingston, D. M., An essential role for p300/CBP in the cellular response to hypoxia. *P Natl Acad Sci USA* **1996,** *93* (23), 12969-12973.

74.   Hallam, T. M.; Bourtchouladze, R., Rubinstein-Taybi syndrome: molecular findings and therapeutic approaches to improve cognitive dysfunction. *Cellular and Molecular Life Sciences* **2006,** *63* (15), 1725-1735.

75.   Tanaka, Y.; Naruse, I.; Hongo, T.; Xu, M. J.; Nakahata, T.; Maekawa, T.; Ishii, S., Extensive brain hemorrhage and embryonic lethality in a mouse null mutant of CREB-binding protein. *Mechanisms of Development* **2000,** *95* (1-2), 133-145.

76.   Kung, A. L.; Rebel, V. I.; Bronson, R. T.; Ch'ng, L. E.; Sieff, C. A.; Livingston, D. M.; Yao, T. P., Gene dose-dependent control of hematopoiesis and hematologic tumor suppression by CBP. *Gene Dev* **2000,** *14* (3), 272-277.

77.   Giles, R. H.; Peters, D. J. M.; Breuning, M. H., Conjunction dysfunction: CBP/p300 in human disease. *Trends in Genetics* **1998,** *14* (5), 178-183.

78.   Tanaka, Y.; Naruse, I.; Maekawa, T.; Masuya, H.; Shiroishi, T.; Ishii, S., Abnormal skeletal patterning in embryos lacking a single Cbp allele: A partial similarity with Rubinstein-Taybi syndrome. *P Natl Acad Sci USA* **1997,** *94* (19), 10215-10220.

79.   Petrij, F.; Giles, R. H.; Dauwerse, H. G.; Saris, J. J.; Hennekam, R. C. M.; Masuno, M.; Tommerup, N.; Vanommen, G. J. B.; Goodman, R. H.; Peters, D. J. M.; Breuning, M. H., Rubinstein-Taybi Syndrome Caused by Mutations in the Transcriptional Coactivator Cbp. *Nature* **1995,** *376* (6538), 348-351.

80.   Kasper, L. H.; Fukuyama, T.; Biesen, M. A.; Boussouar, F.; Tong, C. L.; de Pauw, A.; Murray, P. J.; van Deursen, J. M. A.; Brindle, P. K., Conditional knockout mice reveal distinct functions for the global transcriptional coactivators CBP and p300 in T-cell development. *Mol Cell Biol* **2006,** *26* (3), 789-809.

81.   Chan, H. M.; La Thangue, N. B., p300/CBP proteins: HATs for transcriptional bridges and scaffolds. *Journal of Cell Science* **2001,** *114* (13), 2363-2373.

82.   Nettles, K. W.; Gil, G.; Nowak, J.; Metivier, R.; Sharma, V. B.; Greene, G. L., CBP is a dosage-dependent regulator of nuclear factor-kappa B suppression by the estrogen receptor. *Mol Endocrinol* **2008,** *22* (2), 263-272.

83.   Rebel, V. I.; Kung, A. L.; Tanner, E. A.; Yang, H.; Bronson, R. T.; Livingston, D. M., Distinct roles for CREB-binding protein and p300 in hematopoietic stem cell self-renewal. *P Natl Acad Sci USA* **2002,** *99* (23), 14789-14794.

84.   Li, Z. Y.; Liu, D. P.; Liang, C. C., New insight into the molecular mechanisms of MLL-associated leukemia. *Leukemia* **2005,** *19* (2), 183-190.

85.   Chen, X.; Cheung, S. T.; So, S.; Fan, S. T.; Barry, C.; Higgins, J.; Lai, K. M.; Ji, J.; Dudoit, S.; Ng, I. O.; Van De Rijn, M.; Botstein, D.; Brown, P. O., Gene expression patterns in human liver cancers. *Mol Biol Cell* **2002,** *13* (6), 1929-39.

86.   Malkin, D., The role of p53 in human cancer. *J Neurooncol* **2001,** *51* (3), 231-43.

87.   Herzig, S.; Long, F.; Jhala, U. S.; Hedrick, S.; Quinn, R.; Bauer, A.; Rudolph, D.; Schutz, G.; Yoon, C.; Puigserver, P.; Spiegelman, B.; Montminy, M., CREB regulates hepatic gluconeogenesis through the coactivator PGC-1. *Nature* **2001,** *413* (6852), 179-83.

88.   Yaghmai, R.; Cutting, G. R., Optimized regulation of gene expression using artificial transcription factors. *Molecular Therapy* **2002,** *5* (6), 685-694.

89.   Urnov, F. D.; Rebar, E. J., Designed transcription factors as tools for therapeutics and functional genomics. *Biochem Pharmacol* **2002,** *64* (5-6), 919-923.

90.   Urnov, F. D.; Miller, J. C.; Lee, Y. L.; Beausejour, C. M.; Rock, J. M.; Augustus, S.; Jamieson, A. C.; Porteus, M. H.; Gregory, P. D.; Holmes, M. C., Highly efficient endogenous human gene correction using designed zinc-finger nucleases. *Nature* **2005,** *435* (7042), 646-651.

91.   Fuller, G. N.; Su, X. H.; Price, R. E.; Cohen, Z. R.; Lang, F. F.; Sawaya, R.; Majumder, S., Many human medulloblastoma tumors overexpress repressor element-1 silencing transcription (REST) neuron-restrictive silencer factor, which can be functionally countered by REST-VP16. *Mol Cancer Ther* **2005,** *4* (3), 343-349.

92.   Weatherman, R. V., Chemical approaches to studying transcription. *Organic & Biomolecular Chemistry* **2003,** *1* (19), 3257-3260.

93.   Stanojevic, D.; Young, R. A., A highly potent artificial transcription factor. *Biochemistry-Us* **2002,** *41* (23), 7209-7216.

94.   Ansari, A. Z.; Mapp, A. K.; Nguyen, D. H.; Dervan, P. B.; Ptashne, M., Towards a minimal motif for artificial transcriptional activators. *Chemistry & Biology* **2001,** *8* (6), 583-592.

95.   Jung, D. J.; Shimogawa, H.; Kwon, Y.; Mao, Q.; Sato, S.; Kamisuki, S.; Kigoshi, H.; Uesugi, M., Wrenchnolol Derivative Optimized for Gene Activation in Cells. *J Am Chem Soc* **2009,** *131* (13), 4774-4782.

96.   Liu, B.; Alluri, P. G.; Yu, P.; Kodadek, T., A potent transactivation domain mimic with activity in living cells. *J Am Chem Soc* **2005,** *127* (23), 8254-8255.

97.   Cochran, A. G., Antagonists of protein-protein interactions. *Chemistry & Biology* **2000,** *7* (4), R85-R94.

98.   Berg, T., Modulation of protein-protein interactions with small organic molecules. *Angewandte Chemie-International Edition* **2003,** *42* (22), 2462-2481.

99.   Arkin, M. R.; Wells, J. A., Small-molecule inhibitors of protein-protein interactions: Progressing towards the dream. *Nature Reviews Drug Discovery* **2004,** *3* (4), 301-317.

100.   Pagliaro, L.; Felding, J.; Audouze, K.; Nielsen, S. J.; Terry, R. B.; Krog-Jensen, C.; Butcher, S., Emerging classes of protein-protein interaction inhibitors and new tools for their development. *Current Opinion in Chemical Biology* **2004,** *8* (4), 442-449.

101.   Stockwell, B. R., Exploring biology with small organic molecules. *Nature* **2004,** *432* (7019), 846-854.

102.   Arkin, M., Protein-protein interactions and cancer: small molecules going in for the kill. *Current Opinion in Chemical Biology* **2005,** *9* (3), 317-324.

103.   Fletcher, S.; Hamilton, A. D., Protein surface recognition and proteomimetics: mimics of protein surface structure and function. *Curr Opin Chem Biol* **2005,** *9* (6), 632-8.

104.   Yin, H.; Hamilton, A. D., Strategies for targeting protein-protein interactions with synthetic agents. *Angew Chem Int Ed Engl* **2005,** *44* (27), 4130-63.

105.   Fletcher, S.; Hamilton, A. D., Targeting protein-protein interactions by rational design: mimicry of protein surfaces. *J R Soc Interface* **2006,** *3* (7), 215-33.

Chapter II

iTADs Target the KIX Domain of CBP[a]

A. Abstract

Small molecule replacements of transcription factors are highly sought after due to their value as mechanistic probes and their potential therapeutic value. Here we examine the mechanism of a small molecule TAD mimic using *in vitro* and cellular strategies. Prevailing evidence suggests that TADs interact with several components of the transcriptional machinery to facilitate the initiation of transcription. The results show that iTAD **1** exhibits a multiprotein binding profile *in vitro*, similar to natural activators. In addition, one target was identified as the KIX domain of the Creb binding protein (CBP), a target of natural activators. In addition, iTAD-mediated activation correlates with the availability of CBP in cells, analogous to some endogenous TADs. These results suggest that iTADs function with a mechanism similar to that of natural activators.

---

[a] Portions of this chapter are reported in Buhrlage, S.J.; Bates, C.A.; Rowe, S.P.; Minter, A.R.; Brennan, B.B.; Majmudar, C.Y.; Wemmer, D.E.; Al-Hashimi, H. M.; Mapp, A.K. "Amphipathic small molecules mimic the binding mode and function of endogenous transcription factors." *ACS Chem. Biol.*, **2009**, 4(5), 335-344.

B. Introduction

In 2006, the Mapp lab reported the first small molecule TAD that upregulates transcription in cells.[1] This small molecule TAD was designed to mimic amphipathic activators through a display of hydrophobic and polar functionality around a rigid scaffold. To this end, a five-membered isoxazolidine was synthesized bearing benzyl, hydroxyethyl, and isobutyl functionality around the rigid ring structure, iTAD **1** (Figure II-1). This compound was found to upregulate transcription 80 fold in a cellular 2-hybrid system (*vide infra*). In addition, stereo- and positional isomers of iTAD **1** also activated transcription, mimicking endogenous TADs in the lack of importance of specific sequences or orientation of functionality. A fully hydrophobic isoxazolidine, however, bearing an olefin in replacement of the hydroxyl group was unable to activate transcription.[1-3]

CT-I   **Alkene**   **SJB-III**   **iTAD 1**

R = DBD for activity assay
R = N$_3$ for HSQC NMR
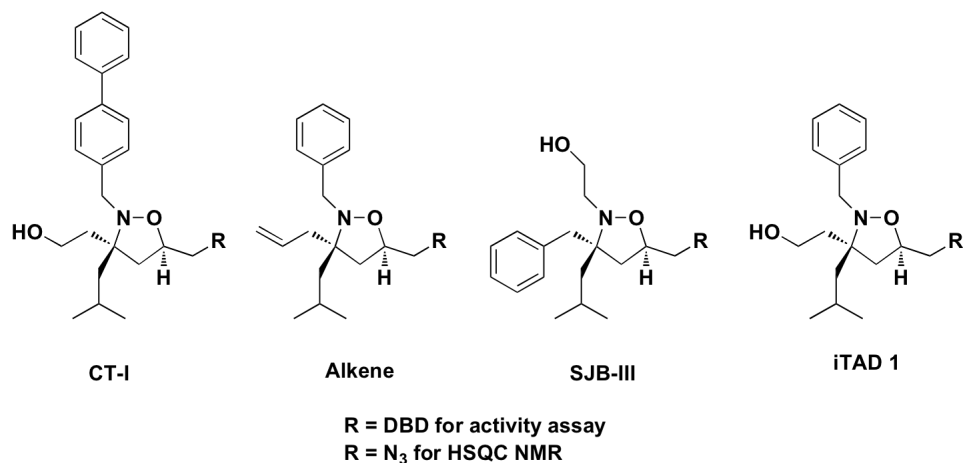
Figure II-1. Isoxazolidine TAD-mimics. **CT-1** contains a biphenyl moiety in place of the benzyl, Alkene is the fully hydrophobic iTAD, **SJB-III** is a positional isomer of iTAD **1**.

Here we show that iTAD **1** interacts with multiple protein binding partners *in vitro* using photocrosslinking, and one target is identified as the Creb binding protein (CBP). Furthermore, the CBP·iTAD binding interaction was further explored using HSQC NMR. These experiments showed that iTAD **1** binds to the KIX domain of CBP, specifically the site utilized by natural activators MLL, Jun, Tat, and Tax. CBP

is a node of many cell-signaling pathways, and this class of small molecules will be invaluable tools for further probing the molecular recognition events that occur during CBP binding.

C. Small Molecule·Protein Interactions

As described in Chapter I, the Mapp lab introduced the first small molecule TAD in 2004. These studies were continued in cells, and showed that a small molecule isoxazolidine bearing amphipathic functionality, could upregulate gene transcription when tethered to a DNA-binding domain (iTAD **1**-DBD), thus reconstituting the function of natural activators.[1, 4] At this time, however, it was unclear as to the mechanism by which iTAD **1** was activating transcription, if it was via a mechanism similar to endogenous TADs or by a novel mechanism.

To elucidate the mechanism by which iTAD **1** regulates transcription, the protein targets of iTAD **1** needed to be identified. A classical way to identify novel protein binding partners is with a pulldown assay, where the molecule of interest is attached to a bead and incubated with cellular extracts.[5] Protein targets of the molecule of interest will bind and thus be localized to the bead. The remaining unbound extracts are removed by washing and the bound proteins are eluted and characterized by SDS-PAGE, Western blot, MS-MS, or a variety of other techniques. This strategy was advantageous, in this case, because there are no modifications to the molecule required; one can simply replace the linker to a DBD for a linker to a solid support. Two strategies for attaching iTAD **1** to a bead; the first was simply to directly attach iTAD **1** through a short PEG linker, the second was to biotinylate iTAD **1** and bind the small molecule conjugate to streptavidin beads (Figure II-2).
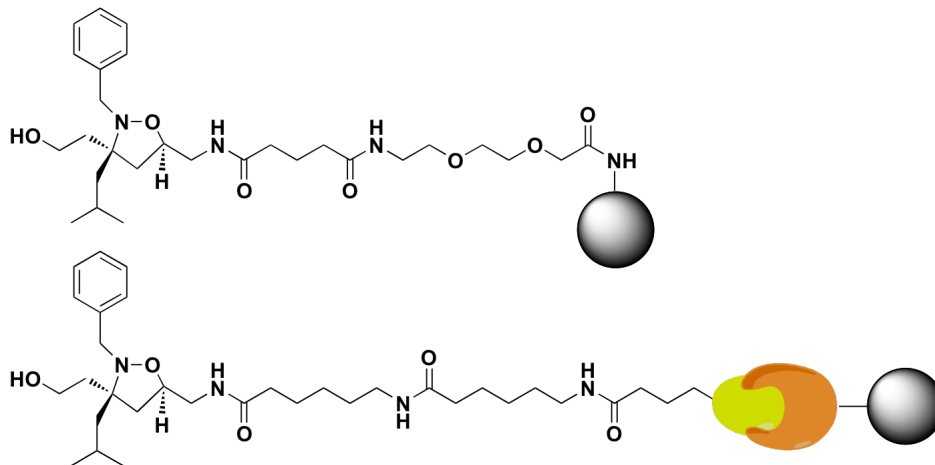
Figure II-2. Beads functionalized with iTAD **1**. In the top example, the isoxazolidine is directly tethered to a bead whereas in the bottom case, it is bound through a biotin·streptavidin (yellow and orange, respectively) interaction.

Both constructs were incubated with HeLa nuclear extracts and then washed with buffer to remove unbound proteins. The beads were then washed with increasingly stringent salt and detergent conditions to elute proteins bound to iTAD **1**, and the eluent was analyzed by SDS-PAGE (Figure II-3). Even with the least stringent wash conditions, there were no bands observable other than BSA (incubated with the beads to decrease nonspecific binding) and a faint band at 49 kDa. This is not altogether surprising; endogenous TADs typically have a low-affinity interaction with their targets and exhibit a multiprotein binding profile.[6-20] The limit of detection for a pulldown experiment is mid-to-low micromolar K_D; iTAD **1** may not achieve tight enough binding to effectively pull out protein targets.[5]

1 2 3 4 5

← 49 kDa

Lane 1: Ladder

Lane 2: 10% input

Lane 3: First wash

Lane 4: Second wash

Lane 5: Final wash

Figure II-3. Pulldown of HeLa nuclear extracts with iTAD **1**. Beads functionalized with iTAD **1** were incubated with HeLa nuclear extracts followed by washing and SDS-PAGE analysis. Silver stained gel is shown above.

Additionally the Uesgui lab performed a pulldown with a small molecule TAD dubbed Wrenchnolol, and, although the specificity of this molecule for a particular protein is touted, the gel from their pulldown experiment showed up to 10 bands.[21] In the pulldown with iTAD **1**, the 49 kD band is very intense in the lanes 2 and 3, indicating this protein is most likely in high concentration in the sample is simply sticking to the beads, not binding the small molecule. Despite the exploration of several different incubation and washing buffer conditions, the target proteins were not binding with high enough affinity to the small molecule to be detected over non-specific binding.

Thus, in order to identify the protein binding partner(s) of iTAD **1** it was necessary to utilize another method for detecting protein·small molecule interactions that would ameliorate complications from low-affinity binding. We chose to pursue a photocrosslinking strategy, described in the sections below.

D. Photocrosslinking

Photocrosslinking is a method that is used to trap small molecule·protein or protein·protein interactions through formation of a covalent bond. This strategy entails appending a photoreactive group to the molecule of interest (the probe), which upon irradiation with UV light forms a highly reactive intermediate that then forms a new covalent bond with a nearby protein.[22-32] In each case, the probe bears a tag, biotin for example, which is used for detection or purification of the crosslinked protein(s). Although this method requires appending a photoactive group to the probe molecule, the formation of a covalent bond between the probe and the target greatly facilitates target identification. This technique, when coupled with tryptic digests and mass spectrometric methods, can be used to generate a high-resolution binding site map of an interaction surface.

Common photoreactive groups include aryl azide, diazirine, tetrafluorophenyl azide, and benzophenone (Figure II-4). The aryl azides form highly reactive nitrene species, through the extrusion of N_2 gas, that react very quickly and irreversibly. Benzophenone, however, forms a triplet biradical upon irradiation with 365 nm light, which may relax electronically back to the ground state. In addition, the aryl azides and diazirines are quite sensitive to ambient light, generally requiring special equipment to synthesize, while benzophenone is largely unaffected by ambient light sources.[27, 28, 32-39] Thus, there are several options for photoreactive moieties, differing in reactivity, size, and electronics. For our purposes, benzophenone had clear advantages over the other groups: its stability and longer irradiation wavelength, made it an easier functionality to work with thus facilitating the synthesis of our photoprobe.
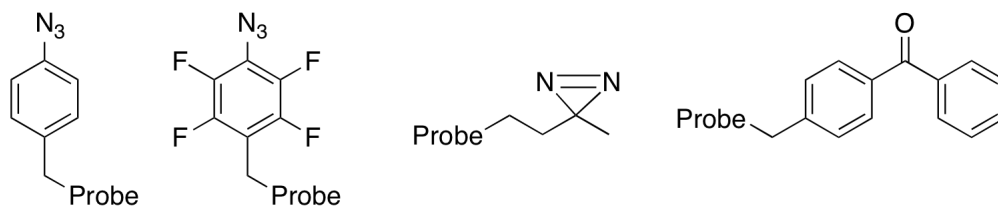
Figure II-4. Common photoreactive groups. Probe: Functional portion of molecule, i.e. TAD.

To identify the targets of iTAD **1**, benzophenone was appended to the molecule, in addition to a biotin affinity handle. Previous work has shown that the hydroxyl and aromatic functionalities are critical for iTAD **1**-mediated transcriptional activation, although they can be placed at C3 or N2. The first generation crosslinking molecule replaced the N2-benzyl moeity of iTAD **1** with a 4-methylbenzophenone group. This molecule was tested for activation in HeLa cells prior to use in crosslinking experiments (*vide infra*).

E. Synthesis and Evaluation of Photoactive iTAD

The first step towards generating target isoxazolidine (iTAD-BP, **10**) was a 1,3-dipolar cycloaddition between oxime **1** (generated under standard conditions from valeraldehyde)[40] and allyl alcohol (Scheme II-1). Accordingly, allyl alcohol and oxime **2** were dissolved in toluene and sodium hypochlorite (bleach) was added resulting in a 1,3-dipolar cycloaddition and the generation of isoxazoline **3**.[41, 42] Treatment of this product with a Lewis acid and allyl magnesium chloride afforded addition of the Grignard reagent to the C=N bond and generating isoxazolidine **4** in 73% yield and with good diastereoselectivity. Treatment with methanesulfonyl chloride followed by displacement with sodium azide generated azide **5**.
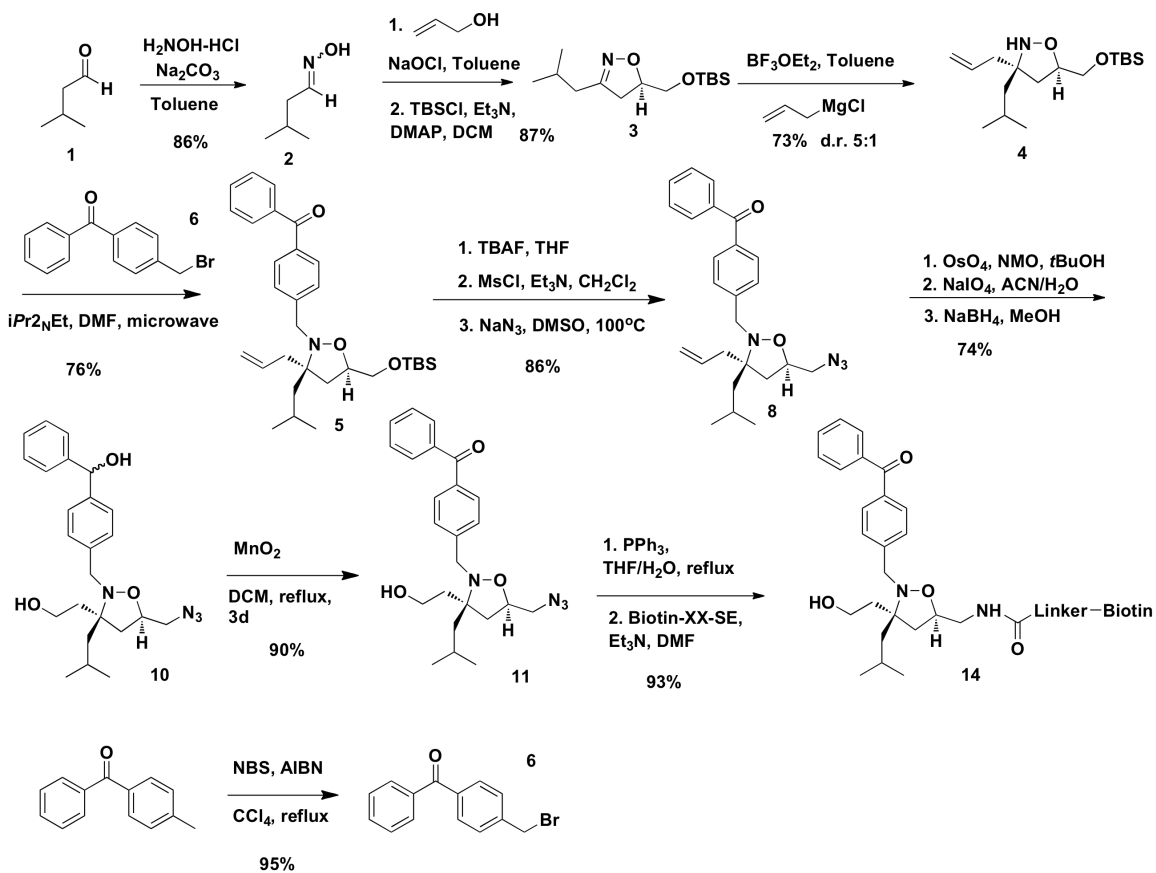
Scheme II-1. Synthesis of first generation photoactive iTAD.

Bromomethylbenzophenone (**6**) was generated from 4-methylbenzophenone, N-bromosuccinimide (NBS), and AIBN in refluxing CCl₄. TBS-protected isoxazolidine **4** was underwent alkylation under microwave-accelerated conditions with 4-bromomethylbenzophenone to afford **5**.[4] Following deprotection with TBAF, the resulting primary alcohol was mesylated and displaced with sodium azide to afford azide **8**. To achieve the desired primary alcohol at the C5 position of the isoxazolidine, azide **8** was treated with a catalytic amount of OsO₄ and a stoichiometric quantity of the co-oxidant NMO. The resulting diol was treated with excess NaIO₄ to cleave the diol to an aldehyde, and the crude material subsequently reduced with NaBH₄ to afford the primary alcohol. Unfortunately, of the several reducing agents tried in this step, all reduced the benzophenone carbonyl and the aliphatic aldehyde. The α,α′,β,β′ unsaturated alcohol was then subjected to oxidation

conditions, using MnO_2 in refluxing dichloromethane to yield alcohol **10**. The azide was subjected to Staudinger reduction conditions with triphenylphosphine and the resulting amine coupled to either biotin-XX, SE (to yield **14**) for use in crosslinking, or to AEEA-OxDex (to yield **13**-AEEA-OxDex) for use in a 2-hybrid system to measure the activity of the compound (Figure II-5).
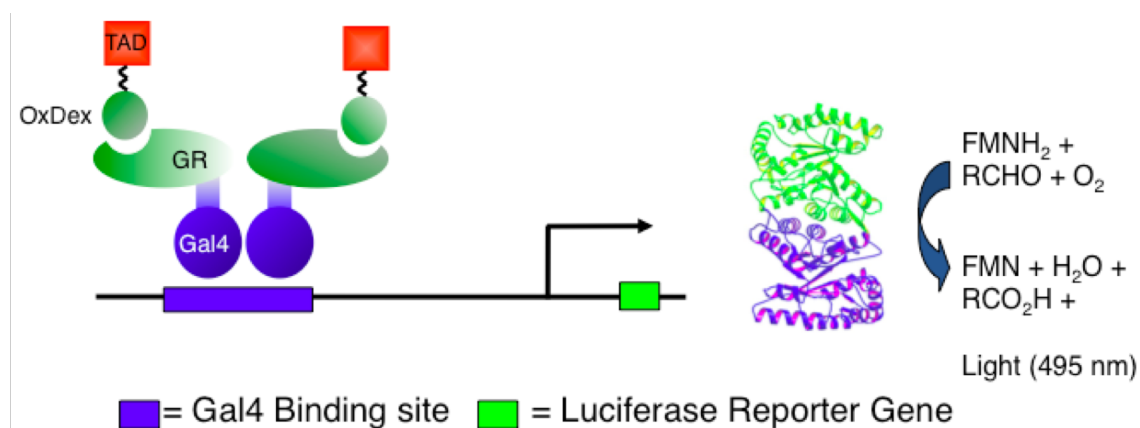
Figure II-5. Two-hybrid cell-based transcriptional activation assay.[43, 44]

Unfortunately, when the ability of this compound to activate transcription was assessed, it was completely inactive, possibly due to the large steric changes made at the N2 position (benzyl, to 4-methylbenzophenone, Figure II-6). Coincidentally, Dr. Jean-Paul Desaulniers, was testing N2-napthyl and biphenyl derivatives of the isoxazolidine scaffold for transcriptional activation and found that those too were inactive, supporting the model that the iTAD binding sites on its target coactivators cannot tolerate bulkier substituents at that position.[45]

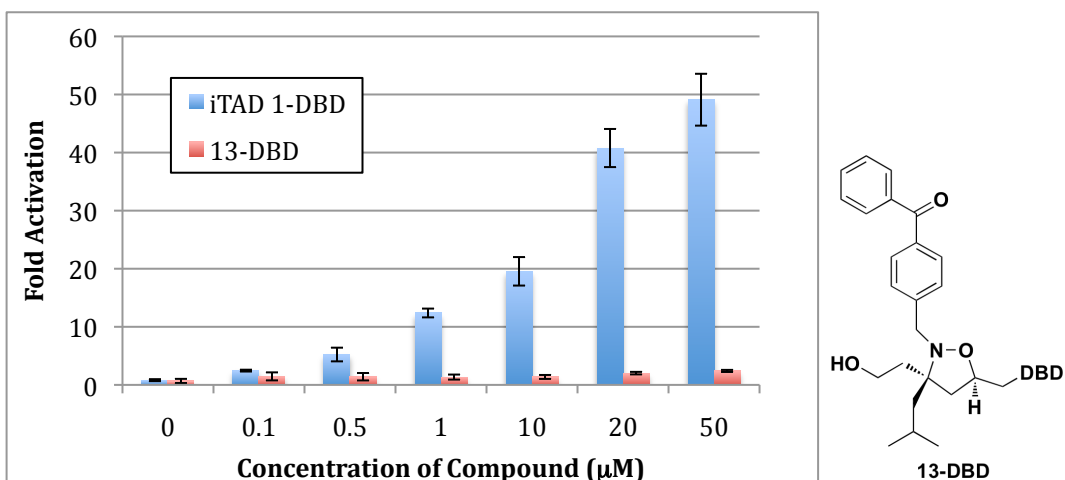**Figure II-6. 13**-DBD function in cell culture. Briefly, HeLa cells were transfected with a plasmid expressing the Gal4 DBD-GR LBD fusion protein, a second plasmid bearing five Gal4-binding sites upstream of a firefly luciferase reported gene, and a third plasmid expressing *Renilla* luciferase as a transfection control, as has been previously described. Compound was added to the cells as a DMSO solution 4 h after transfection such that the final concentration of DMSO in all wells was 1% (vol/vol). The firefly and *Renilla* luciferase activities were measured 24 h after compound addition. Fold activation was determined at each concentration by first dividing the firefly luciferase activity by that of the *Renilla* luciferase. This value was then divided by the amount of activity observed with OxDex- AEEA. Each value is the average of at least three independent experiments with the indicated error (SDOM).

Data from previous work showed that changes at the C5 position appeared well tolerated; thus the second-generation photoactive molecule design appended benzophenone at the C5 position through an amide bond (iTAD-BpA, Scheme II-2).[46] The synthesis began analogously to that described previously, with the exception that benzyl bromide was used as the alkylating agent to afford the N-benzyl compound (not N-4methylbenzophenone). After the Staudinger reduction of the azide, *p*-benzoyl-*l*-phenylalanine (BpA) was coupled to the amine using standard peptide coupling conditions. After removal of the Fmoc protecting group, the amine was acylated with either biotin-XX, SE or AEEA-OxDex to afford **21** or **30**, respectively. These compounds were both purified by reverse-phase HPLC prior to use.
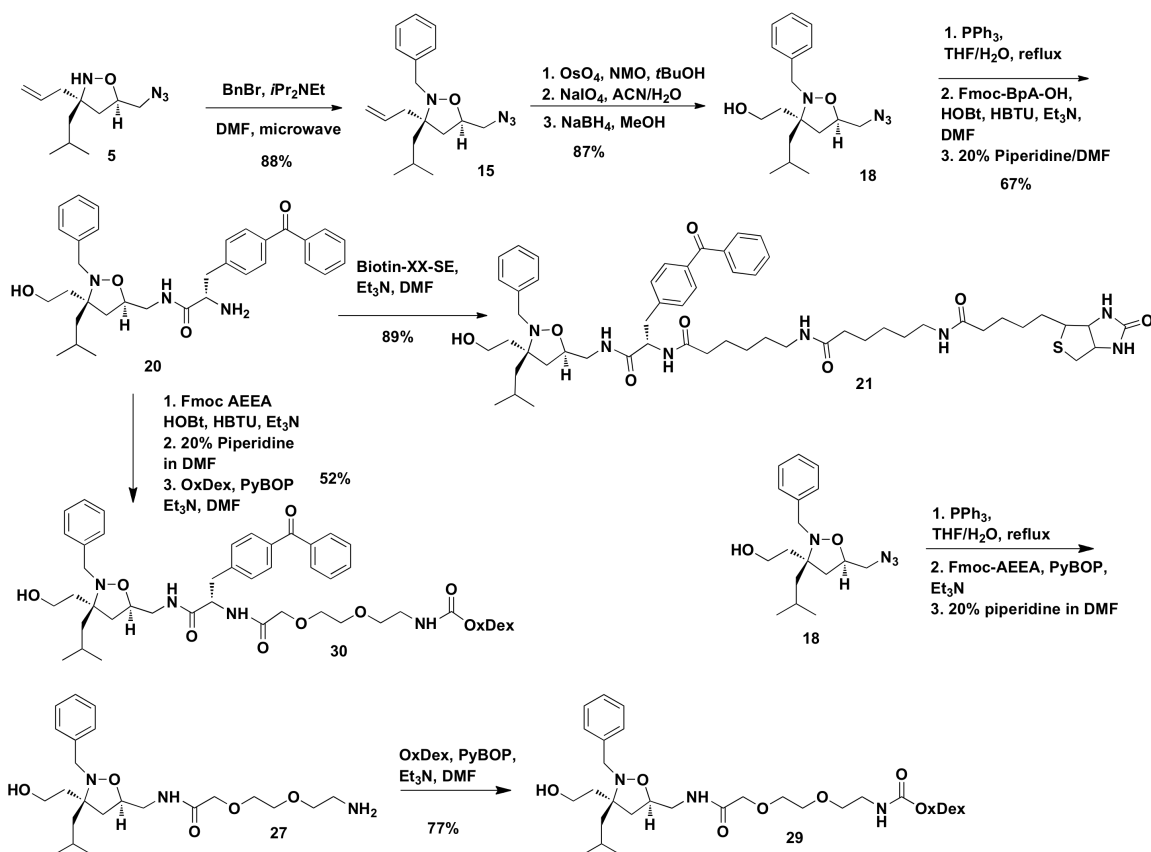
Scheme II-2. Synthesis of second generation photoactive iTAD.

BpA derivative **30** activated transcription in the cellular assay (Figure II-7a); however, there was concern that having added a large hydrophobic group to the molecule had altered its protein-binding pattern relative to iTAD **1**, rendering it an unacceptable probe molecule. To test this, a competitive inhibition experiment was carried out. In this experiment, iTAD-BpA was localized to DNA as a transcriptional activator and the impact of increasing concentrations of free iTAD **1** (no DBD) on the transcriptional activity was assessed. Figure II-7b shows that the activity of iTAD-BpA decreased as the concentration of iTAD **1** increased, indicating that these two molecules share overlapping binding surfaces within the transcriptional machinery. Thus, iTAD-BpA was an appropriate molecule for probing interactions with coactivator targets bound during iTAD **1**-driven gene expression.

37

a)

b)
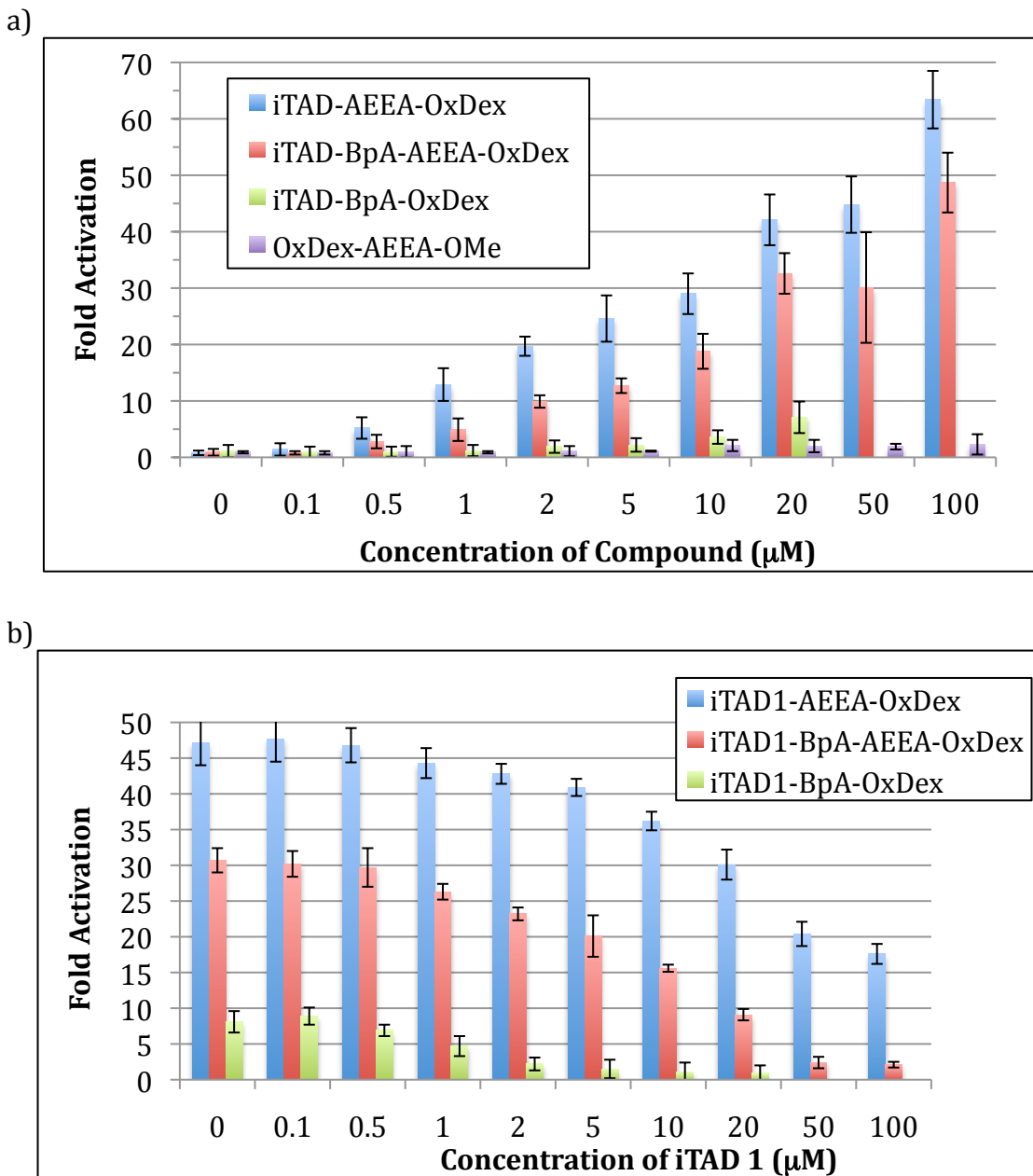
Figure II-7. iTAD-BpA function in cell culture. a) iTAD-BpA activates transcription nearly as well as iTAD-AEEA-OxDex. b) iTAD-BpA is squelched by free iTAD **1**. Activation assay was performed as in a), but with a single concentration of iTAD-BpA-DBD and increasing concentrations of iTAD **1**.

To identify putative coactivator targets of iTAD-BpA, *in vitro* photocrosslinking experiments were performed. The photoactive iTAD tethered to biotin (**21**) was exposed to nuclear extracts from HeLa cells and irradiated with a

handheld UV lamp at 365 nm. Following irradiation, the samples were purified using NeutrAvidin® beads to isolate covalently modified proteins. After extensive washing, the bound proteins were eluted and analyzed by SDS-PAGE and Western blot. To optimize crosslinking conditions, several combinations of buffers, washing and incubation times, and irradiation times were explored. This is a critical step for several reasons: 1) certain buffers caused proteins to precipitate over the course of the experiment, 2) mild washing conditions increased the likelihood of detecting nonspecific interactions, while extremely stringent conditions may have washed away proteins of interest (detergent and high salt concentration may disrupt the biotin·streptavidin interaction), and 3) longer irradiation times increased the chances of forming non-specific interactions, while using too short an irradiation time risked missing interactions with proteins in very low concentration. Figure II-8 shows a Western blot using Streptavidin-HRP (to detect the biotin tag) where each lane represents a different irradiation time. Not surprisingly, longer irradiation times resulted in greater numbers of crosslinked proteins.

Lane 1: 1 min

Lane 2: 2 min

Lane 3: 4 min

Lane 4: 8 min

Lane 5: 12 min
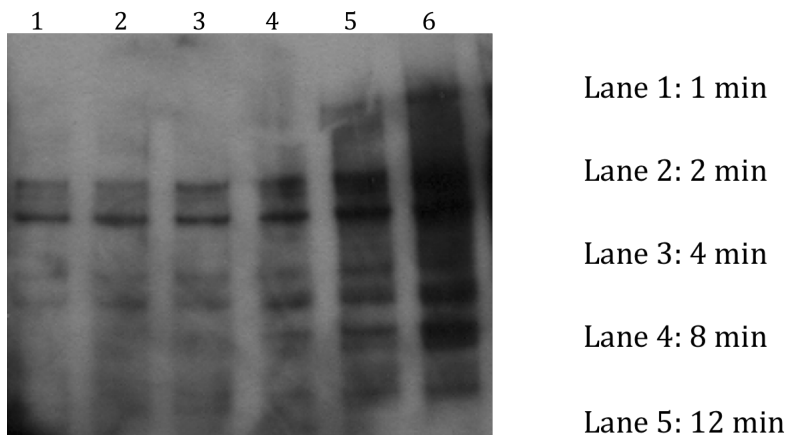
Figure II-8. Time course of the photocrosslinking reaction. Isoxazolidine **21** at a concentration of 50 µM was incubated for 12 h with HeLa nuclear extracts and then individual aliquots were irradiated for varying lengths of time with 365 nm light using a hand-held UV lamp. The mixtures were then immunoprecipitated with Neutravidin beads and then resolved by PAGE. Visualization was accomplished with a streptavidin-HRP conjugate (1:1000). A band corresponding to the molecular weight of CBP can be observed at the 4 minute time point (Lane 4).

Based on this experiment, 5 minutes was chosen for the remainder of the crosslinking experiments, as the number of bands remained constant at longer times, but the intensity of the bands and the background noise increased at longer times. Using these optimized conditions, an additional photocrosslinking experiment was performed (Figure II-9). The appearance of multiple, discrete bands showed that iTAD **1** has a distinct, multiprotein binding profile similar to that of natural activators.[6, 7, 9-11, 15, 17, 18, 20]

	1	2	3	4	5	6

220 kDa -   ← CBP

120 kDa -

80 kDa -

1-Ladder
2- 10% Nuclear Extracts
3-Affinity Purified Extracts
4-Xlinked and Purified Extracts
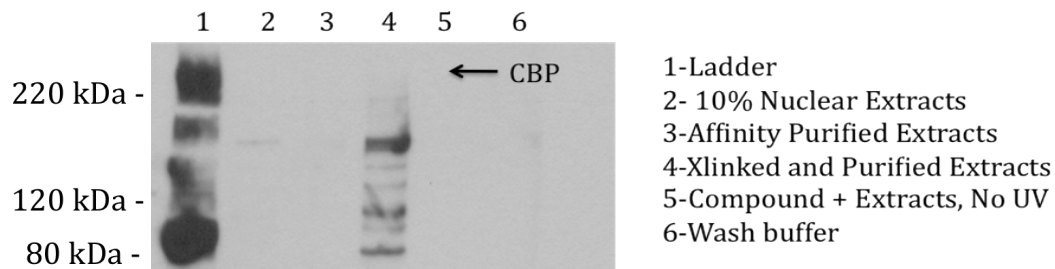5-Compound + Extracts, No UV
6-Wash buffer

Figure II-9. Crosslinking indicates multiprotein binding profile of iTAD-BpA. Crosslinking experiment was carried out as previously described using optimized irradiation time and buffer conditions.

These bands appeared at >260kDa, ~130kDa, ~120kDa, ~95kDa, and ~62kDa. Based on these molecular weights there are a number of putative transcription factor targets, outlined in Figure II-10.

The Creb-binding protein (CBP) is a large, multidomain protein that interacts with a plethora of natural activators including CREB and p53, and has a chromatin-modifying histone acetyltransferase (HAT) domain.[47-49] Med12 is a subunit of the Mediator complex (also known as the TRAP or DRIP complex); mutations in Med12 are known to cause two types of mental retardation.[50] SAP130 is part of the HDAC1-Sin3a corepressor complex that deacetylates histones, repressing transcription.[51] HDAC5 also deacetylates histones, and is important in transcriptional regulation and cell cycle progression.[52] Med24 and Med16 are both components of the Mediator complex; Med24 is important for integrity of the complex, while Med16 is required for transcription of lipopolysaccharide- and heat-shock response genes.[53, 54] p97 has multiple functions, including nuclear transport and ubiquitin-ligase

activity.[55] Med15, another Mediator subunit, is important for sterol-responsive gene expression and is a target of natural activators.[53, 54] Cdc23 is part of the Anaphase-promoting complex (APC) that catalyzed the ubiquitylation of B-type cyclins and cohesin, initiating the transition out of metaphase into anaphase.[56] MOP9 is a coactivator targeted by activators involved in response to hypoxia and regulating circadian rhythms.[57] The multiprotein binding profile of iTAD-BpA was a promising result; however, these bands needed further investigation to determine not only the identity of these proteins, but also the relevance of the interaction to iTAD-mediated gene expression.

MW	Protein	Complex
265	CBP	Multiple
260	Med12	Mediator
130	SAP130	HDAC1/Sin3a
124	HDAC5	Multiple
100	Med24	Mediator
97	p97	Multiple
95	Med16	Mediator
87	Med15	Mediator
66	Cdc23	Anaphase-promoting Complex
62	MOP9	Multiple

Figure II-10. Possible iTAD-BpA binding partners by molecular weight. Complex indicates name of multiprotein complex where the specified protein is found. Multiple complexes indicates the specified protein is known to be in > 10 complexes.

Western blots were performed under optimized conditions using antibodies against CBP, SAP130, Med15, and Cdc23 to identify additional binding partner of **21**.

These experiments confirmed CBP as a binding partner of iTAD-BpA (*vide infra*), though none of the other proteins were detected by Western blot (Figure II-11).
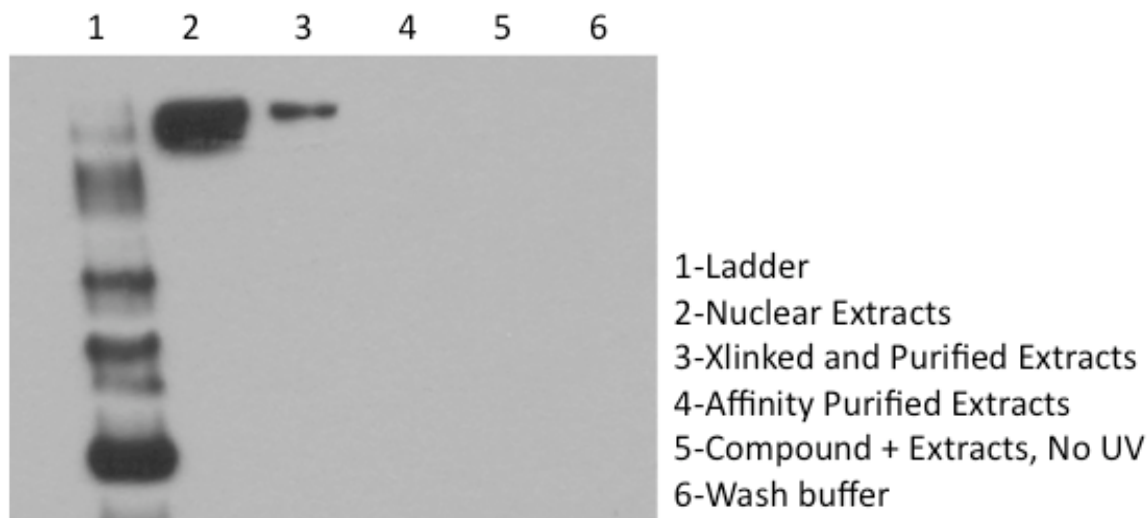

1-Ladder
2-Nuclear Extracts
3-Xlinked and Purified Extracts
4-Affinity Purified Extracts
5-Compound + Extracts, No UV
6-Wash buffer

Figure II-11. Crosslinking identified CBP as a binding partner of iTAD-BpA. HeLa nuclear extracts were incubated with **21** for 12 h followed by 30 min of irradiation of the mixture with 365 nm light. Following immunoprecipitation with streptavidin, Western blot analysis demonstrates that one interaction partner of **21** is CBP. In the absence of UV irradiation (Lane 5), no CBP is observed, consistent with a direct interaction between **21** and CBP. Lane 2 contains nuclear extracts alone. UV indicates irradiation with 365 nm light.

During the period when these crosslinking experiments were conducted, a colleague, Ryan Casey, was examining the ability of small amphipathic natural products to act as TADs when tethered to a DBD.[45] One example he discovered was the natural product santonin with its lactone opened (Ryan Casey). This molecule shares some properties with iTAD **1**; a rigid scaffold and amphipathic functionality, but is otherwise dissimilar. This merits a comparison of protein binding partners between the two molecules, and between **15** (iTAD-alkene), an isoxazolidine unable to activate transcription and a peptidic minimal TAD from the natural activator MLL (Dr. Will Pomerantz). These molecules were tethered to BpA and biotin and used in crosslinking experiments analogously to those described previously (Figure II-12a). This provided a comparison in the protein binding profile of four molecules, three of which activated transcription and one that did not

Shown below is a Western blot probed for biotin (Figure II-12b). In the case of iTAD **1**, the multiprotein binding profile is observed. Both santonin-RO and MLL-19 also show multiprotein binding profiles and appear to share some targets with each other and with iTAD **1**. The panel at the far right shows proteins crosslinked with the methyl ester of BpA tethered to biotin, demonstrating little to no overlap with the other probes. Interestingly, the alkene, which does not activate transcription, has the fewest number of targets. This suggests that although the alkene clearly binds to at least four different proteins, these interactions are nonproductive towards initiating transcription.
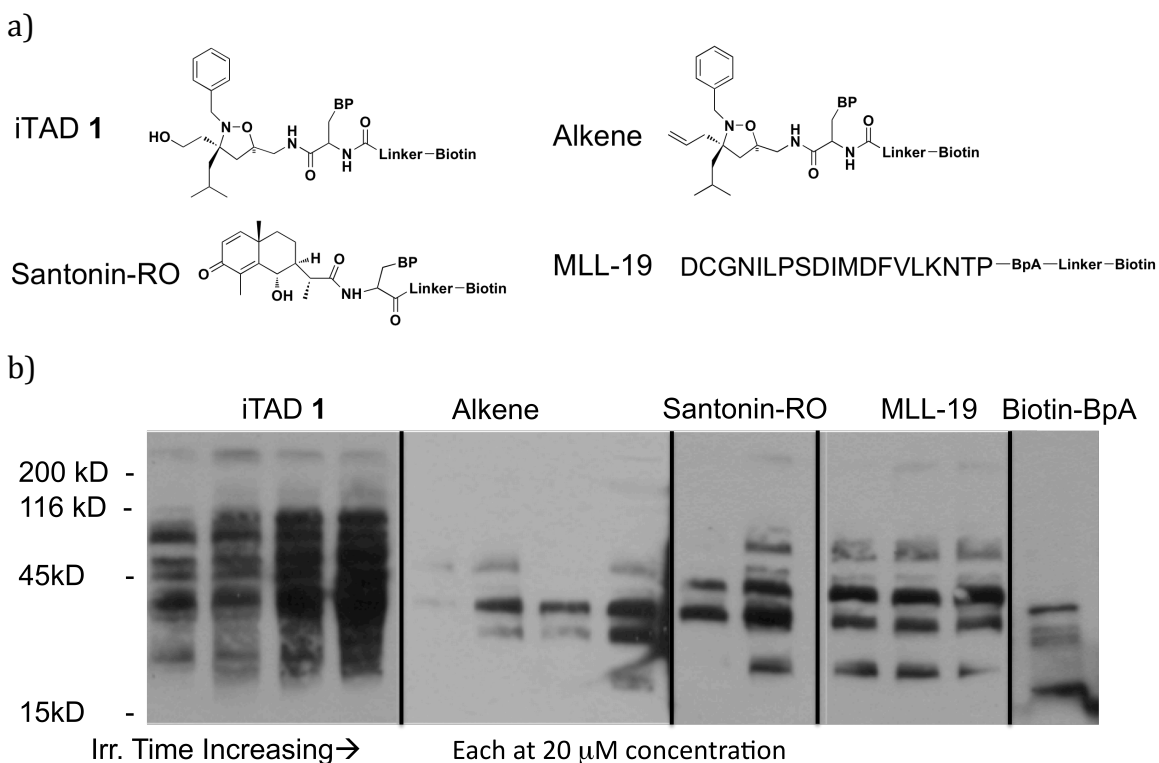
a)

b)

Figure II-12. Binding profiles of other small molecule TADs. a) Four molecules tested. BP = benzophenone. b) Crosslinking experiments were performed individually with each compound as previously described. Western blots are shown above for four small molecules and an unfunctionalized biotin-BpA control (far right).

To further examine these small molecule TADs, each crosslinking sample was also probed with an anti-CBP antibody to determine if other small molecule TADs bind CBP (Figure II-13). These data indicate that both iTAD **1** and santonin-RO interacted with the Creb binding protein (CBP), a known target of natural activators, while the alkene and control did not. MLL-19 (minimal TAD from an endogenous CBP-binding activator) showed a very faint band in the CBP Western blot, likely due in part to limited solubility of the 19-mer in the buffer used.[13]
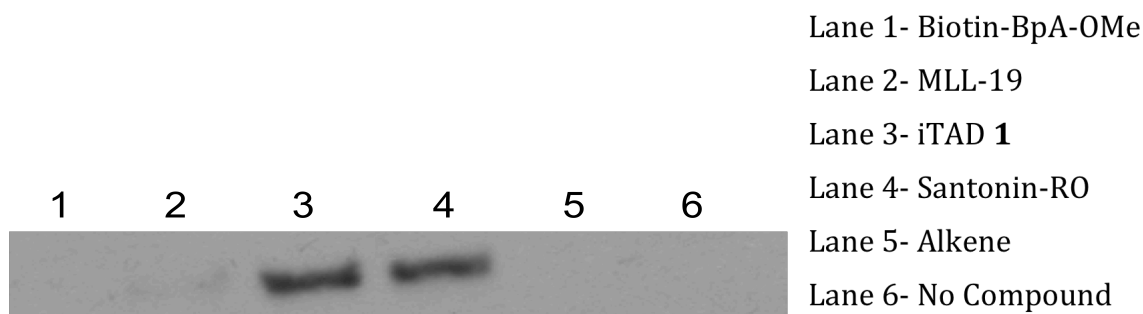
Lane 1- Biotin-BpA-OMe
Lane 2- MLL-19
Lane 3- iTAD **1**
Lane 4- Santonin-RO
Lane 5- Alkene
Lane 6- No Compound

**Figure II-13.** A subset of small molecule TADs bind CBP.

These data suggest that the iTADs, and possibly other small molecule amphipathic TAD mimics, function in a mechanism similar to that of natural activators, with a multipartner binding profile and binding of a known target of endogenous activators, although more work was necessary to elucidate the importance of the iTAD·CBP binding interaction.

## F. Activity of iTAD correlates with availability of CBP

CBP is a large protein containing multiple domains that interact with activators. It is a key node in many cell signaling networks, minimally with roles in growth and development, learning and memory, angiogenesis, lipid homeostasis, and certain viral pathogenesis.[47-49, 58-85] Illustrating the fundamental role of CBP in transcription, CBP interacts with >300 transcriptional activators through five protein binding domains.

To assess the importance of the iTAD·CBP interaction in a cellular context, a series of experiments were conducted where the amount of CBP in cells, or its availability for iTAD binding, were altered. When a plasmid encoding full-length CBP was transfected into HeLa cells the activity of iTAD **1**-DBD increased significantly, while that of the negative control MeO-AEEA-OxDex was unchanged (Figure II-14a).[47] However, this could be the result of a general increase in transcription due to an increased amount of a key transcriptional regulator. We next transfected a short-hairpin (sh) RNA-expression vector with a sequence targeting the CBP gene, or a scramble of that sequence.[86] This anti-CBP shRNA will bind to the CBP mRNA and induce its degradation, resulting in lower CBP expression (Figure II-14b).

a)
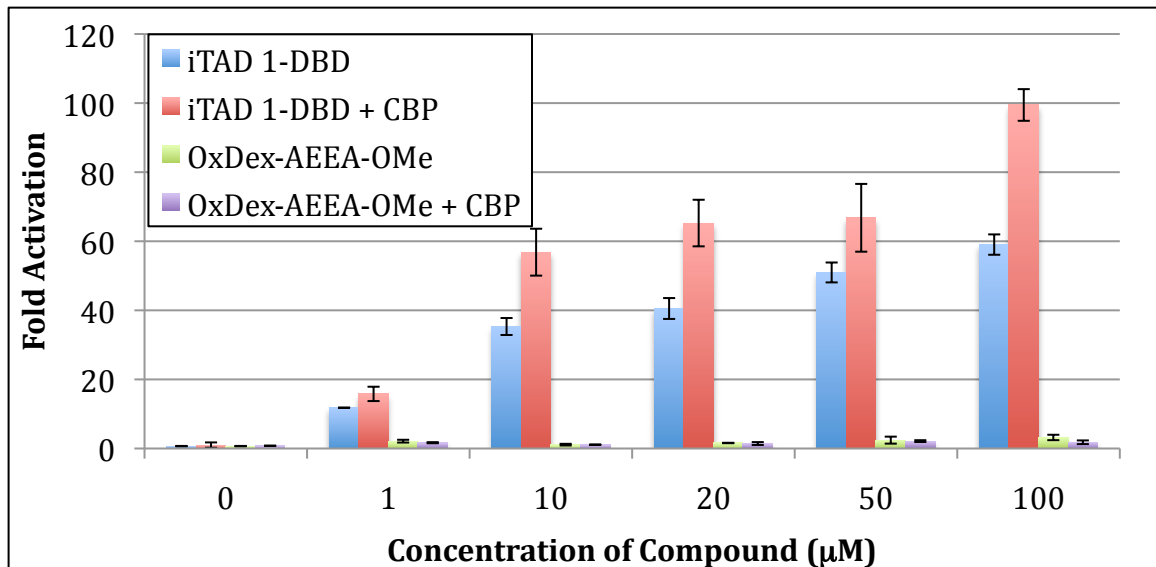
b)
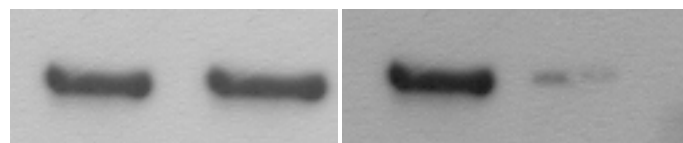
Lane 1- No shRNA   Lane 2- 50 ng shRNA   Lane 3- No shRNA   Lane 4- 100 ng shRNA
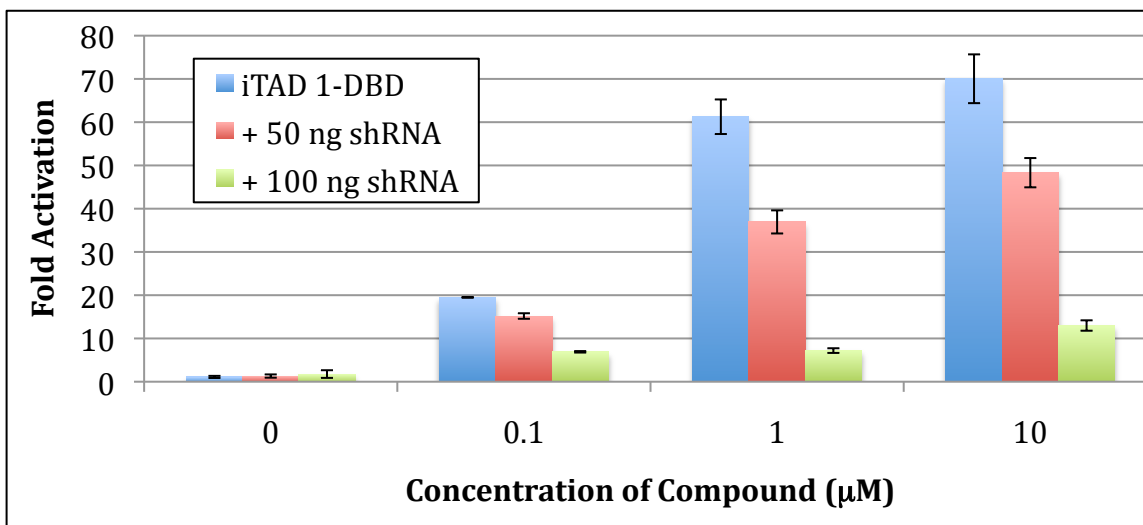
c)

Figure II-14. Function of iTAD **1** in cell culture is dependent upon CBP. a) Addition of full-length CBP by transfection. Briefly, HeLa cells were transfected with a plasmid expressing the Gal4 DBD-GR LBD fusion protein, a second plasmid bearing five Gal4-binding sites upstream of a firefly luciferase reported gene, a third plasmid expressing *Renilla* luciferase as a transfection control, and a fourth plasmid encoding full-length CBP. Compound was added to the cells as a DMSO solution 4 h after transfection such that the final concentration of DMSO in all wells was 1% (v/v). The firefly and *Renilla* luciferase activities were measured 24 h after compound addition. Fold activation was determined at each concentration by first dividing the firefly luciferase activity by that of the *Renilla* luciferase. This value was then divided by the amount of activity observed with OxDex- AEEA. Each value is the average of at least three independent experiments with the indicated error (SDOM). b) Decrease in amount of available CBP with addition of anti-CBP shRNA.[86] Cells were lysed at room temperature with RIPA buffer and a protease inhibitor cocktail (Roche). Samples were centrifuged and subjected to PAGE separation as described previously followed by Western blot analysis using anti-CBP antibody (1:500) and anti-mouse secondary antibody (1:1000). c) Function of iTAD **1**-DBD in cell culture with decreased amounts of CBP. Transfection occurred as described in a), but using a CBP-shRNA plasmid instead of full-length CBP.

The decrease in available CBP results in a decrease in iTAD **1**-driven transcription in a dose-dependent manner. Furthermore, when additional CBP is transfected into cells with the anti-CBP shRNA, the additional CBP rescues the activity of iTAD **1**-DBD (Figure II-15).
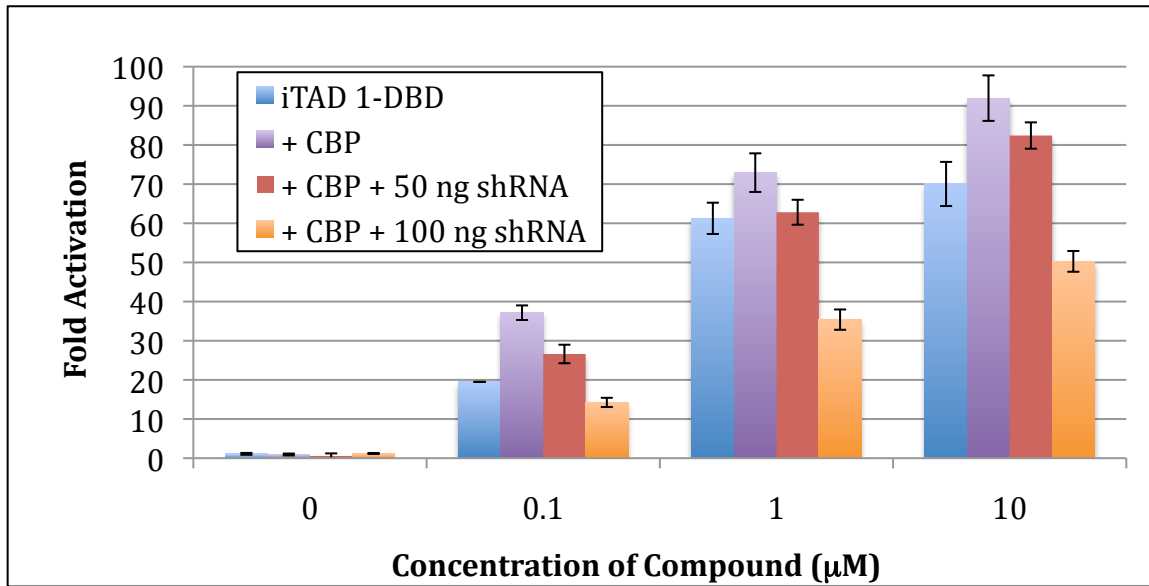
Figure II-15. CBP rescues iTAD **1**-DBD activity. Transfections and activity calculations were performed as described previously.
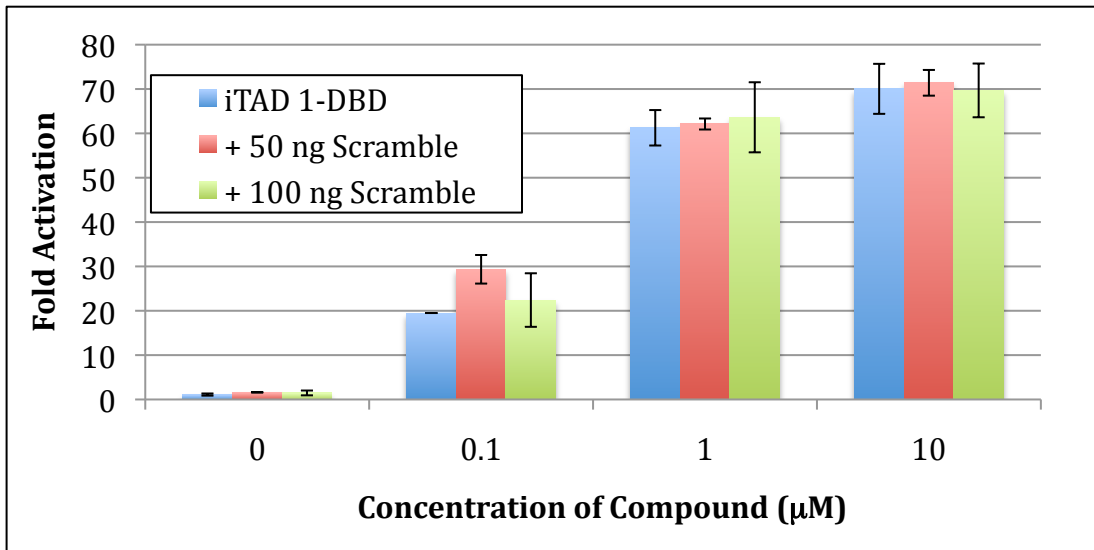

Figure II-16. iTAD **1**-DBD function is unaffected by scrambled shRNA. Transfections and activity calculations were performed as described previously.

In the case of the anti-CBP shRNA, the activity of iTAD **1**-DBD decreases significantly, but is unchanged when the scrambled shRNA is used (Figure II-16). In each case a change in the levels of CBP result in a change in iTAD **1** activity. When CBP is greatly knocked down, however, the result is not complete abrogation of activity of iTAD **1**-DBD, simply a decrease in activity (Figure II-14c). In addition,

NMR spectroscopic and fluorescence polarization binding data show a correlation between the ability of an iTAD to bind CBP and its ability to activate transcription (Figure II-17). When taken together, these data suggest that the iTAD·CBP interaction is important for cellular function of the iTADs; however, it is not the only factor required for activity.
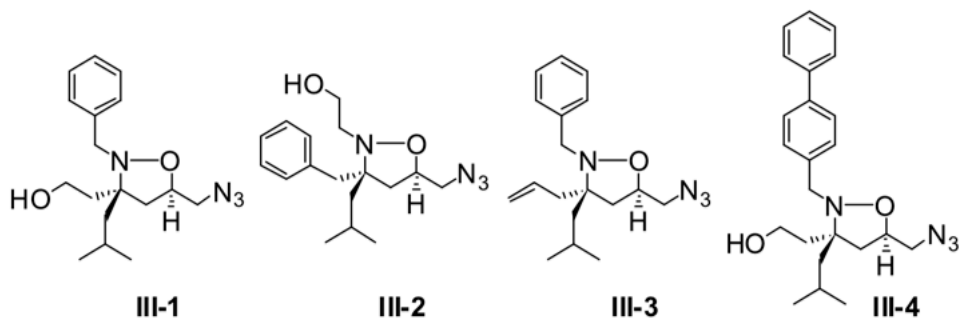
	III-1	III-2	III-3	III-4
Functions as an iTAD	+	+	-	-
CBP	+	+	-	-
Sur2	+	nd	+	+
Tra1	+	nd	nd	nd
Med15	+	nd	nd	+

Figure II-17. Summary of identified isoxazolidine coactivator binding partners. Compounds used in binding experiments were synthesized by Sara Buhrlage and designated **SJB-III-1 – 4**. nd = not determined.

To elucidate the importance of the iTAD·KIX interaction, HeLa cells were transfected with a plasmid encoding full-length E1A.[87] This is a viral protein known to bind the CH1 and KIX domains in cells and sequester CBP for use in expressing the viral genome. When transfected with E1A and treated with iTAD **1**-DBD, activity levels were dramatically decreased, while non-KIX-binding alkene **15** and VP16 (an

activator not known to contact CBP) activity levels remained the same both with
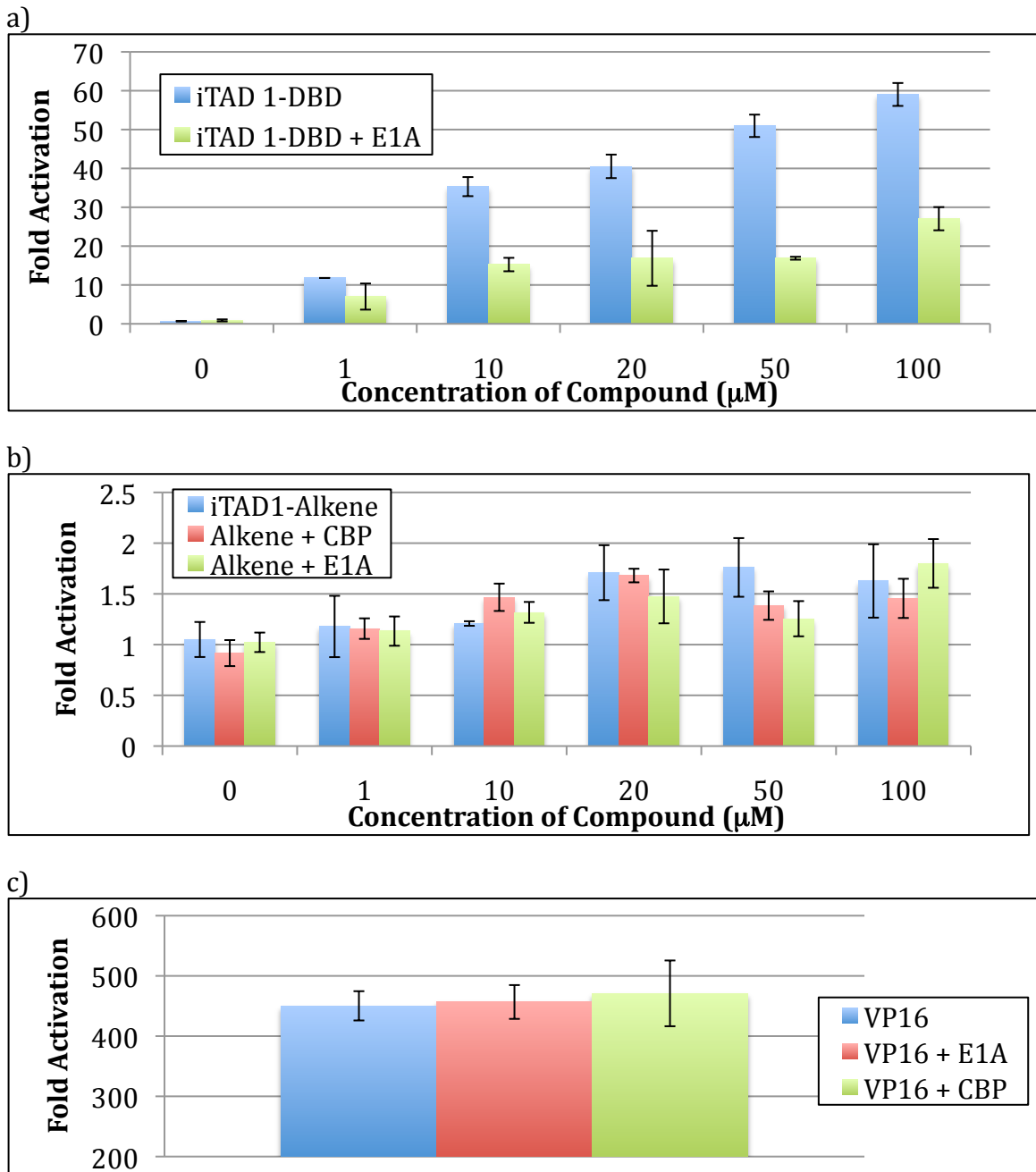E1A and additional CBP (Figure II-18a-c).

a)

b)

c)

Figure II-18. CBP-sequestering adenoviral protein early-region 1A (E1A) alters iTAD **1** function in cell culture, but not non-KIX-binding TADs. a) Effect of E1A transfection on iTAD **1**-driven luciferase expression.[87] b) Effect of E1A and CBP transfection on iTAD-alkene (**15**) function. c). Effect of CBP and E1A transfection on viral protein 16 (VP16)-driven luciferase expression.

Furthermore, a mammalian expression plasmid was constructed containing the KIX domain sequence followed by a nuclear localization signal (NLS) (Dr. Will Pomerantz). When this plasmid was transfected into cells treated with iTAD **1**-DBD, there was a dose-dependent decrease in iTAD **1**-DBD activity; as the levels of KIX-NLS increased the activity of iTAD **1**-DBD decrease (Figure II-19). This is likely due to iTAD binding the exogenously expressed KIX domain, forming a nonfunctional KIX·iTAD complex and thus decreasing the amount of iTAD available for productive interactions with CBP. These data suggest that specifically the KIX domain within CBP is a critical binding partner of iTAD **1**-DBD in cells.
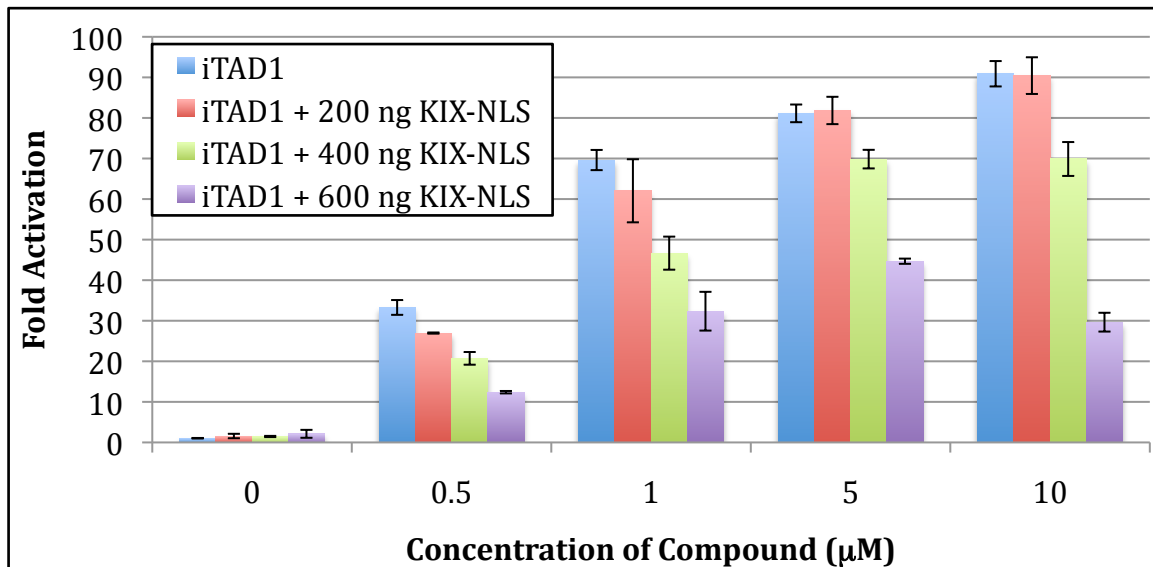

Figure II-19. Effect of KIX-NLS on iTAD **1**-DBD activity in cell culture. Transfections and activity calculations were performed as previously described.

These studies further highlight the importance of CBP binding in transcriptional activation. However, more experiments were necessary in order to determine the domain(s) of CBP that may interact with iTAD **1** and to assess if the iTAD·CBP interaction is merely one determinant of activity or a critical binding interaction.

G. Characterization of iTAD 1 Binding Site

CBP interacts with >300 transcriptional activators through five protein binding domains. As such, it was important to further characterize the binding interaction between iTAD **1** and CBP. Competitive inhibition experiments suggested iTAD **1** might interact with the KIX domain of CBP, that was first identified in CBP but has since been found in coactivators ranging from mammals to plants and fungi, and is thought to be a conserved TAD binding motif. The solution structure of the 87 residue KIX domain of CBP was solved by Peter Wright's lab in 1997.[7]

The KIX domain of CBP consists of 3 α-helices and two 3_{10} helices and interacts with over 15 transcriptional activators through two distinct hydrophobic binding sites.[12, 19, 88, 89] The larger, shallower site formed by helices α-1 and α-3 is bound by Myb and CREB (Figure II-20a and b), while the smaller, deeper binding cleft formed by the C-termini of α-1 and α-3, and the N-terminus of α-2 is bound by MLL, Jun, Tat, and Tax.[7, 13, 19, 90] Key residues from KIX binding TADs are listed in Figure II-13c. The determinants of binding site selection within the KIX domain are currently unknown, thus our investigation also involved binding site selectivity within this domain.

a)
CREB/Myb Site:

Myb   291 KEKRIKELELLLMSTENELKGQQAL 315
Creb   119 TDSQKRREILSRRPSYRKILNDLSSDAPG 147
MLL/Jun/Tat/Tax Site:

MLL   2840 DCGNILPSDIMDFVLKNTP 2858
cJun   47 GSLKPHLRAKNSDLLTSPDVGLLKLASPELERLIIQSSNGHIT 89
Tat   1 MEPVDPRLEPWKHPGSQPKTACTN 24
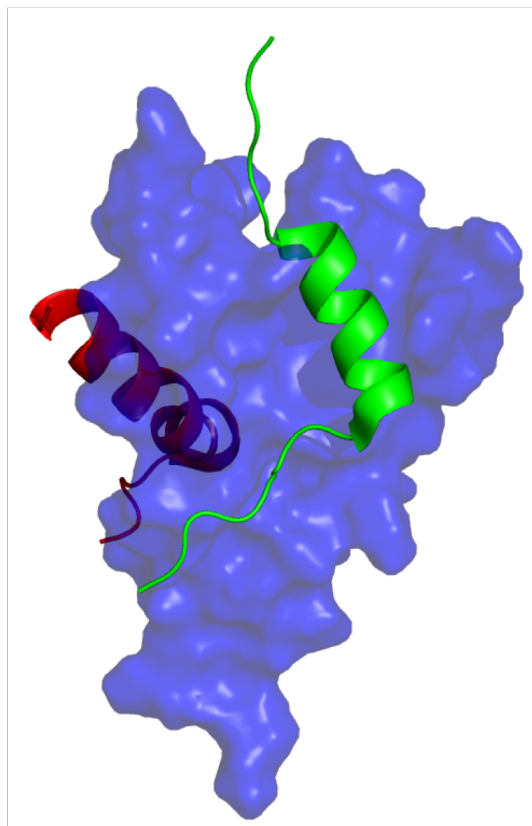Tax   59 IDGRVIGSALQFLIPRLPSFPTQRTSKTLKVLTPPIT 95

Figure II-20. CBP KIX domain and its TAD binding partners. a) Sequences of KIX binding TADs. b) Solution structure of KIX·MLL·Myb. KIX is shown in blue, MLL in green, and Myb in red.[19] Figure adapted from 2agh.

To assess how iTAD **1** interacts with the KIX domain, my colleague Sara Buhrlage carried out one-dimensional ^{1}H, ^{13}C -HSQC experiments using ^{13}C labeled iTAD **1** (at the benzylic position), in the presence and absence of hexahistidine-tagged murine KIX domain [CBP(586-6720)] with a polar linker (His$_6$KIX) (Figure II-21). In the spectrum of the small molecule alone contained two resonances, one for each benzylic proton. The spectrum recorded in the presence of His$_6$KIX (with excess small molecule), a second set of resonances appeared, corresponding to the small molecule bound to the protein. The appearance of these distinct peaks suggests that the molecule is binding in the slow exchange regime.
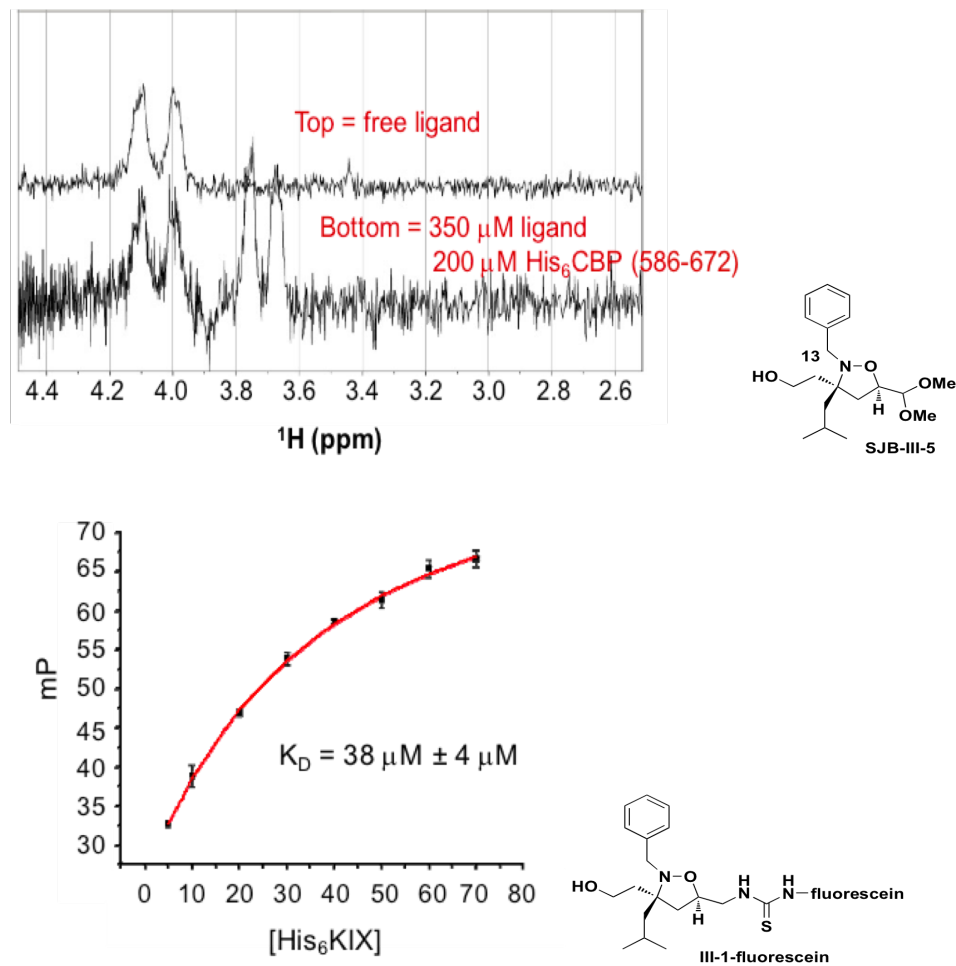
Figure II-21. iTAD **1** binds the CBP KIX domain. a) 1D ^{13}C, ^{1}H-HSQC of **SJB-III-5** in the presence and absence of His$_6$KIX. b) This interaction occurs with a K$_D$ of 38 µM ± 4 µM (Dr. Steve Rowe).

To evaluate the affinity of iTAD **1** for the KIX domain, another colleague, Steve Rowe conducted fluorescence polarization binding experiments with iTAD-Fluorescein (III-1-fluorescein) and His$_6$KIX, and yielded a KD of 38 µM +/- 4 µM (Figure II-21). This is consistent with K$_D$s from endogenous KIX ligands (dissociation constants ranging from 300 nM to 40 µM).[7, 12, 13, 90, 91] NMR spectroscopy was then used to further characterize the binding interaction to determine the location(s) of the binding site(s) within the KIX domain.

The spectrum of this fragment of CBP without a tag was assigned by Peter Wright's lab using ^{1}H, ^{15}N-HSQC.[7] To exploit this assignment, His$_6$KIX uniformly labeled with ^{15}N was overexpressed and purified and a ^{1}H- ^{15}N-HSQC spectrum of the protein was recorded in the presence and absence of iTAD **1**. Approximately 90% of the KIX residue assignments could be transposed to our spectrum; not all residues could be assigned due to chemical shift degeneracy and line broadening effects. The full spectrum is shown in Figure II-22. Residues from the linker between the histidine-tag and the KIX domain are indicated by red boxes and stars.
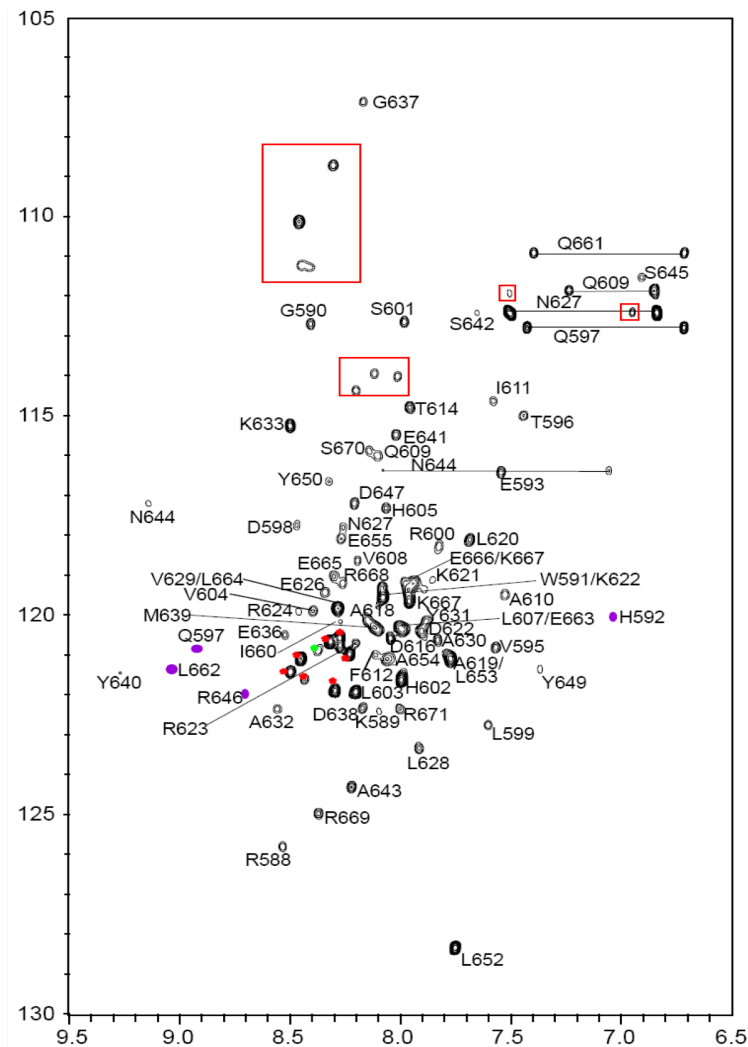

Figure II-22. 2D ^{15}N, ^{1}H-HSQC of ^{15}N-His$_6$KIX. Resonances from the linker between the KIX domain and histidine tag are indicated by red boxes and stars. Purple

resonances are not observed at the contour level shown here, but are visible at higher contours.

To further probe the nature of the iTAD·KIX binding interaction, a titration experiment was carried out by adding increasing amounts of small molecule to the protein and recording the spectra. Progressive changes were observed in the ^{1}H and ^{15}N resonances, suggesting that complexation is occurring in the fast exchange regime (Figure II-23a). Surprisingly, the small molecule exhibits slow exchange, while the protein exhibits fast exchange. While unusual, this behavior has been observed for the TAD of CREB (Kid) in complex with KIX. The Wright and Lumb groups have conducted similar evaluations for three endogenous TADs that bind the KIX domain. These experiments have shown that Jun and Tax interact with KIX on the fast exchange regime and MLL binds in the slow exchange regime.[12, 19, 91] Based on these experiments we can conclude that iTAD **1** displays kinetic behavior similar to that of a subset of KIX-binding activators.

To identify the binding site of iTAD **1**, the changes in chemical shift were quantified and mapped onto the KIX residues (Figure II-23b). This method has proven reliable for the identification of binding sites within the KIX domain.[12, 16, 91] The magnitude of the chemical shift perturbation was similar to that observed for endogenous ligands. The residues that experienced the greatest chemical shift change (at least 1 standard deviation over the average chemical shift change) are V608, I611, T614, A618, L620, K621, R623, R624, and E665. These shifts correspond to the C-terminus of α1, L12, G2, and the N-terminus of α2, overlaying with the MLL/Jun/Tat/Tax binding site (Figure II-23c).

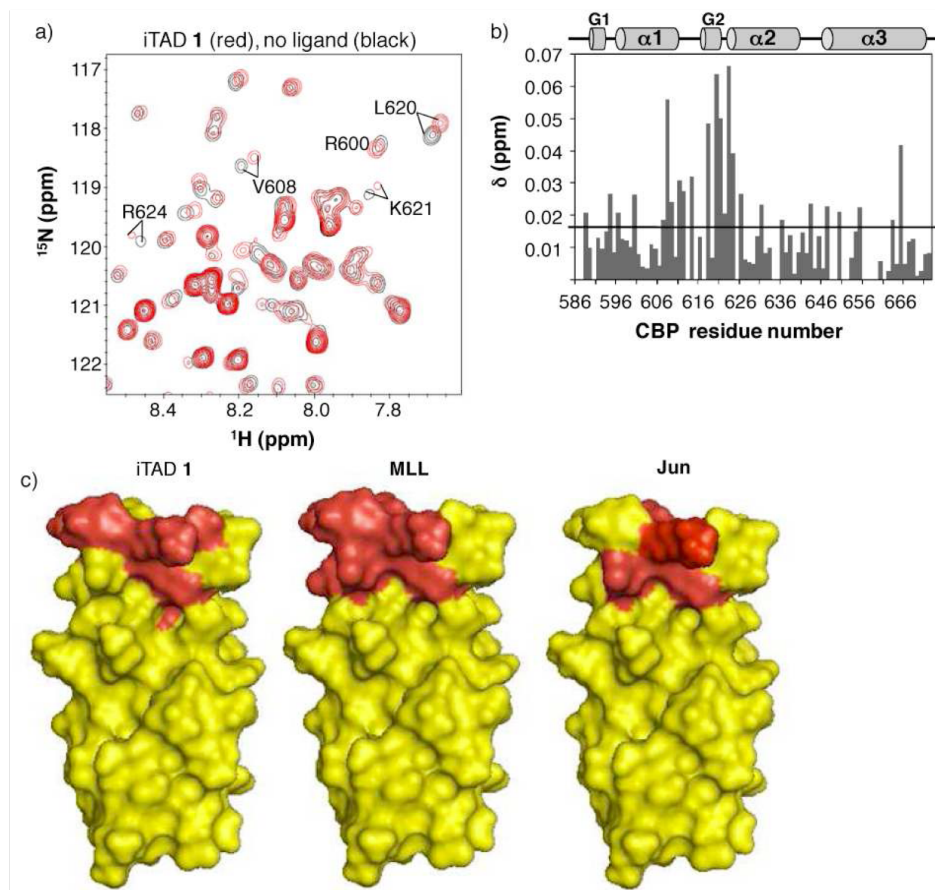**Figure II-23.** iTAD **1** binds the MLL/Jun/Tat/Tax site. a) ^{15}N, ^{1}H-HSQC spectrum of ^{15}N-His$_6$KIX in the presence of 5-fold excess iTAD **1** (red) is overlayed on the spectrum of free His$_6$KIX (black). b) Chemical shift perturbation map of KIX upon binding iTAD **1**. c) iTAD **1**, MLL and Jun share a binding site. The residues in red in the space filling diagrams experience the largest chemical shift upon binding the respective ligand. Figures adapted from 1kdx.

These experiments have shown that iTAD **1** functions at least in part through utilization of a subset of coactivator binding sites used by its endogenous counterparts. Furthermore, the binding characteristics of iTAD **1** mimic those of a subset natural TADs in both thermodynamic and kinetic parameters. This is the first example of a small molecule that binds selectively to one of the KIX binding sites utilized by endogenous TADs. This class of small molecules will serve as useful implements for the study of CBP molecular recognition events.

These data highlight two important aspects of iTAD·coactivator interactions. First, iTAD **1** exhibits a low affinity, multiprotein binding profile analogous to endogenous activators, and what was observed through *in vitro* crosslinking and binding studies. Second, these experiments revealed a property of certain iTADs was to bind the KIX domain of CBP. During the course of this work the Wright lab published a solution structure of a portion of the MLL TAD in complex with the KIX domain. This facilitates a more meticulous comparison of the binding mode of iTAD **1** and endogenous TADs. The Wright group used a short fragment of the MLL TAD (2842-2857) to solve the structure of the KIX·MLL co-complex, but only 11 residues (2847-2857) form an amphipathic helix upon binding the KIX domain (Figure II-17a). The side chains of five residues make important contacts to a shallow groove in the KIX domain: one polar (T2847) and four hydrophobic (I2849, F2852, V2853, and L2854), each contributing to a K_D of 3 μM.[13, 19]

In Figure II-24 the KIX domain is viewed from the top face, where three of the five critical residues can be observed: Leu, Phe, and Thr. Surprisingly, the side-chain functionality of these residues is nearly identical to the three functional groups of iTAD **1**, one polar (C3 hydroxyethyl), and two hydrophobic (N2 benzyl and C3 isobutyl), for binding the KIX domain (Figure II-24). Examination of this structure provides possible explanations for the inability of the N2-biphenyl and N2-benzophenone compounds to bind to the KIX domain, as the phenylalanine binding pocket cannot accommodate larger residues.[19] Further examination of TADs that bind this region of KIX show only one containing a large hydrophobic residue (W11 of Tat) that would be similar in size to biphenyl.[12, 16, 91] It has also been shown that a F2852Y mutation in the MLL TAD completely abrogates binding to the KIX domain and concomitantly decreases MLL-mediated transcription by 60%.[92] The low tolerance for large hydrophobic groups at this site further explains the inactivity of the N2-BP iTAD.
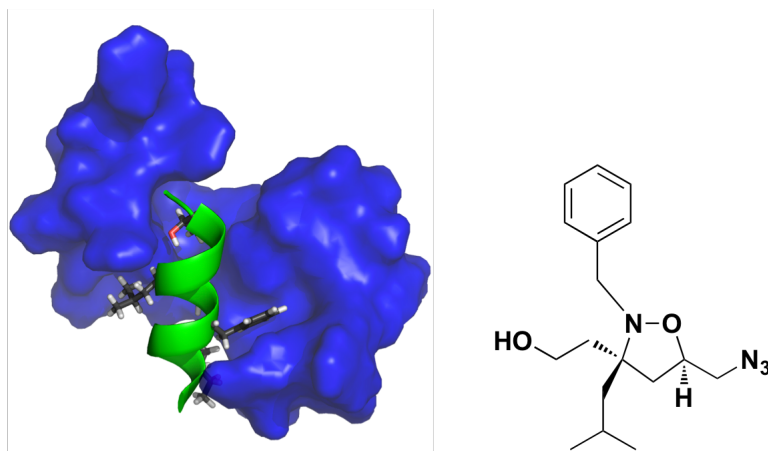
Figure II-24. MLL·KIX solution structure. The KIX domain is shown in blue and the MLL peptide in green. I2849, F2852, V2853, L2854, and T2857 of MLL form extensive hydrophobic contacts with the KIX domain upon binding. From this position, F2852 can be seen in the hydrophobic pocket, and L2854 and T2857 can be seen along the back side of the helix. Figure adapted from 2agh. Similar functionality is seen in iTAD **1**.

Although the N2 position has been intolerant of steric modification, the substituent at C5 (attachment of DBD in the context of transcriptional activation) has been shown in previous experiments not to contribute significantly to binding interactions, as an analog containing a dimethylacetal at C5 demonstrates nearly identical binding interactions via HSQC. In addition, the spatial orientation of the iTAD **1** functional groups suggests a similar binding mode to that of the MLL TAD. Although the core of the isoxazolidine is smaller than the α-helix of MLL, this binding site on the KIX domain has been shown to undergo significant structural rearrangement upon binding and may thus enable the recognition of a much smaller ligand.[19, 89] Consistent with this hypothesis, several residues in and around the binding pocket are line broadened in these experiments (for example, V608, K621, R624, and K621), suggesting conformational flexibility in that region. Further, Dr. Sara Buhrlage synthesized a positional isomer of iTAD **1** (SJB-III-2) and showed that it was also recognized by the KIX domain, indicating that that binding site can in fact adapt to accommodate iTADs with differing functional group orientation (Figure II-18). Also, alkene **15** does not bind the KIX domain by Fp or NMR, consistent with a

polar group mimicking serine or threonine functionality, and the necessity of possessing both hydrophobic and polar groups for this interaction.

To further probe the nature of this binding mode, three compounds containing groups at the *para* position of the benzyl group and a compound with an N2-isopentyl group were synthesized (Scheme II-3). The synthesis of **41** and **42** proceeded as previously described, using p-methylbenzylbromide and p-fluorobenzylbromide respectively. The synthesis of *p*-OH and N-alkyl compounds (carried out by Dr. Will Pomerantz) was slightly different, beginning with the corresponding aldehydes that were coupled using a reductive amination with NaBH(OAc)$_3$.
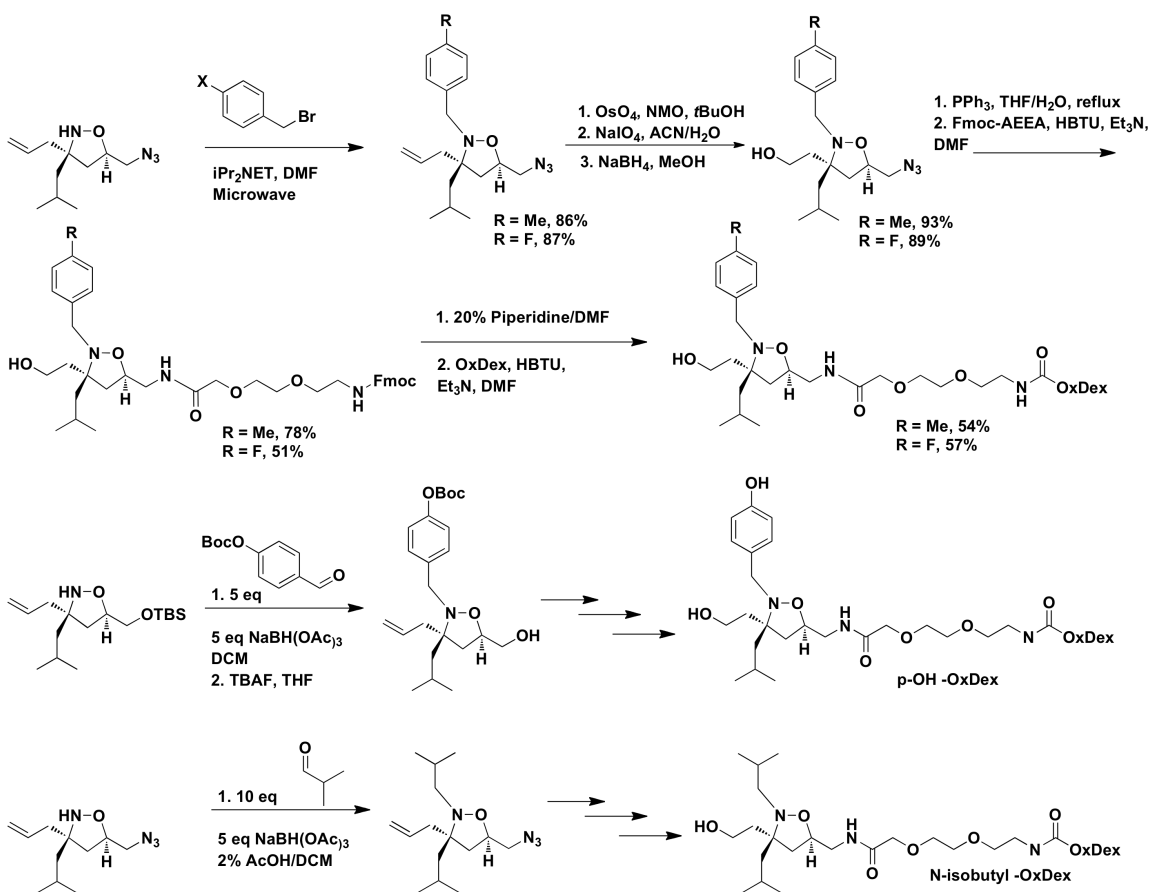
Scheme II-3. Synthesis of N2 analogues.

These compounds were tethered to OxDex and tested for activity as previously described (Figure II-5). Consistent with the postulated binding mode, the N-isobutyl derivative does not activate transcription, while the *p*-fluoro and *p*-Me activate only very slightly. Althought the *para* hydroxy compound binds by NMR, it does not activate transcription, suggesting a possible altered binding or stability profile or a difference in intracellular distribution.
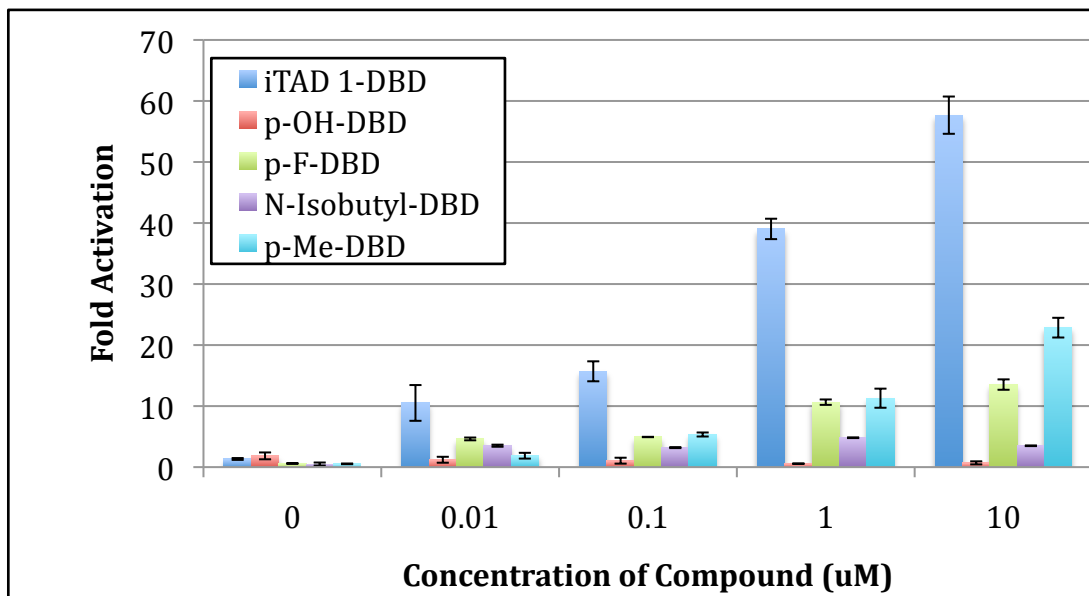

Figure II-25. Function of N2-substituted iTADs in cell culture. Transfections and activity calculations were performed as previously described.

H. Conclusions

Through NMR and crosslinking experiments, we have shown that a small molecule isoxazolidine TAD binds to the KIX domain of CBP. This is the first reported example of a small molecule that binds a specific site within the KIX domain. Furthermore, iTAD **1** shows remarkable similarity to the natural TAD MLL, both in terms of binding site and functional group content, and *in vitro* binding experiments show that iTAD **1** binds with similar thermodynamic parameters to this site as the endogenous TADs.

Knockdown, sequestration, and squelching experiments have confirmed that the iTAD·CBP interaction, and more specifically the iTAD·KIX interaction, is critical for iTAD function. This suggests that screening for molecules that bind the KIX domain may yield additional small molecule TADs; however, this strategy has thus far proven unsuccessful. The Montminy lab screened 762 compounds by NMR and found only two that bound the KIX domain, and neither bound to a site used by endogenous activators, suggesting the isoxazolidine architecture may be particularly useful in this endeavor.[93] Not surprisingly, modification of the functional group orientation of the isoxazolidine ring alters the KIX binding profile of the iTAD. This suggests that different combinations of functional groups may yield a degree of specificity for particular coactivator classes or binding sites.

I. Experimental

General.

Unless otherwise noted, starting materials were obtained from commercial suppliers and used without further purification. Toluene, CH_2Cl_2, THF, and Et_2O were dried by passage through activated alumina columns.[94] All reactions involving air- or moisture-sensitive compounds were performed under a dry N_2 atmosphere. Unless otherwise noted, organic extracts were dried over Na_2SO_4, filtered, and concentrated under reduced pressure on a rotary evaporator. $BF_3 \cdot OEt_2$ and Et_3N were distilled from CaH_2. DMF was distilled under reduced pressure from P_2O_5. NBS was recrystallized from EtOH/water. Purification by column chromatography was carried out with E. Merck Silica Gel 60 (230-400 mesh) according to the procedure of Still, Kahn and Mitra.[95] Reverse-phase HPLC purification was performed on a Varian ProStar 210 equipped with Rainin Dynamix UV-D II detector using a C18 (8 x 100 mm) Radial PakTM cartridge using a gradient mixture of 0-80% 0.1% TFA/water and acetonitrile, unless otherwise specified. UV-Vis spectra were recorded in ethanol. In order to determine the concentrations of all OxDex

conjugates, the characteristic UV-Vis absorption of dexamethasone at 242 nm with an extinction coefficient of 12,000 $M^{-1}cm^{-1}$ was used. Once concentration was determined, the sample was aliquoted, lyophilized, and stored at -80°C. ^1H and ^{13}C NMR spectra were recorded in $CDCl_3$ at 400 MHz and 125 MHz, respectively, unless otherwise specified. IR spectra were measured as thin films on NaCl plates using a Perkin Elmer Spectrum 1000 FT-IR. High-resolution mass spectra were measured on a VG-250-S Micromass, Inc., mass spectrometer at the University of Michigan Mass Spectrometry Laboratory. Full-length CBP plasmid was purchased from Addgene. CBP shRNA plasmid was prepared as previously reported.[86]

Pulldown Experiments.

Covalent attachment of iTAD **1**- The beads were swelled in MeOH for 10 minutes followed by 1:9 MeOH/blocking buffer (PBS, pH 7.4, 10% (v/v) glycerol, 1% (v/v) BSA, 0.1% (v/v) Nonidet NP-40) for 10 minutes. The beads were then incubated with HeLa nuclear extracts (15 µL, 13.5 mg/mL, Promega) in binding buffer (PBS, pH 7.4, 5% (v/v) glycerol) at 4°C for 10 hours. Biotinylated iTAD **1**-Streptavidin beads were incubated with excess biotinylated iTAD **1** in blocking buffer (same as above) for 1 hour at 4°C. The beads were then incubated with HeLa nuclear extracts as described above. After incubation, each set of beads was washed with wash buffer (PBS, pH 7.4, 10% (v/v) glycerol, 0.2% (v/v) Nonidet NP-40) three times, with each elution being kept for SDS-PAGE analysis. The eluted proteins were mixed with 4x Nu-PAGE loading dye (Invitrogen), and heated at 95°C for 10 minutes. Samples were subjected to SDS-PAGE analysis using a 4-12% Bis-Tris gel in MES buffer and run for 60 min (400V, 200 mA). Gels were stained using the SilverXpress staining kit (Invitrogen).

In Vitro Crosslinking.

HeLa nuclear extracts (25 uL, 13.5 mg/mL, Promega) were incubated with 30 μM compound **21** with gentle mixing in Buffer A (10mM PBS, pH 7.4, 10% (v/v) glycerol) plus 1% (v/v) DMSO at 4 °C for 12 hrs. Samples were transferred to a 96-well plate and irradiated with a handheld UV lamp (365 nm) at 4°C for 30 minutes. The irradiated solution was transferred to an Eppendorf tube containing Neutravidin beads (50μL, Pierce) in Buffer A (plus 1% (v/v) BSA, 0.1% (v/v) Nonidet NP-40) and incubated 1 hour at 4°C. The beads were then washed 3x with Buffer A (plus 0.1% (v/v) Nonidet NP-40), resuspended in elution buffer (Buffer A plus 25% (v/v) 4x Nu-PAGE loading dye (Invitrogen)), and heated at 95°C for 10 minutes.

Western Blot.

General procedure: Samples were mixed with loading dye (25% final vol.) and BME (1% final vol.) and heated at 95°C for 10 minutes. 20 μL of sample was loaded per well on a 4-12% Bis-Tris gel in MES buffer and run for 60 min (400V, 200 mA). Proteins were transferred to a PVDF membrane for 75 min (45V, 200 mA).

(For photocrosslinking) Crosslinked samples were separated by SDS-PAGE and transferred to a PVDF membrane (Invitrogen). Membranes were blocked (10mM PBS, pH 7.4, 1% (v/v) Tween-20, 10% (v/v) non-fat milk) and analyzed via Western blot. Mouse monoclonal anti-CBP antibody (1:1000, Santa Cruz Biotechnology) was added followed by horseradish peroxidase-labeled goat anti-mouse antibody (1:1000, Santa Cruz Biotechnology). Bands were visualized using the ECL plus Western Blot Detection System (GE Healthcare).

Cell-based Activity Assay.

HeLa cells were purchased from the American Tissue Culture Center (ATCC) and plated onto treated polystyrene petri dishes (Corning) with 10 mL of D-MEM (+ 4.5 g/L d-glucose, + l-glutamine, - sodium pyruvate, + 10% FBS, + NEAA) (invitrogen). The cells were grown at 37°C 5% and 5% CO_2 to 80-90% confluence. Upon reaching the desired confluence, the D-MEM was removed and 4 mL 0.25% trypsin was added. The cells were incubated with the trypsin solution for 5 minutes at 37°C and 5% CO_2. Following the inubation, 10 mL of D-MEM were added and the resultant solution was pipetted up and down several times to ensure removal of all cells from the dish surface. The solution was centrifuged in a 15-mL Falcon tube at 1000 rpm for 2 minutes in a Fisher Centrific centrifuge. The supernatant was removed and the cell pellet was resuspended in 10 mL of D-MEM. The concentration of cells was calculated using a Hausser Scientific improved Neubauer phase counting chamber hemocytometer. Based on the determined concentration the cells were diluted to 100,000/mL in D-MEM. 100 μL of the cell solution was then added to each well of a Microtest flat-bottom, low-evaporation-lid 96-well plates (Becton-Dickinson) and the plated cells were incubated overnight at 37°C and 5% CO_2. The media was removed from the plated cells and they were washed once with Opti-MEM (+ HEPES, + 2.4 g/L sodium bicarbonate, + l-glutamine) (Invitrogen) and then transfected.

The transfection procedure consisted of first mixing appropriate plasmids and Lipofectamine 2000® together in Opti-MEM® media for each well being transfected. After a 20 minute incubation at room temperature 100 μL of the solution was placed in the appropriate wells and the cells were incubated for 5 hours at 37°C and 5% CO_2. At the end of the 5-hour incubation, the transfection solution was removed and 100 μL fresh D-MEM was added to each well. To the media was added 1 μL of either DMSO or the appropriate concentration of a

molecule being tested dissolved in DMSO (the final concentration of DMSO in all the wells was 1%). The cells were then incubated for 24 hours at 37°C and 5% CO_2.

Following the 24-hour incubation, the media was removed from each well and the cells were washed once with PBS buffer. 20 µL of passive lysis buffer (Promega) was added to each well and the cells were incubated for 20 minutes at room temperature on an orbital shaker. Subsequently, the total volume of each well was added to a cuvette along with 25 µL of Luciferase Assay Reagent II (Promega) and the luminescence was recorded. Then 25 µL Stop & Glo reagent was added and the Renilla luminescence was recorded again on a Berthold FB12 single cuvette luminometer.[43]

General procedure for nitrile oxide cycloadditions.

Oximes were prepared in accordance with standard procedures.[40]
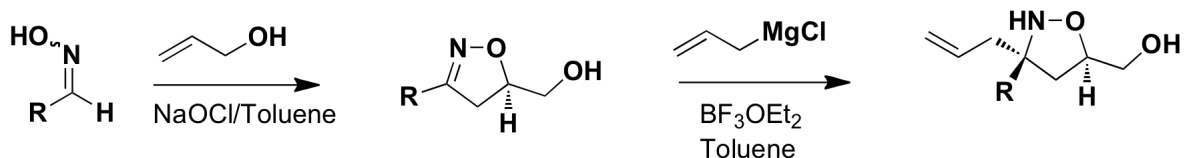
To a solution of oxime (6.07 g, 60 mmol, 1.0 eq) and allyl alcohol (13.67 mL, 200 mmol, 3.33 eq) in toluene (600 mL) cooled in an ice-water bath was added sodium hypochlorite (220 mL, 150 mmol) dropwise over 30-40 minutes from an addition funnel. The reaction was allowed to come up to room temperature and stirred for 12-18 h. Sat. sq. NH_4Cl (100 mL) was added to the reaction mixture followed by an aqueous workup. The isolated material was purified by column chromatography and carried through to the Grignard addition.

**General procedure for Grignard addition to isoxazoline.**

To a solution of isoxazoline in toluene cooled in a dry ice/acetone bath was added $BF_3•Et_2O$ dropwise over 20 min and the reaction was stirred for 1 h with

65

continued cooling. Allylmagnesium chloride was added dropwise and the reaction was stirred for 8 h with continued cooling. The reaction was then slowly warmed to rt and quenched with addition of sat. aq. NH₄Cl followed by aqueous workup.[41, 42] The aqueous layer was extracted with EtOAc (5 x 10 mL) and the combined organic layers were washed with water (20 mL) and brine (20 mL). Products were purified by flash chromatography to provide isoxazolidines **3-5**, **15**, and **18**, which have been previously reported.[1, 4, 45, 96] Spectroscopic data on the purified products was consistent with reported values for those compounds.

General procedure for solid-phase synthesis.

Wang resin was swelled in CH_2Cl_2 for 5 min. Acids were dissolved in DMF or CH_2Cl_2 and 1-methylimidazole and MSNT were added and stirred until dissolved. The solvent was removed from the beads by suction and the reaction mixture was added. The mixture was agitated at rt for either 4 or 12 h. The beads were washed with DMF (5 x 10 mL) and CH_2Cl_2 (5 x 10 mL). Fmoc deprotections were carried out using 20% piperidine in DMF for 20 min at rt. Further amide couplings used HOBt and HBTU in DMF, with repeated washing, and deprotection where appropriate. Microcleavages were carried out at each step to assess product purity. Cleavage of final product from resin used 95:2.5:2.5 TFA/H₂O/TIPS for 20 min at rt.

**Small Molecule Synthesis and Characterization.**
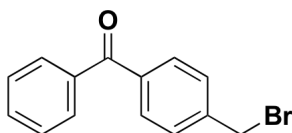
(4-bromomethylbenzophenone) (6): To a stirring solution of 4-methylbenzophenone (200 mg, 1.01 mmol, 1.0 eq) in freshly distilled CCl₄ (10 mL) were added AIBN (16.4 mg, 0.1 mmol, 0.10 eq) and N-bromosuccinimide (216 mg, 1.21 mmol, 1.2 eq) and heated to reflux for 8 h. Solution was cooled to rt and Et₂O

(10 mL) was added. Solution is filtered to remove solids and washed with water (20 mL) and placed at 4°C for 2 h. Solution was filtered to removed crystals which were recrystallized from hot EtOH to yield 239 mg of **6** in 86% yield as shiny white flakes. IR: 3084, 3060, 1666, 1601, 1449, 1277, 808, 761, 622 cm^{-1}. ^{1}H NMR: δ 4.49 (s, 2H), 7.32-7.54 (m, 4H), 7.65-7.80 (m, 5H); ^{13}C NMR: 33.6, 128.2, 129.0, 129.9, 132.1, 134.9, 136.2, 138.0, 143.2, 196.3; HRMS (ESI) calcd for [C$_{14}$H$_{11}$BrO + H]$^+$: 275.0072, found 275.0080.
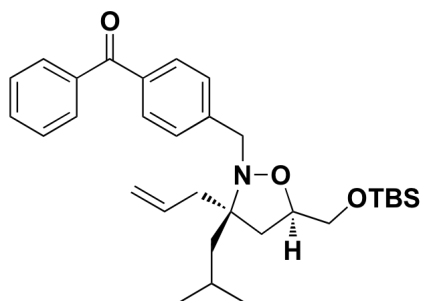
((4-(((3*S*,5*R*)-3-allyl-5-(((*tert*-butyldimethylsilyl)oxy)methyl)-3-isobutylisoxazolidin-2-yl)methyl)phenyl)(phenyl)methanone) (5): To a solution of **4** (100 mg, 0.32 mmol, 1.0 eq) in DMF (3.2 mL) was added 4-bromomethylbenzophenone (106 mg, 0.38 mmol, 1.2 eq) and iPr$_2$NEt (66 μL, 0.38 mmol, 1.2 eq) and the solution was heated in a microwave at 20% power for 15 s and allowed to cool to rt. This was repeated 20 times until SM was consumed by TLC. Water (15 mL) and ether (15 mL) were added followed by aqueous workup. The combined organic layers were washed with brine (20 mL) and purified by flash chromatography (1:5 to 1:1 EtOAc/hexanes) to give 158 mg of **5** in 97% yield as a light yellow oil. IR: 2952, 2855, 1664, 1454, 1360, 1253, 1120, 832 cm^{-1}; ^{1}H NMR: δ 0.05 (s, 6H), 0.94 (d, 6H), 0.98 (s, 9H), 1.32-1.39 (m, 2H), 1.58-1.63 (dd, 2H), 2.39-2.48 (m, 2H), 3.04-3.12 (dd, 2H), 3.72-3.78 (m, 2H), 4.10-4.20 (m, 2H), 4.55-4.65 (m, 2H), 5.20-5.40 (m, 1H), 7.41-7.79 (m, 9H); HRMS (ESI) calc for [C$_{31}$H$_{45}$NO$_3$Si + Na]$^+$: 530.3066, found: 530.3039.
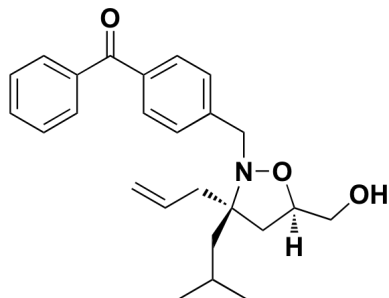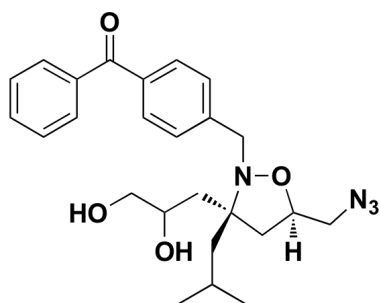
((4-(((3*S*,5*R*)-3-allyl-5-(hydroxymethyl)-3-isobutylisoxazolidin-2-yl)methyl)phenyl)(phenyl)methanone) (7): To a solution of **5** (158 mg, 0.31 mmol, 1.0 eq) in THF (16 mL) cooled in an ice-water bath was added TBAF (1 mL of a 1M solution in THF, 3.0 eq) dropwise. The reaction was allowed to warm to rt and stir for 4 h. The reaction was quenched with NH_4Cl (5 mL), followed by H_2O (10 mL). The aqueous layer was extracted with EtOAc (3 x 10 mL) and the combined organic extracts were purified by flash chromatography (95:5 hexanes/EtOAc) to give 116 mg of **7** as a clear oil in 95% yield. IR: 3394, 2952, 2863, 1666, 1450, 1028, 733 cm^{-1}; ^{1}H NMR: δ 0.94 (d, 6H), 1.32-1.39 (m, 2H), 1.58-1.63 (dd, 2H), 2.39-2.48 (m, 2H), 3.04-3.12 (dd, 2H), 3.72-3.78 (m, 2H), 4.10-4.20 (m, 2H), 4.55-4.65 (m, 2H), 5.20-5.40 (m, 1H), 7.41-7.79 (m, 9H); ^{13}C NMR δ 24.12, 24.45, 25.21, 38.58, 38.70, 43.88, 53.38, 65.56, 66.71, 68.48, 75.40, 117.78, 128.2, 129.0, 129.9, 132.1, 134.9, 136.2, 138.0, 143.2, 196.3; HRMS (ESI) calcd for $[C_{25}H_{31}NO_3 + Na]^+$: 416.2202, found 416.2212.
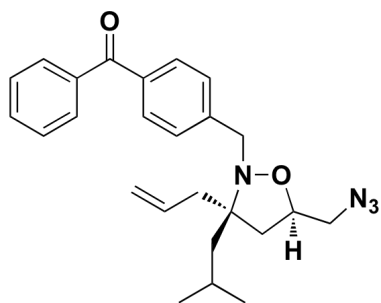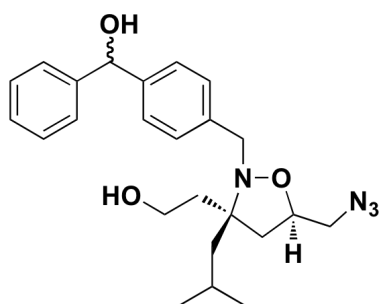

((4-(((3*S*,5*R*)-3-allyl-5-(azidomethyl)-3-isobutylisoxazolidin-2-yl)methyl)phenyl)(phenyl)methanone) (8): To a stirring solution of **7** (750 mg,

1.91 mmol, 1.0 eq) in CH_2Cl_2 (20 mL) cooled in an ice-water bath was added Et_3N (600 μL, 4.19 mmol, 2.2 eq), and DMAP (23 mg, 0.19 mmol, 0.1 eq). Methanesulfonylchloride (300 μL, 3.81 mmol, 2.0 eq) was added and the reaction was stirred with continued cooling for 2 h. Following aqueous workup, the crude product was dissolved in DMSO (10 mL) and NaN_3 (1.24 g, 19.1 mmol, 10.0 eq) was added and the reaction was heated at 100°C for 2 h. Water (20 mL) and Et_2O (30 mL) were added and the aqueous layer was extracted with Et_2O (3 x 10 mL). Purification by flash chromatography (98:2 heaxanes/EtOAc) gave 680 mg of **8** in 85% yield. IR: 2955, 2869, 2099, 1666, 1454, 1278, 916, 732 cm^{-1}; ^{1}H NMR: δ 0.94 (d, 6H), 1.32-1.39 (m, 2H), 1.58-1.63 (dd, 2H), 2.39-2.48 (m, 2H), 3.0-3.10 (dd, 2H), 3.14-3.18 (m, 2H), 4.10-4.20 (m, 2H), 4.55-4.65 (m, 2H), 5.2-5.4 (m, 1H), 7.41-7.79 (m, 9H); ^{13}C NMR δ 24.11, 24.62, 25.22, 38.68, 40.21, 43.56, 53.28, 54.39, 68.29, 74.49, 117.78, 128.2, 129.0, 129.9, 132.1, 134.9, 136.2, 138.0, 143.2, 196.3; HRMS (ESI) calcd for $[C_{25}H_{30}N_4O_2 + Na]^+$: 441.2266, found: 441.2254.
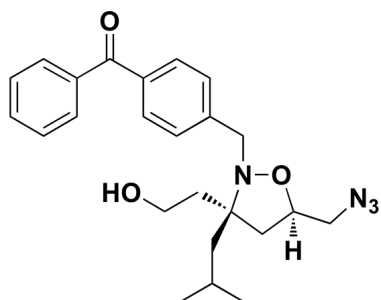

((4-(((3S,5R)-5-(azidomethyl)-3-(2,3-dihydroxypropyl)-3-isobutylisoxazolidin-2-yl)methyl)phenyl)(phenyl)methanone) (9): To a stirring solution of **8** (1.43 g, 3.42 mmol, 1.0 eq) in THF (7 mL) was added *t*BuOH (26 mL) and H_2O (1.7 mL). The mixture was cooled in an ice-water bath and NMO (481 mg, 4.1 mmol, 1.2 eq) was added, stirring until dissolved. OsO_4 (4.2 mL of a 2.5% solution in 2-propanol, 0.1eq) was added dropwise and the reaction was stirred for 20 h. Sodium sulfite (1.83 g) was added and the solution was stirred for 1 h. Water (30 mL) and EtOAc (50 mL) were added and the aqueous layer was

extracted with EtOAc (3 x 20 mL). Combined organic extracts were washed with brine (30 mL) and purified by flash chromatography (1:1-1:2 hexanes/EtOAc). 1.42 g of **9** was isolated as a clear yellow oil in 92% yield. IR: 3374,2957, 2869, 2100, 1666, 1454, 1281,1069, 918, 735, 697 cm^{-1}; ^{1}H NMR δ 0.89-1.0 (m, 6H), 1.30-1.50 (m, 1H), 1.55-1.76 (m, 3H), 1.85-2.15 (m, 2H), 2.26-2.60 (m, 1H), 3.19-3.3 (m, 1H), 3.35-3.64 (m, 3H), 3.70-3.91 (m, 4H), 4.10-4.18 (m, 1H), (m, 9H) 7.41-7.79; HRMS (ESI) calcd for [$C_{25}H_{32}N_4O_4$ + Na]$^+$: 475.2321, found: 475.2318.

(2-((3S,5R)-5-(azidomethyl)-2-(4-(hydroxy(phenyl)methyl)benzyl)-3-isobutylisoxazolidin-3-yl)ethanol) (10): To a stirring solution of **9** (710 mg, 1.57 mmol, 1.0 eq) in acetonitrile (16 mL) and H_2O (16 mL) was added NaIO$_4$ (403 mg, 1.88 g, 1.2 eq) and the reaction was stirred at rt for 3 h. H_2O (30 mL) and ether (30 mL) were added and the aqueous layer was extracted with Et$_2$O (3 x 20 mL). The crude aldehyde was dissolved in MeOH (16 mL) and NaBH$_4$ (149 mg, 3.93 mmol, 2.5 eq) was added in 3 portions. The reaction was stirred at rt for 30 min then quenched with water (5 mL) and partitioned between H_2O (40 mL) and Et$_2$O (40 mL). The aqueous layer was extracted with Et$_2$O (3 x 20 mL). Purification by flash chromatography gave 566 mg of **10** in 86% yield as a clear colorless oil. IR: 3373,2957, 2869, 2109, 1454, 1281,1069, 918, 735, 697; ^{1}H NMR: δ 0.94 (d, 3H, *J* = 6.6), 0.94 (d, 3H, *J* = 6.6), 1.31-1.35 (m, 1H), 1.59 (dd, 1H, *J* = 14.4, 4.9), 1.81-1.88 (m, 1H), 1.90-1.96 (m, 1H), 2.20 (dd, 1H, *J* = 12.0, 8.8), 2.25-2.45 (m, 2H), 3.46-3.56 (m, 1H), 3.66 (dd, 1H, *J* = 10.3, 5.9), 3.77-3.85 (m, 2H), 4.00-4.10 (m, 1H), 4.24-4.30 (m, 2H), 4.60-4.67 (m, 2H), 4.78 (s, 1H), 7.21-7.58 (m, 9H); ^{13}C NMR: δ 24.31, 24.90,

25.24, 35.61, 40.82, 43.01, 53.69, 54.49, 59.67, 70.43, 75.61, 117.78, 128.2, 129.0, 129.9, 132.1, 134.9, 136.2, 138.0, 143.2; HRMS (ESI) calcd for $[C_{24}H_{32}N_4O_3 + Na]^+$: 477.2478, found: 477.2471.
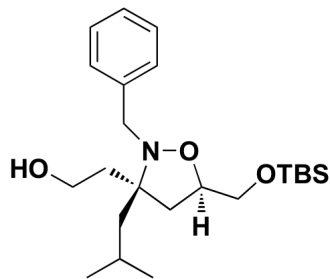

((4-(((3S,5R)-5-(azidomethyl)-3-(2-hydroxyethyl)-3-isobutylisoxazolidin-2-yl)methyl)phenyl)(phenyl)methanone) (11): To stirring solution of **10** (50 mg, 98 µmol, 1.0 eq) in CH_2Cl_2 (2 mL) cooled in an ice-water bath was added powdered activated 4 angstrom molecular sieves (50 mg) followed by NMO (23 mg, 196 µmol, 1.0 eq) and TPAP (3.6 mg, 10 µmol, 0.1 eq). The reaction was taken directly to flash chromatography (1:1 hexanes/EtOAc) giving 29 mg of **11** in 58% yield. IR: 3358, 2955, 2870, 2100, 1666, 1455, 1280, 1045, 733, 697 cm^{-1}; ^{1}H NMR: δ 0.99 (s, 3H), 1.00 (s, 3H), 1.50-1.55 (m, 2H), 1.58-1.64 (m, 3H), 1.78-2.06 (dd, 1H, J = 8.1, 12.7), 2.36 (dd, 1H, J = 8.0, 12.7), 3.41 (d, 2H, J = 4.7), 3.78-3.93 (m, 3H), 4.05 (d, 1H, J = 13.9), 4.19-4.28 (m, 1H), 7.44-7.52 (m, 4H), 7.58-7.61 (m, 1H), 7.78-7.85 (m, 4H); ^{13}C NMR: δ 24.31, 24.90, 25.24, 35.61, 40.82, 43.01, 53.69, 54.49, 59.67, 70.43, 117.78, 128.2, 129.0, 129.9, 132.1, 134.9, 136.2, 138.0, 143.2, 196.3; HRMS (ESI) calcd for $[C_{24}H_{30}N_4O_3 + Na]^+$: 445.2216, found: 445.2204.
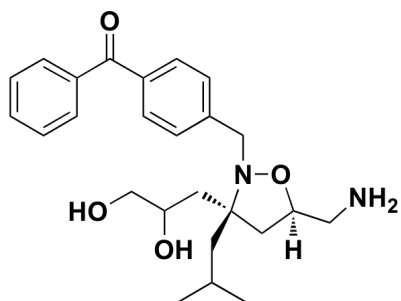
((4-(((3S,5R)-5-(aminomethyl)-3-(2,3-dihydroxypropyl)-3-isobutylisoxazolidin-2-yl)methyl)phenyl)(phenyl)methanone) (12): To a stirring solution of diol **9** (87 mg, 0.19 mmol, 1.0 eq) in 1:1 THF/H$_2$O (3 mL) and PPh$_3$ (152 mg, 0.58 mmol, 3.0 eq) was added. The reaction was refluxed at 80°C for 4 h. An acid, base workup yielded 66 mg of crude amine **12** (81%) that was carried on without further purification. HRMS (ESI) calcd for [C$_{25}$H$_{34}$N$_2$O$_4$ + Na]$^+$: 449.2416, found 449.2428.
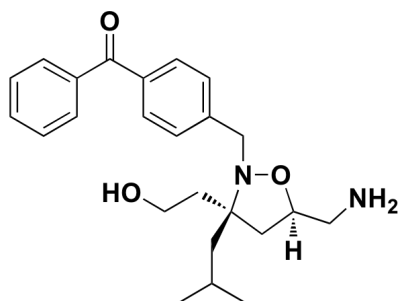
((4-(((3S,5R)-5-(aminomethyl)-3-(2-hydroxyethyl)-3-isobutylisoxazolidin-2-yl)methyl)phenyl)(phenyl)methanone) (13): Azide **11** was reduced as described previously using **9** (126 mg, 0.3 mmol, 1.0 eq), PPh$_3$ (235 mg, 0.84 mmol, 3.0 eq), THF/H$_2$O (4 mL, 1:1). **13** was obtained in 87% yield as 104 mg of a yellow oil. Crude amine **13** was carried on without further purification. HRMS (ESI) calcd for [C$_{24}$H$_{32}$N$_2$O$_3$ + H]$^+$: 397.2491, found: 397.2482.
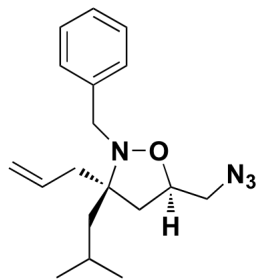
(2-((3S,5R)-5-(azidomethyl)-2-benzyl-3-isobutylisoxazolidin-3-yl)ethanol)

(16): Prepared from **4** as previously described. Purification by flash chromatography (9:1 hexanes/EtOAc) provided 278 mg of **16** in 94% yield of as a colorlesss oil. Spectral data matched published values.[4]
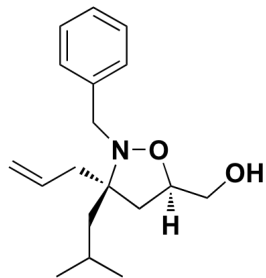
(((3S,5R)-3-allyl-2-benzyl-3-isobutylisoxazolidin-5-yl)methanol) (17): To a stirring solution of silyl ether **16** (2.0 g, 4.95 mmol, 1.0 eq) in THF (14 mL) cooled in an ice-water bath was added TBAF (13 mL, 12.4 mmol, 3.0 eq) drop wise and the reaction was allowed to ward to rt. Sat. aq. NH_4Cl (5 mL) was added after 2 h followed by aq. workup. Purification by flash chromatography (8:2 hexanes/EtOAc) provided 1.41 grams of **17** in 98% yield as a clear, colorless oil. IR: 3394, 2952, 2863, 1450, 1028, 733 cm^{-1}; ^{1}H NMR: δ 0.97 (d, 3H, J = 4.8), 0.98 (d, 3H, J = 3.8), 1.39 (dd, 1H, J = 14.6, 6.6), 1.62 (dd, 1H, J = 14.7, 4.8), 1.86-1.92 (m, 1H), 2.00-2.08 (m, 1H), 2.18-2.25 (br s, 1H), 2.29 (dd, 1H, J = 12.5, 8.8), 2.45 (dd, 1H, J = 13.9, 7.3), 3.52-3.61 (m, 2H), 3.82 (d, 1H, J = 14.6), 3.9 (d, 1H, J = 14.3), 4.02-4.10 (m, 1H), 5.08-5.12 (m, 2H), 5.88-5.99 (m, 1H), 7.20-7.40 (m, 5H); ^{13}C NMR: δ 24.10, 24.40, 25.20, 38.59, 38.71, 43.87, 53.38, 65.55, 68.47, 75.41, 117.78, 126.95, 127.90, 128.42, 135.18, 138.18, 138.92; HRMS (ESI) calcd for $[C_{18}H_{27}NO_2 + Na]^+$: 316.1889, found 316.1899.
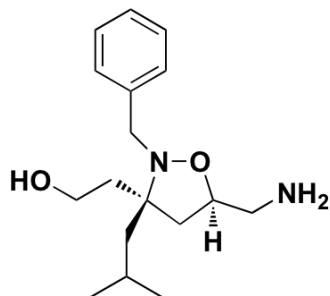
((3*S*,5*R*)-3-allyl-5-(azidomethyl)-2-benzyl-3-isobutylisoxazolidine) (15): To a stirring solution of alcohol **17** (1.25 g, 6.25 mmol, 1.0 eq) in CH_2Cl_2 (65 mL) cooled in an ice-water bath was added Et_3N (.92 mL, 6.6 mmol, 1.05 eq). Methane sulfonylchloride (0.51 mL, 6.6 mmol, 1.05 eq) was added dropwise and the reaction was allowed to warm to rt. After 1 h H_2O (30 mL) and Et_2O (30 mL) were added. The aqueous layer was extracted with Et_2O (3 x 20 mL), and the combined organic extracts were washed with brine. The crude material was then dissolved in DMSO (50 mL) and NaN_3 (3.11 g, 47.9 mmol, 10 eq) was added. The flask was fitted with a reflux condenser and heated to 100°C for 12 h. The reaction was cooled to rt and diluted with H_2O (200 mL) and extracted with Et_2O (3 x 50 mL), and the combined organic extracts were washed with brine. Purification by flask chromatography (95:5 hexanes/EtOAc) provided 1.82 grams of **15** in 93% yield as a clear colorless oil. IR: 2955, 2869, 2099, 1454, 1278, 916, 732 cm^{-1}; ^{1}H NMR: δ 0.96 (d, 3H, *J* = 6.6), 0.98 (d, 3H, *J* = 6.6), 1.38 (dd, 1H, *J* = 6.6, 14.7), 1.58 (dd, 1H, *J* = 14.5, 5.5), 1.80-1.90 (m, 2H), 2.26 (dd, 1H, *J* = 7.4, 13.9), 2.31 (dd, 1H, *J* = 8.6, 12.7), 3.87 (m, 1H), 3.90 (m, 1H), 4.10-4.15 (m, 1H), 5.05-5.15 (m, 2H), 5.85-5.97 (m, 1H), 7.18-7.42 (m, 5H); ^{13}C NMR: δ 24.10, 24.60, 25.21, 38.65, 40.18, 43.54, 53.26, 54.37, 68.28, 74.47, 117.8, 126.67 128.0, 128.1, 134.9, 138.6; HRMS (ESI), calcd for [C18H27N4O + H]$^{+}$: 315.2185, found 315.2167.
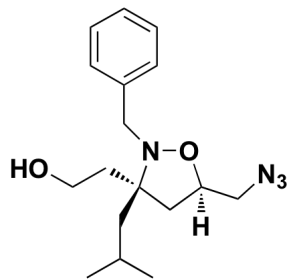
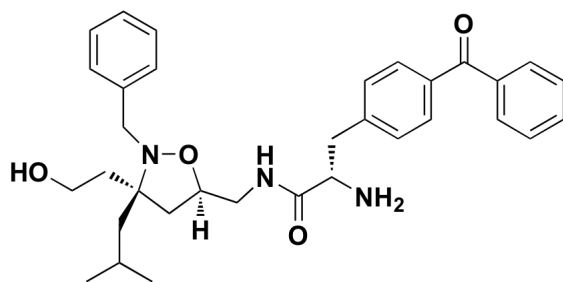**(2-((3*S*,5*R*)-5-(azidomethyl)-2-benzyl-3-isobutylisoxazolidin-3-yl)ethanol)**
(18): Oxidative cleavage of the allyl group was carried out according to published procedures.[96] Purification by flash chromatography yielded 378 mg of **18** in 92% yield as a clear, colorless oil. IR: 3358, 2955, 2870, 2100, 1455, 1280, 1045, 733, 697 cm^{-1}; ^{1}H NMR: δ 0.99 (s, 3H), 1.00 (s, 3H), 1.50-1.60 (m, 1H), 1.64-1.95 (m, 5H), 2.06 (dd, 1H, *J* = 8.1, 12.7), 2.36 (dd, 1H, *J* = 8.0, 12.7), 3.41 (d, 2H, *J* = 4.7), 3.78-3.93 (m, 3H), 3.99 (d, 1H, *J* = 13.9), 4.19-4.28 (m, 1H), 7.22-7.37 (m, 5H); ^{13}C NMR: δ 24.31, 24.90, 25.24, 35.61, 40.82, 43.01, 53.69, 54.49, 59.67, 70.43, 127.2, 128.4, 128.6, 137.6; HRMS (ESI) calcd for $[C_{17}H_{27}N_4O_2 + Na]^+$: 341.1953, found 341. 1965.
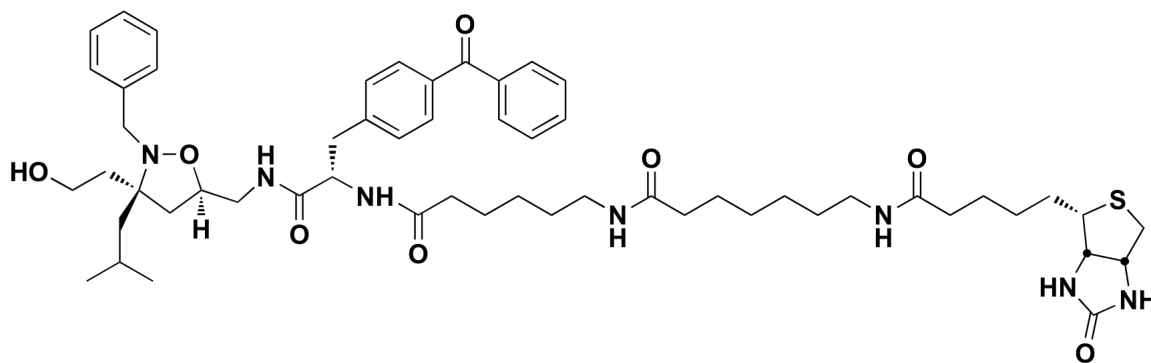

(2-((3*S*,5*R*)-5-(aminomethyl)-2-benzyl-3-isobutylisoxazolidin-3-yl)ethanol)
(19): Reduction of **18** (17 mg) was accomplished under conditions identical to those used for azide **9.** Purification of the crude mixture by flash chromatography (90:10 CH$_2$Cl$_2$/MeOH) provided 15 mg of amine **19** in 94% yield as clear oil. IR: 3454, 2953, 2867, 1454, 1365, 1045, 733, 697 cm-1; ^{1}H NMR (CD$_3$OD): δ 0.96, (d, 3H, *J* = 6.6), 0.99 (d, 3H, *J* = 6.6), 1.35-1.42 (dd, 1H, *J* = 14.1, 6.5), 1.59-1.66 (dd, 1H, *J* = 14.1, 5.1), 1.76-1.94 (m, 5H), 2.39-2.46 (dd, 1H, *J* = 12.7, 8.1), 2.71-2.87 (m, 2H), 3.70-3.79 (m, 2H), 3.86 (s, 2H), 4.02-4.11 (m, 1H), 7.17-7.37 (m, 5H); δ ^{13}C NMR: δ

24.85, 25.57, 25.85, 37.58, 42.86, 45.09, 46.70, 55.22, 60.08, 70.45, 127.9, 129.3, 129.5, 140.3; HRMS (ESI) calcd for $[C_{17}H_{28}N_2O_2 + H]^+$: 293.2229, found: 293.2214.

(2-amino-3-(4-benzoylphenyl)-*N*-(((3*S*)-2-benzyl-3-(2-hydroxyethyl)-3-isobutylisoxazolidin-5-yl)methyl)propanamide) (20): To a solution of amine **19** (100 mg, 0.34 mmol, 1.0 eq) in DMF (3.4 mL) was added HOBt (69 mg, 0.51 mmol, 1.5 eq) and HBTU (194 mg, 0.51 mmol, 1.5 eq) and the mixture was stirred at room temperature for one hour. Fmoc-BpA-OH (250 mg, 0.51 mmol, 1.5 eq) and triethylamine (48 μL, 0.34 mmol, 1.0 eq) were added and the reaction was stirred at room temperature for 12 hours. Piperidine (900 μL, .012 mmol, 0.35 eq) was added and the reaction was stirred for 10 minutes. The solvent was removed under high vacuum and the product was purified by reverse-phased HPLC yielding 99 mg of **20** as a white powder in 53% yield. IR: 2560, 1686, 1677, 1279, 1200, 1137 cm^{-1}; ^{1}H NMR (CD$_3$OD): δ 0.99 (d, 3H, J = 6.6), 1.01 (d, 3H, J = 6.6), 1.54-1.64 (m, 1H), 1.71-1.82 (m, 2H), 1.85-2.02 (m, 2H), 2.39- 2.46 (m, 2H), 3.00-3.12 (m, 2H), 3.13-3.24 (m, 2H), 3.46-3.58 (m, 2H), 3.74-3.84 (m, 2H), 3.98-4.10 (m, 1H), 4.13-4.23 (m, 1H), 7.18-7.42 (m, 6H), 7.46-7.54 (m, 2H), 7.58-7.64 (m, 2H), 7.66-7.76 (m, 4H); HRMS (ESI) calcd for $[C_{33}H_{41}N_3O_4 + H]^+$: 544.3175, found: 544.3190.

(N-((S)-3-(4-benzoylphenyl)-1-(((3S,5R)-2-benzyl-3-(2-hydroxyethyl)-3-isobutylisoxazolidin-5-yl)methylamino)-1-oxopropan-2-yl)-6-(6-(5-biotinyl)hexanamido)hexanamide) (21): To a solution of **20** (5 mg, 9.2 μmol, 1.0 eq) in DMF (920 μL) was added Biotin-XX-SE (6.2 mg, 11 μmol, 1.2 eq) and triethylamine (1.3 μL, 9.2 μmol, 1.0 eq). The reaction was stirred at rt for 12 hrs then the solvent was removed under vacuum. The product was purified by reverse phase HPLC yielding 6.8 mg of **21** as a white powder in 74% yield. HRMS (ESI) for [$C_{55}H_{77}N_7O_8S$ + Na]$^+$: 1018.5452, found: 1018.5474.
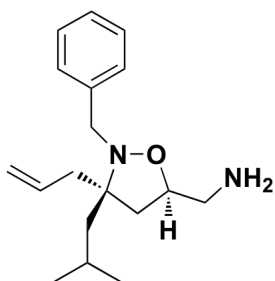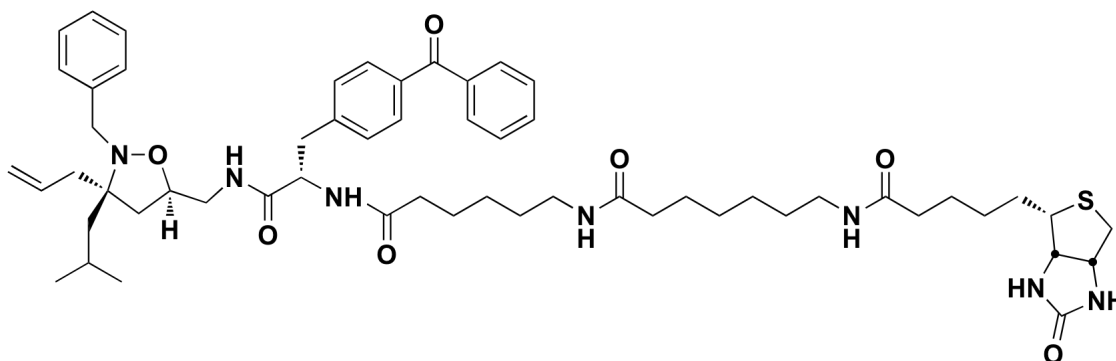

(((3S,5R)-3-allyl-2-benzyl-3-isobutylisoxazolidin-5-yl)methanamine) (22): To a solution of azide **15** (30 mg, 0.096 mmol, 1.0 eq) in THF/H_2O (5 mL, 1:1) was added PPh$_3$ (50 mg, 0.198 mmol, 2.0 eq). The mixture was allowed to stir at reflux for 4 h. The mixture was then poured into a biphasic mixture of 1N HCl (15 mL) and ether (20 mL). The layers were partitioned and the organic layer was extracted with 1N HCl (2 x 10 mL). The combined aqueous layers were basified with 3N NaOH (until pH 10 or greater). The aqueous mixture was then extracted with Et$_2$O (3 x 20 mL) and the combined organics were dried over Na$_2$SO$_4$, filtered, and concentrated

in vacuo. The crude material was purified by flash chromatography (95:5 CH$_2$Cl$_2$:MeOH) to provide 11 mg of amine **22** in 83% yield as a clear oil. IR: 2955, 2869, 1455, 1278, 916, 732 cm-1; ^{1}H NMR (CD$_3$OD): δ 0.93 (d 3H, *J* = 6.8), 0.96 (d, 3H, *J* = 6.6), 1.32 (dd, 1H, *J* = 14.5, 6.4), 1.38-1.52 (m, 2H), 1.58 (dd, 1H, *J* = 14.5, 4.9), 1.76-1.89 (m, 2H), 2.21-2.30 (m, 2H), 2.39 (dd, 1H, *J* = 13.9, 7.4), 2.59-2.69 (m, 1H), 2.75-2.87 (m, 1H), 3.79-3.92 (m, 3H), 5.06-5.15 (m, 2H), 5.85-5.98 (m, 1H), 7.20-7.45 (m, 5H); ^{13}C NMR: δ 24.12, 24.61, 25.20, 38.89, 40.56, 43.72, 46.79, 46.83, 53.48, 68.40, 117.6, 126.7, 127.9, 128.2, 135.2, 139.2; HRMS (ESI) calcd for [C$_{18}$H$_{28}$N$_2$O + H]$^+$: 289.2280, found 289.2291.
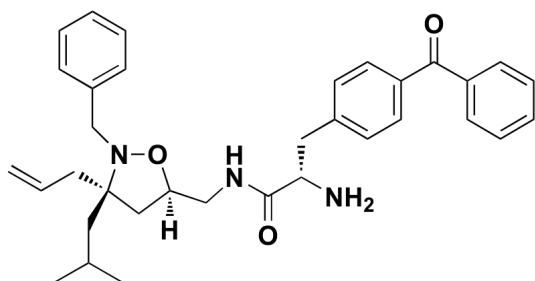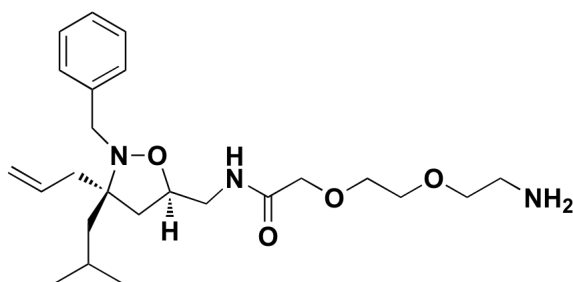

((S)-N-((($3S$,$5R$)-3-allyl-2-benzyl-3-isobutylisoxazolidin-5-yl)methyl)-2-amino-3-(4-benzoylphenyl)propanamide) (23): To a solution of Fmoc-BpA-OH (67 mg, .136 mmol, 1.5 eq) in DMF (1 mL) was added Et$_3$N (19 μL, .136 mmol, 1.5 eq) and PyBOP (71 mg, .136 mmol, 1.5 eq). The reaction mixture was allowed to stir for 20 minutes at rt. Amine **22** (20 mg, .068 mmol, 1.0 eq) in DMF (500 μL) was added and the reaction was stirred overnight. Piperidine (500 μL) was added and the reaction was stirred for an additional 20 minutes. The solvent was removed *in vacuo* and the residue was suspended in 1:1 ACN/0.1% TFA (1 mL), filtered, and purified by reverse phase HPLC to provide 24 mg of **23** in 65% yield as a white powder. IR: 2598, 2870, 1677, 1459, 1280, 937 cm^{-1}; ^{1}H NMR (CD$_3$OD): δ 0.99 (d, 3H, J = 6.6), 1.01 (d, 3H, J = 6.6), 1.54-1.64 (m, 1H), 1.71-1.82 (m, 2H), 1.85-2.02 (m, 2H), 2.39- 2.46 (m, 2H), 3.00-3.12 (m, 2H), 3.13-3.24 (m, 3H), 3.46-3.58 (m, 2H), 3.74-3.84 (m, 2H), 5.06-5.15 (m, 2H), 5.85-5.98 (m, 1H), 7.18-7.38 (m, 6H), 7.46-7.54 (m,

2H), 7.58-7.64 (m, 2H), 7.66-7.76 (m, 4H); HRMS (ESI) calcd for $[C_{34}H_{41}N_3O_3 + H]+$: 539.3148, found 539.3141.
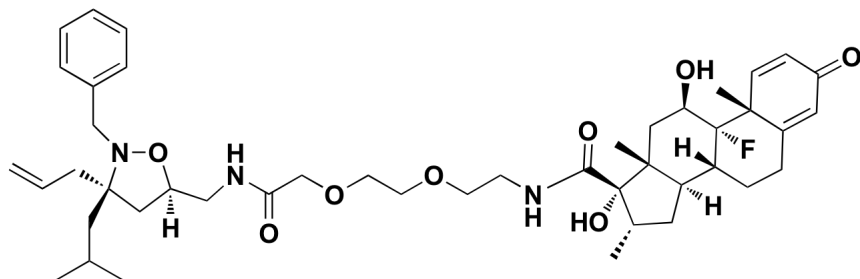

(N-((S)-1-((((3S,5R)-3-allyl-2-benzyl-3-isobutylisoxazolidin-5-yl)methyl)amino)-3-(4-benzoylphenyl)-1-oxopropan-2-yl)-6-(6-(5-(2-oxohexahydro-1H-thieno[3,4-d]imidazol-4-yl)pentanamido)hexanamido) hexanamide) (24): Amine **23** (20 mg, .037 mmol, 1.0 eq) was dissolved in DMF (500 μL) and Biotin-XX-SE (25 mg, .044 mmol, 1.2 eq) and Et$_3$N (6.1 μL, .044 mmol, 1.2 eq) in DMF (500 μL) were added. The reaction was allowed to stir for 12h at rt then the solvent was removed *in vacuo*. The residue was dissolved in ACN/0.1% TFA (500 μL) and the product isolated by reverse phase HPLC to provide 21 mg of **24** in 55% yield as a white powder. HRMS (ESI) calcd for $[C_{57}H_{79}N_7O_7S + Na]^+$: 1028.5659, found 1028.5669.


(N-(((3S,5R)-3-allyl-2-benzyl-3-isobutylisoxazolidin-5-yl)methyl)-2-(2-(2-aminoethoxy)ethoxy)acetamide) (25): To a solution of Fmoc-AEEA (50 mg, 0.13 mmol, 1.5 eq) dissolved in DMF (2 mL) were added HOBt (18 mg, 0.13 mmol, 1.5 eq)

and HBTU (49 mg, 0.13 mmol, 1.5 eq). This solution was agitated for 15 min. The solution of activated Fmoc-AEEA was added to amine **22** (25 mg, 0.087 mmol, 1.0 eq) dissolved in DMF (1 mL) and Et₃N (18.1 μL, 0.13 mmol, 1.5 eq) and the resulting mixture was allowed to stir for 12 h at which time the reaction mixture was concentrated *in vacuo*. The resulting oil was dissolved in a solution of 20% piperidine in DMF (1 mL) and was allowed to stir for 30 minutes. The resulting solution was dried *in vacuo*. Reverse-phase HPLC purification provided 31 mg of **25** as an oil in 82% yield. ¹H NMR (CD₃OD): δ .97 (d, 3H, *J* = 6.6), 1.05 (d, 3H, *J* = 6.6), 1.44 (dd, 1H, *J* =14.3, 6.3), 1.71 (dd, 1H, *J* = 14.5, 5.1), 1.85-2.01 (m, 3H), 2.35-2.55(m, 3H), 3.0-3.08 (m, 2H), 3.35-3.43 (m, 2H) 3.55-3.65 (m, 6H), 3.91-4.10 (m, 4H), 4.15-4.27 (m, 1H), 5.11-5.21 (m, 2H), 5.91-6.02 (m, 1H), 7.20-7.44 (m, 5H); HRMS (ESI) calcd for [C₂₄H₃₉N₃O₄ + H]⁺: 434.3019, found: 434.3012.
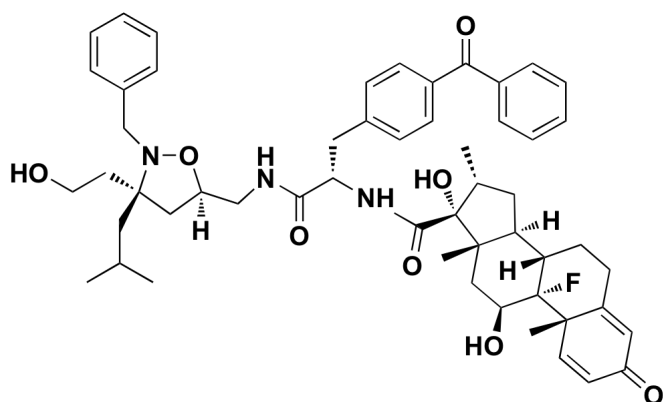

(2-(2-((8*S*,9*R*,10*S*,11*S*,13*S*,14*S*,16*R*,17*R*)-9-fluoro-17-hydroxy-10,11,13,16-tetramethyl-3-oxo-6,7,8,9,10,11,12,13,14,15,16,17-dodecahydro-3*H*-cyclopenta[*a*]phenanthrene-17-carboxamido)ethoxy)ethyl (((3*S*,5*R*)-3-allyl-2-benzyl-3-isobutylisoxazolidin-5-yl)methyl)carbamate) (26): To a solution of OxDex (13 mg, .035 mmol, 1.5 eq) dissolved in DMF (1 mL) was added HOBt (5 mg, .035 mmol, 1.5 eq) and HBTU (13 mg, .035 mmol, 1.5 eq) and the resulting mixture was agitated for 15 min. To this solution was added a solution of isoxazolidine **25** (10 mg, .023 mmol, 1.0 eq) dissolved in DMF (500 μL) and Et₃N (4.8 μL, .035 mmol, 1.5 eq). The resulting mixture was stirred for 12 h at rt. The product was isolated by reverse-phase HPLC purification to provide 14 mg of **26** as a white solid in 62% yield. The purity of compound **26** was confirmed by reverse-phase HPLC analysis.

The identity was verified by mass spectral analysis of the isolated compound. HRMS (ESI) calcd for $[C_{45}H_{64}FN_3O_8 + H]^+$: 794.4756, found: 794.4769.
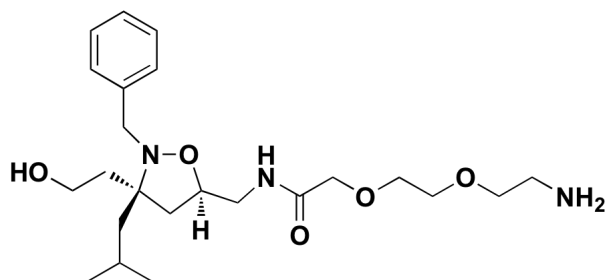

Preparation of **27** was accomplished under conditions identical to those used for **26**. Reverse-phase HPLC purification provided 41 mg of **27** in 70% yield as a white solid. ^1H NMR (CD$_3$OD): δ 0.96 (d, 3H, J = 6.6), 1.00 (d, 3H, J = 6.6), 1.45 (dd, 1H, J = 13.7, 6.3), 1.66-1.85 (m, 2H), 1.90 (t, 2H, J = 6.8), 1.98-2.07 (m, 1H), 2.45 (dd, 1H, J = 12.7, 8.0), 3.00 (t, 2H, J = 5.1), 3.37 (dd, 1H, J = 13.7, 7.4), 3.43-3.61 (m, 6H), 3.72-3.79 (m, 3H), 3.90-4.00 (m, 4H), 4.17-4.27 (m, 1H), 7.21-7.39 (m, 5H); HRMS (ESI) calcd for $[C_{23}H_{39}N_3O_5 + H]^+$: 438.2968, found: 438.2962.
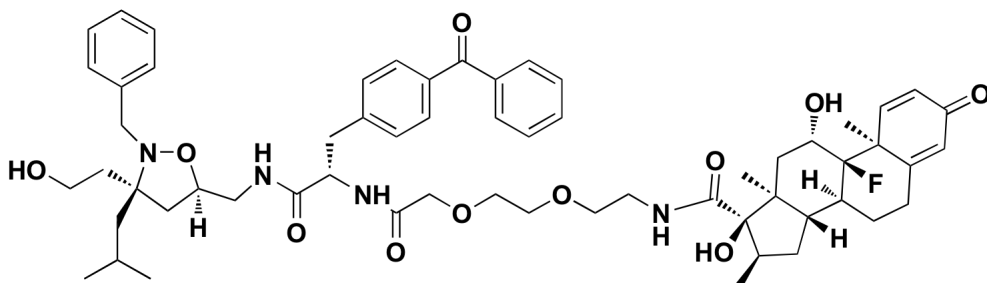

((8S,9R,10S,11S,13S,14S,16R,17R)-N-(((S)-3-(4-benzoylphenyl)-1-(((($3S,5R$)-2-benzyl-3-(2-hydroxyethyl)-3-isobutylisoxazolidin-5-yl)methyl)amino)-1-oxopropan-2-yl)-9-fluoro-17-hydroxy-10,11,13,16-tetramethyl-3-oxo-6,7,8,9,10,11,12,13,14,15,16,17-dodecahydro-3H-cyclopenta[a]phenanthrene-17-carboxamide) (28): To a solution of OxDex (20 mg, 53 μmol, 1.5 eq) in DMF

81

(700 μL) were added HOBt (7.2 mg, 53 μmol, 1.5 eq), HBTU (20.1 mg, 53 μmol, 1.5 eq), and Et$_3$N (3.6 mg, 15 μL, 1.0 eq) and the reaction was stirred for 20 min. **20** (20.6 mg, 35 μmol, 1.0 eq) was added in DMF (500 μL) and the reaction was stirred for 12h at rt. The solvent was removed *in vacuo* and the residue was dissolved in 1:1 ACN/0.1% TFA and purified by reverse phase HPLC providing 16.1 mg of **28** in 48% yield. HRMS (ESI) calcd for [C$_{55}$H$_{68}$FN$_3$O$_7$ + H]$^+$: 902.5120, found 902.5146.
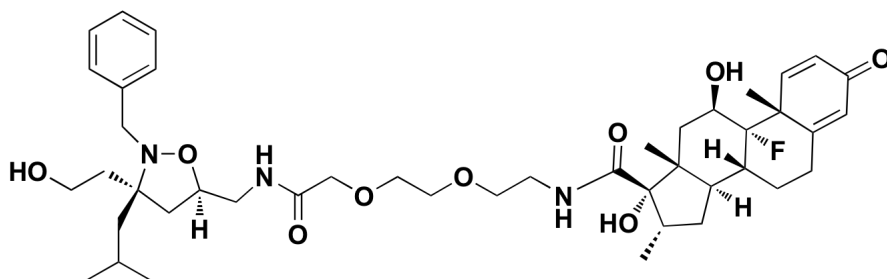

((8*S*,9*R*,10*S*,11*S*,13*S*,14*S*,16*R*,17*R*)-*N*-(2-(2-(2-((((3*S*,5*R*)-2-benzyl-3-(2-hydroxyethyl)-3-isobutylisoxazolidin-5-yl)methyl)amino)-2-oxoethoxy)ethoxy)ethyl)-9-fluoro-17-hydroxy-10,11,13,16-tetramethyl-3-oxo-6,7,8,9,10,11,12,13,14,15,16,17-dodecahydro-3*H*-cyclopenta[*a*]phenanthrene-17-carboxamide) (29): To a solution of **18** (3.85 mg, 13.3 μmol, 1.0 eq) in THF/H$_2$O (1:1) was added PPh$_3$ and the flask was fitted with a reflux condenser and heated at 80° C for 4 h. An acid, base workup yielded the crude amine, which was immediately coupled to Fmoc-AEEA-OH. Towards this, AEEA (10.5 mg, 20 μmol, 1.5 eq) in DMF (0.3 mL) was stirred with PyBOP (10.5 mg, 20 μmol, 1.5 eq) for 15 min. A solution of the crude amine (3.5 mg, 13.1 μmol, 1.0 eq) and ET3N (20 μL, 13.3 μmol, 1.5 eq) in DMF (0.3 mL) was added and the solution stirred for 12 h. Piperidine (150 μL) was added to generate a 20% solution of piperidine in DMF to afford deprotection of the Fmoc group. The product was purified by reverse-phase HPLC using a 0.1% TFA in H$_2$O/ACN gradient. The product was subsequently coupled to OxDex. OxDex (20 mg, 52.9 μmol, 1.5 eq) was stirred with PyBOP (27.5 mg, 52.9 μmol, 1.5 eq) in DMF (0.5 mL) for 15 min at which point **27** was added (3 mg, 6.9 μmol, 1.0 eq) with Et$_3$N (1

μL, 6.9 μmol, 1.0 eq) in DMF and stirred for 12 h. The mixture was then concentrated and purified by reverse-phase HPLC using a 0.1% TFA in H_2O/ACN gradient. HRMS (ESI) calcd for $[C_{44}H_{64}FN_3O_9 + H]^+$: 798.4705, found: 798.4696.


((8S,9R,10S,11S,13S,14S,16R,17R)-N-((S)-4-(4-benzoylbenzyl)-1-((3S,5R)-2-benzyl-3-(2-hydroxyethyl)-3-isobutylisoxazolidin-5-yl)-3,6-dioxo-8,11-dioxa-2,5-diazatridecan-13-yl)-9-fluoro-17-hydroxy-10,11,13,16-tetramethyl-3-oxo-6,7,8,9,10,11,12,13,14,15,16,17-dodecahydro-3H-cyclopenta[a]phenanthrene-17-carboxamide) (30): AEEA-OxDex (65.5 mg, .125 mmol, 1.5 eq) was dissolved in DMF (2 mL) with HOBt (17 mg, .125 mmol, 1.5 eq) and HBTU (47.5 mg, .125 mmol, 1.5 eq) and stirred for 1 h. Amine **19** (45 mg, 0.083 mmol, 1.0 eq) and Et$_3$N (18 μL, .125 mmol, 1.5 eq) in DMF (1 mL) were added dropwise and the reaction stirred for 12 h. The sample was concentrated and the product was purified by reverse-phase HPLC using a 0.1% TFA in H_2O/ACN gradient. HRMS (ESI) calcd for $[C_{61}H_{79}FN_4O_{10} + H]+$: 1047.5858, found: 1047.5877.
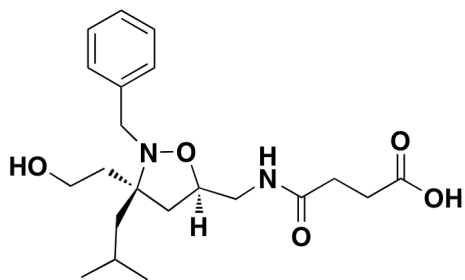
(4-((((3S,5R)-2-benzyl-3-(2-hydroxyethyl)-3-isobutylisoxazolidin-5-yl)methyl)amino)-4-oxobutanoic acid) (31): To a solution of amine **19** (200 mg,

628 µmol, 1.0 eq) in THF (10 mL) cooled in an ice-water bath, were added DMAP (15.3 mg, 126 µmol, 0.2 eq), Et$_3$N (87.5 µL, 628 µmol, 1.0 eq), and TBSOTf (144 µL, 628 µmol, 1.0 eq) and mixture was stirred for 1.5 h with continued cooling. The mixture was diluted with sat. aq. NH$_4$Cl (2 mL), then H$_2$O (5 mL) and extracted with Et$_2$O (3 x 10 mL). The combined organic extracts were washed with brine, concentrated and carried directly to the amine. Towards this, the residue was dissolved in 1:1 THF/H$_2$O (10 mL) and the reduction carried out as described for **12** (PPh$_3$, 494 mg, 1.88 mmol, 3.0 eq). An acid, base workup yielded the crude amine, which was dissolved in DMF (2 mL) and Et$_3$N (131 µL, 942 µmol, 1.5 eq), DMAP (15.3 mg, 126 µmol, 0.2 eq), and succinic anhydride (94.3 mg, 942 µmol, 1.5 eq) were added and the resulting solution was stirred for 12 h. The mixture was diluted with 1:1 H$_2$O/AcOH (10 mL), stirred at rt for 20 minutes and extracted with EtOAc (3 x 20 mL). The combined organic extracts were washed with brine and purified by flash chromatography (99:1 CHCl$_3$/MeOH) providing 271 mg of **31** in 85% yield as a clear oil. ^{1}H NMR (CD$_3$OD): δ 0.97 (s, 3H), 1.00 (d, 3H, J = 6.8), 1.39 (dd, 1H, J = 6.1, 14.4), 1.62 (dd, 1H, J = 5.4, 14.2), 1.80-1.90 (m, 2H), 1.95 (dd, 1H, J = 6.3, 12.6), 2.37-2.42 (m, 1H), 2.44 (dd, 1H, J = 8.8, 12.7), 2.51-2.57 (m, 2H), 2.85 (s, 2H), 2.98 (s, 2H), 3.28 (dd, 1H, J = 6.3, 13.7), 3.33 (dd, 1H, J = 4.9, 13.7), 3.80-3.90 (m, 3H), 4.10-4.15 (m, 1H), 7.18-7.37 (m, 5H); HRMS (ESI) calcd for [C$_{21}$H$_{32}$N$_2$O$_5$ + Na]$^+$: 415.2209, found: 415.2219.
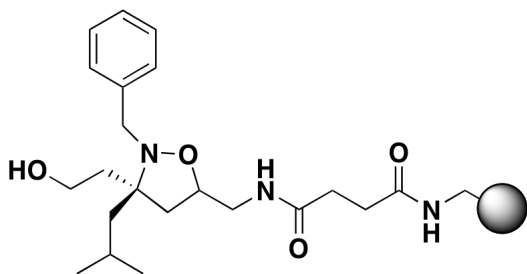

Four types of amine-functionalized resin were used ((aminomethyl)polystyrene, methylbenzylamine, Tentagel-S-NH$_2$, and Jandagel-NH$_2$) with the following procedure: To a stirring solution of **31** (19.1 mg, 46 µmol, 1.0 eq) in THF (2 mL)

cooled in an ice/water bath was added TBAF (138 μL, 138 μmol, 3.0 eq). After 2h, the reaction appeared complete by TLC and the solvent was removed *in vacuo*. The crude alcohol was dissolved in DMF (2 mL), PyBOP (28.7 mg, 56 μmol, 1.2 eq) was added and the reaction stirred for 20 min. Resin (127.6 mg, 37 μmol, 0.8 eq) was swelled in CH_2Cl_2 (5 mL) for 20 min, washed with DMF (5 x 10 mL) and resuspended in 20% piperidine in DMF (5 mL) for 10 min. Resin was washed with DMF (5 x 10 mL) and the reaction mixture plus Et_3N (92 μL, 66.8 μmol, 2.0 eq) was added to resin. The reaction was agitated at room temperature for 24 h. Resin was washed with DMF (5 x 5 mL), then acetylated using acetic anhydride (1 mL) and iPr_2Net (150 μL) at rt for 30 min, and washed with DMF (5 x 5 mL), MeOH (5 x 5 mL), and CH_2Cl_2 (5 x 5 mL), dried by blowing N_2, and stored at 4°C prior to use in pulldown experiments.

J. Appendix of Selected ¹H NMR Spectra and HPLC Traces
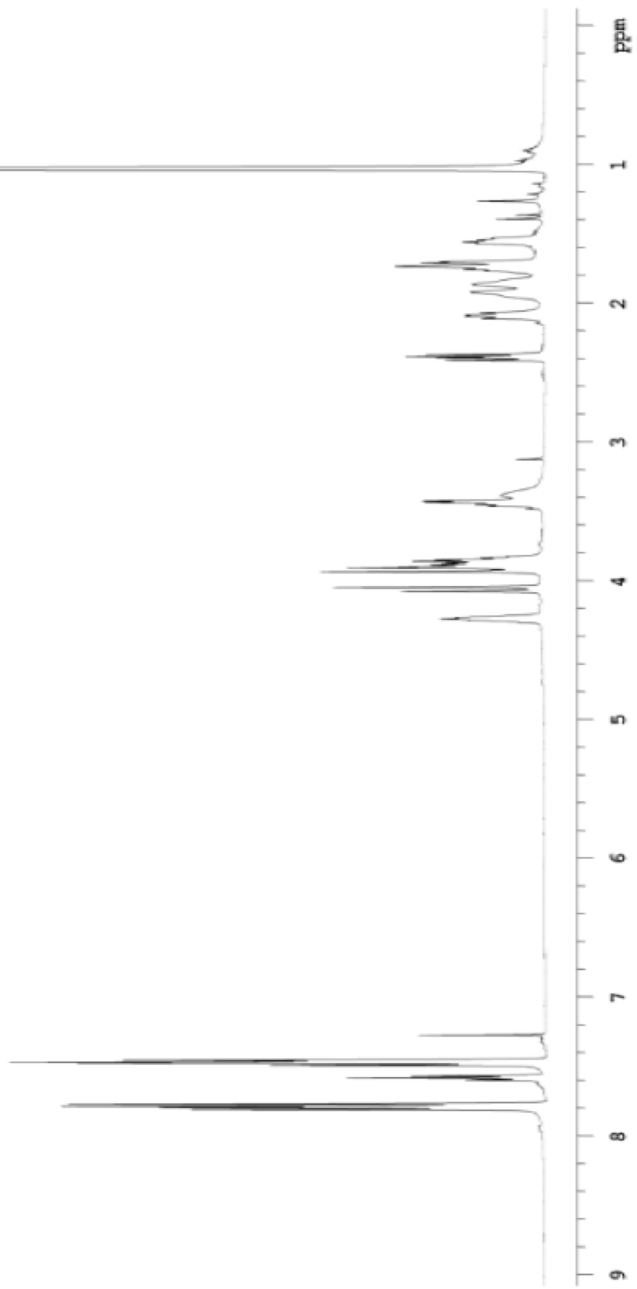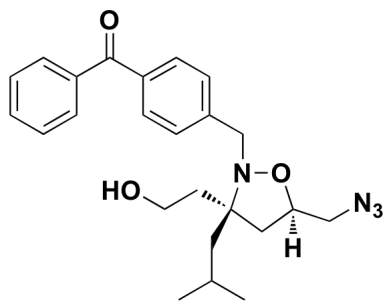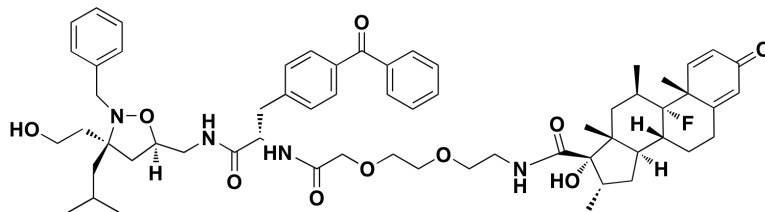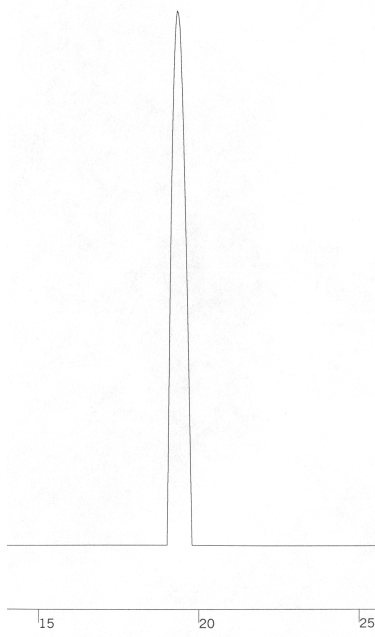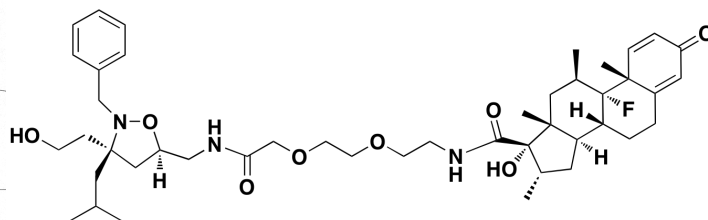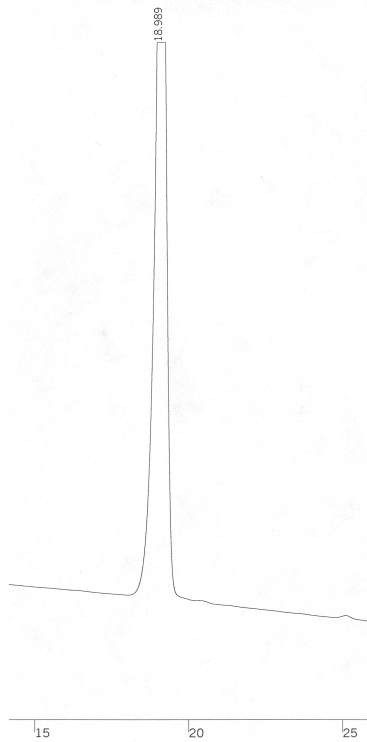
87

89

90
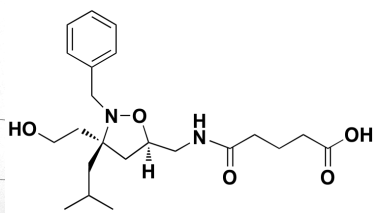
91

28.603

26.011
26.844
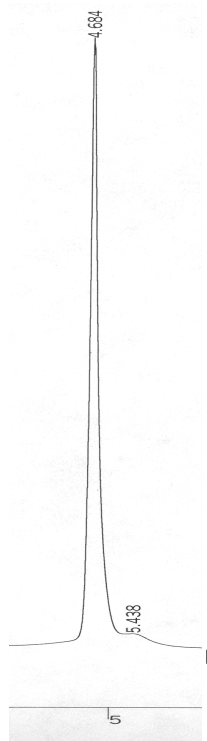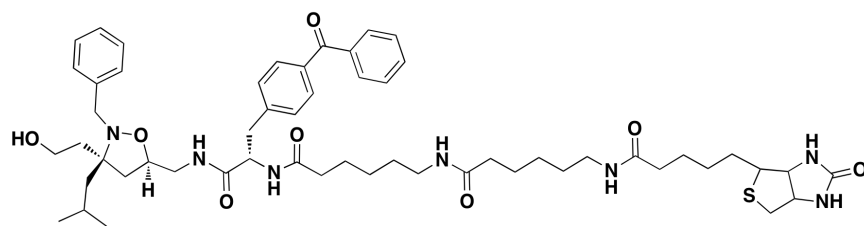27.325

31.961

30

4.684

5.438

5

92
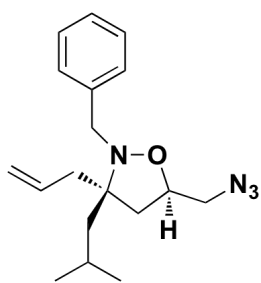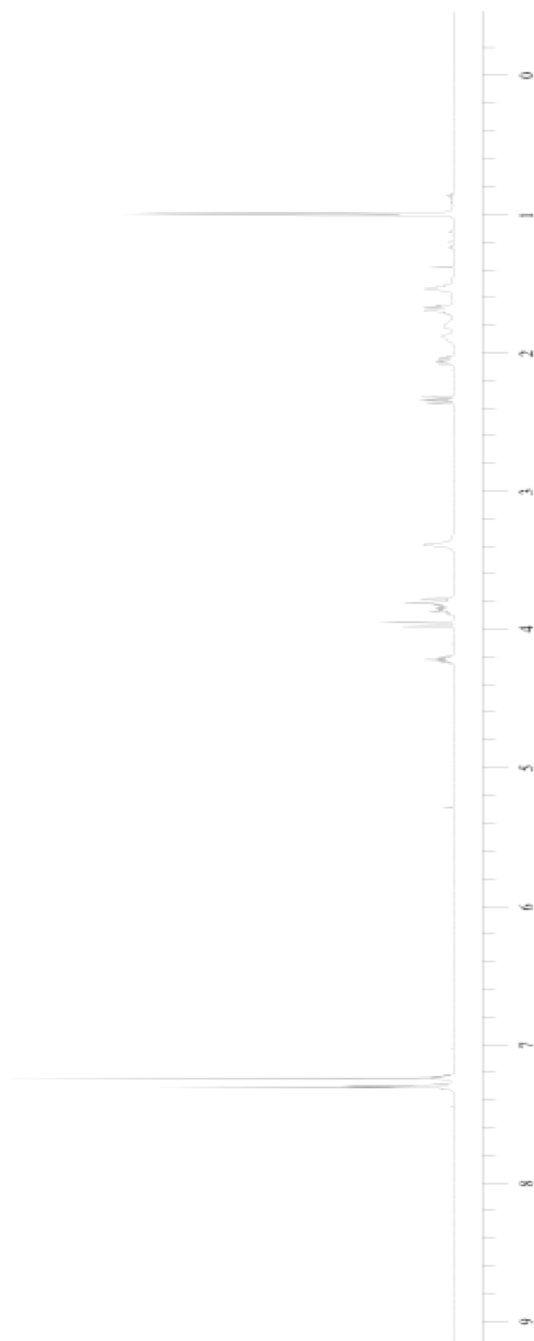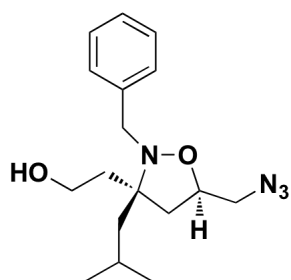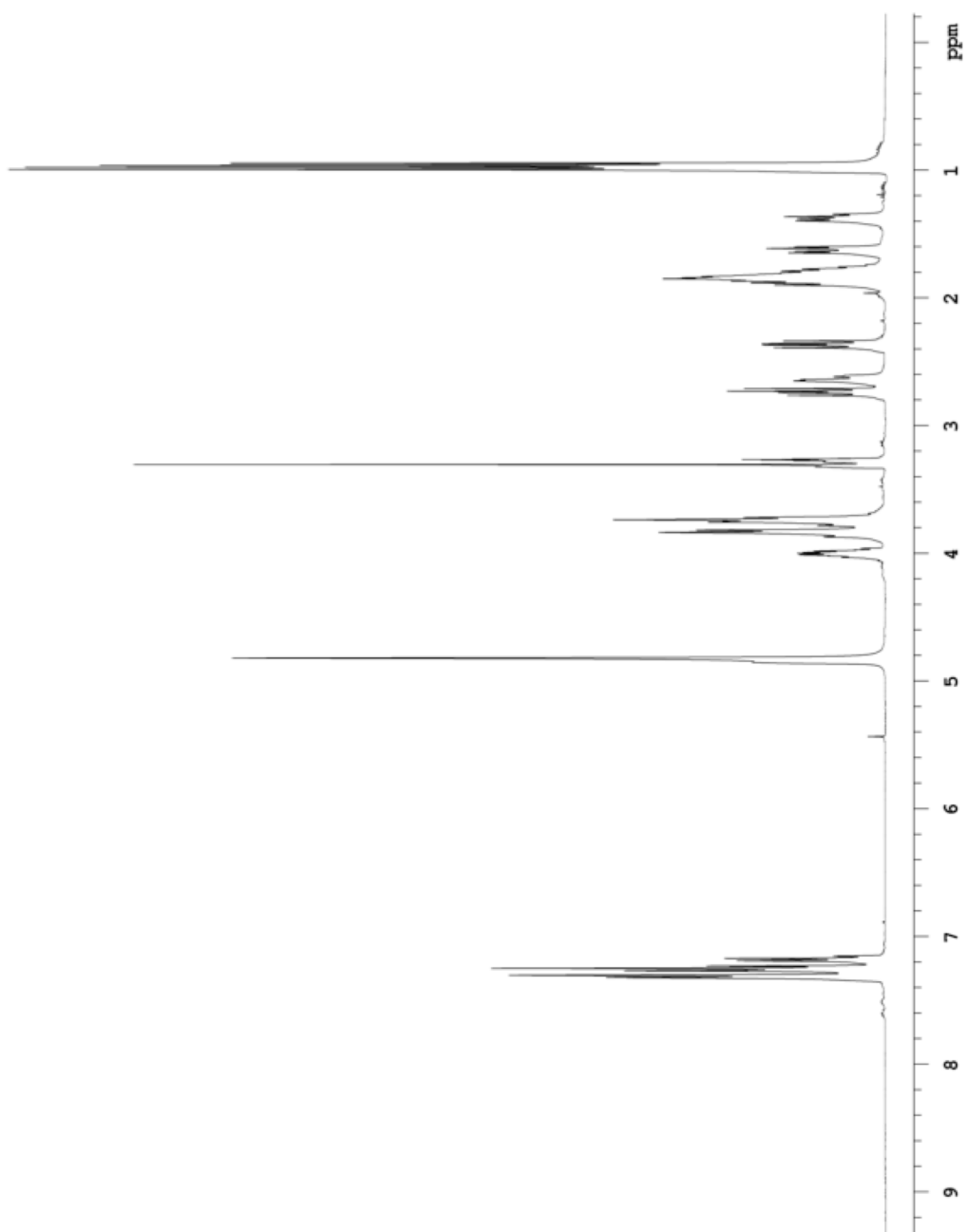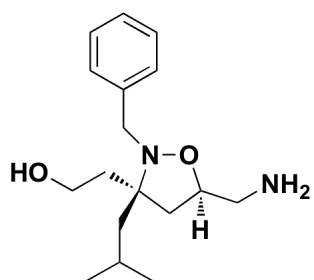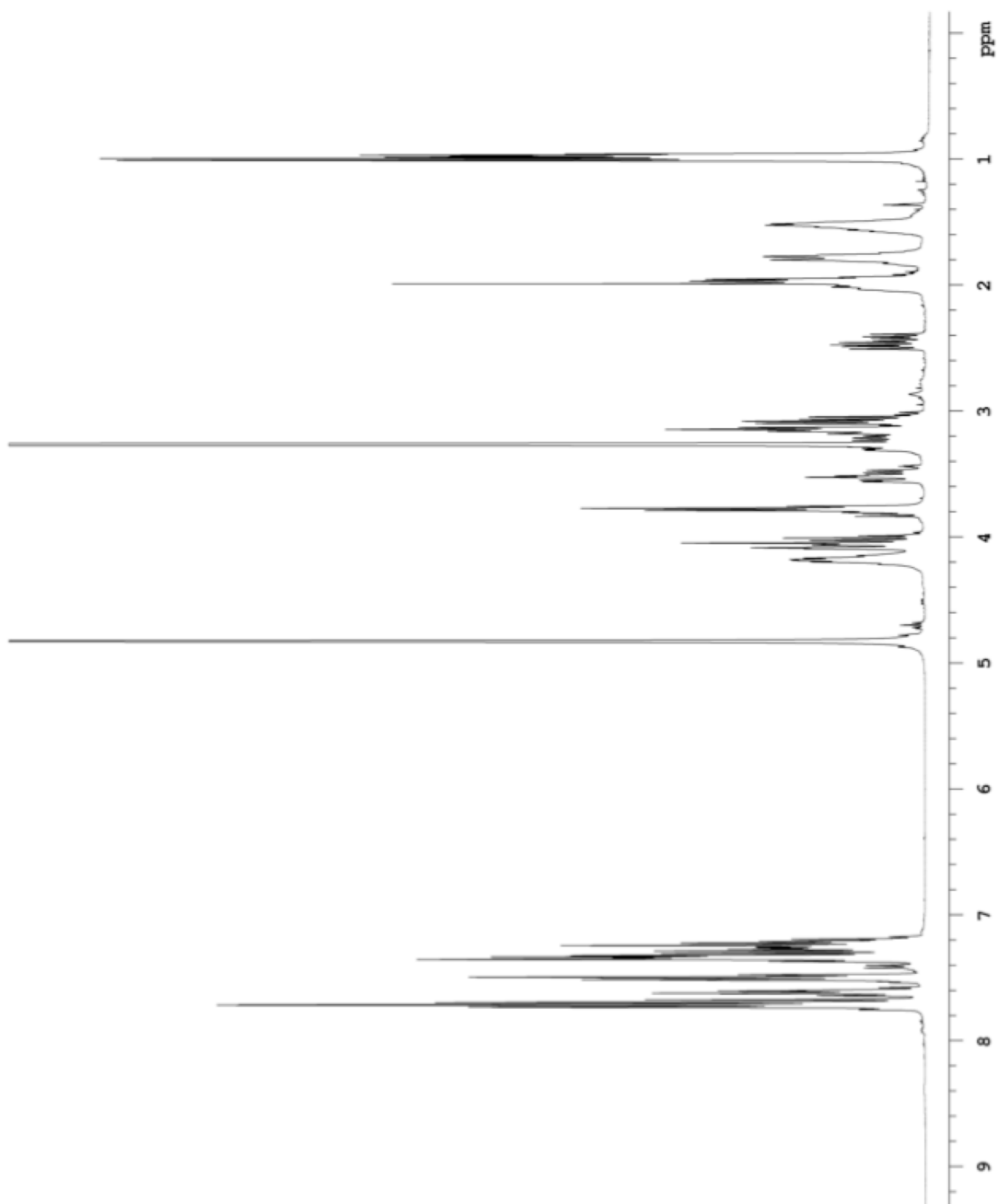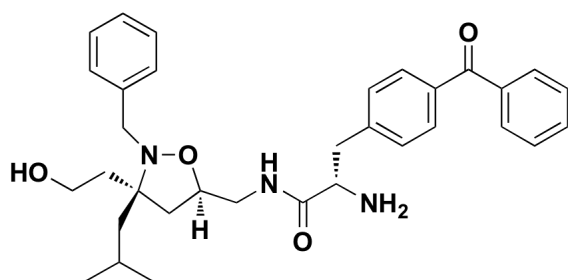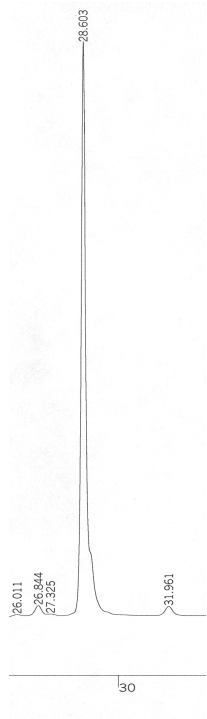
K. References

1. Rowe, S. P.; Casey, R. J.; Brennan, B. B.; Buhrlage, S. J.; Mapp, A. K., Transcriptional up-regulation in cells mediated by a small molecule. *J Am Chem Soc* **2007,** *129* (35), 10654-+.

2. Rowe, S. P.; Mapp, A. K., Assessing the permissiveness of transcriptional activator binding sites. *Biopolymers* **2008,** *89* (7), 578-581.

3. Buhrlage, S. J.; Bates, C. A.; Rowe, S. P.; Minter, A. R.; Brennan, B. B.; Majmudar, C. Y.; Wemmer, D. E.; Al-Hashimi, H.; Mapp, A. K., Amphipathic Small Molecules Mimic the Binding Mode and Function of Endogenous Transcription Factors. *Acs Chem Biol* **2009,** *4* (5), 335-344.

4. Minter, A. R.; Brennan, B. B.; Mapp, A. K., A small molecule transcriptional activation domain. *J Am Chem Soc* **2004,** *126* (34), 10504-10505.

5. Smirnova, E.; Shurland, D. L.; van der Bliek, A. M., Mapping dynamin interdomain interactions with yeast two-hybrid and glutathione S-transferase pulldown experiments. *Regulators and Effectors of Small Gtpases, Pt E* **2001,** *329*, 468-477.

6. Lee, D. K.; Kim, S.; Lis, J. T., Different upstream transcriptional activators have distinct coactivator requirements. *Gene Dev* **1999,** *13* (22), 2934-2939.

7. Radhakrishnan, I.; Perez-Alvarado, G. C.; Parker, D.; Dyson, H. J.; Montminy, M. R.; Wright, P. E., Structural analyses of CREB-CBP transcriptional activator-coactivator complexes by NMR spectroscopy: implications for mapping the boundaries of structural domains. *J Mol Biol* **1999,** *287* (5), 859-65.

8. Frangioni, J. V.; LaRiccia, L. M.; Cantley, L. C.; Montminy, M. R., Minimal activators that bind to the KIX domain of p300/CBP identified by phage display screening. *Nat Biotechnol* **2000,** *18* (10), 1080-5.

9. John V. Frangioni, L. M. L., Lewis C. Cantley, Marc R. Montminy, Minimal activators that bind to the KIX domain of p300/CBP identified by phage display screening. *Nature Biotechnology* **2000,** *18*, 6.

10. Lu, X.; Ansari, A. Z.; Ptashne, M., An artificial transcriptional activating region with unusual properties. *Proc Natl Acad Sci U S A* **2000,** *97* (5), 1988-92.

11. Park, J. M.; Kim, H. S.; Han, S. J.; Hwang, M. S.; Lee, Y. C.; Kim, Y. J., In vivo requirement of activator-specific binding targets of mediator. *Mol Cell Biol* **2000,** *20* (23), 8709-19.

12.   Campbell, K. M.; Lumb, K. J., Structurally distinct modes of recognition of the KIX domain of CBP by Jun and CREB. *Biochemistry-Us* **2002,** *41* (47), 13956-64.

13.   Goto, N. K.; Zor, T.; Martinez-Yamout, M.; Dyson, H. J.; Wright, P. E., Cooperativity in transcription factor binding to the coactivator CREB-binding protein (CBP). The mixed lineage leukemia protein (MLL) activation domain binds to an allosteric site on the KIX domain. *J Biol Chem* **2002,** *277* (45), 43168-74.

14.   Andrew C. Vendel, S. J. M., Kevin J. Lumb, KIX-Mediated Assembly of the CBP-CREB-HTLV-1 Tax Coactivator-Activaor Complex. *Biochemistry-Us* **2003,** *42*, 7.

15.   Wu, Z.; Belanger, G.; Brennan, B. B.; Lum, J. K.; Minter, A. R.; Rowe, S. P.; Plachetka, A.; Majmudar, C. Y.; Mapp, A. K., Targeting the transcriptional machinery with unique artificial transcriptional activators. *J Am Chem Soc* **2003,** *125* (41), 12390-1.

16.   Vendel, A. C.; Lumb, K. J., NMR mapping of the HIV-1 Tat interaction surface of the KIX domain of the human coactivator CBP. *Biochemistry-Us* **2004,** *43* (4), 904-8.

17.   Fishburn, J.; Mohibullah, N.; Hahn, S., Function of a eukaryotic transcription activator during the transcription cycle. *Mol Cell* **2005,** *18* (3), 369-378.

18.   Reeves, W. M.; Hahn, S., Targets of the Gal4 transcription activator in functional transcription complexes. *Mol Cell Biol* **2005,** *25* (20), 9092-102.

19.   De Guzman, R. N.; Goto, N. K.; Dyson, H. J.; Wright, P. E., Structural basis for cooperative transcription factor binding to the CBP coactivator. *J Mol Biol* **2006,** *355* (5), 1005-13.

20.   Mapp, A. K.; Ansari, A. Z., A TAD further: Exogenous control of gene activation. *Acs Chem Biol* **2007,** *2* (1), 62-75.

21.   Shimogawa, H.; Kwon, Y.; Mao, Q.; Kawazoe, Y.; Choi, Y.; Asada, S.; Kigoshi, H.; Uesugi, M., A wrench-shaped synthetic molecule that modulates a transcription factor-coactivator interaction. *J Am Chem Soc* **2004,** *126* (11), 3461-71.

22.   Gilbert, B. A.; Rando, R. R., Modular Design of Biotinylated Photoaffinity Probes - Synthesis and Utilization of a Biotinylated Pepstatin Photoprobe. *J Am Chem Soc* **1995,** *117* (31), 8061-8066.

23.   Oatis, J. E.; Knapp, D. R., Synthesis and photochemistry of two cleavable heterobifunctional benzophenone protein crosslinkers. *Tetrahedron Lett* **1998,** *39* (13), 1665-1668.

24.	Ploug, M., Identification of specific sites involved in ligand binding by photoaffinity labeling of the receptor for the urokinase-type plasminogen activator. Residues located at equivalent positions in uPAR domains I and III participate in the assembly of a composite ligand-binding site. *Biochemistry-Us* **1998,** *37* (47), 16494-16505.

25.	Coupal, M.; De Lean, A.; McNicoll, N.; Fournier, A., Development of p-benzoylbenzoylated [N,C,rANP(1-28)]pBNP32 (pBNP1) derivatives and affinity photolabeling of the bovine NPR-A receptor. *Biochem Bioph Res Co* **1999,** *258* (1), 81-86.

26.	DeSantis, G.; Paech, C.; Jones, J. B., Benzophenone boronic acid photoaffinity labeling of subtilisin CMMs to probe altered specificity. *Bioorgan Med Chem* **2000,** *8* (3), 563-570.

27.	Ding, S. H.; Horn, R., Slow photo-cross-linking kinetics of benzophenone-labeled voltage sensors of ion channels. *Biochemistry-Us* **2001,** *40* (35), 10707-10716.

28.	Ding, S. H.; Horn, R., Slow photocrosslinking kinetics of the voltage sensors of ion channels. *Biophys J* **2001,** *80* (1), 218A-219A.

29.	Stromgaard, K.; Saito, D. R.; Shindou, H.; Ishii, S.; Shimizu, T.; Nakanishi, K., Ginkgolide derivatives for photolabeling studies: Preparation and pharmacological evaluation. *J Med Chem* **2002,** *45* (18), 4038-4046.

30.	Olsen, R. W.; Chang, C. S. S.; Li, G. D.; Hanchar, H. J.; Wallner, M., Fishing for allosteric sites on GABA(A) receptors. *Biochem Pharmacol* **2004,** *68* (8), 1675-1684.

31.	Nakashima, H.; Hashimoto, M.; Sadakane, Y.; Tomohiro, T.; Hatanaka, Y., Simple and versatile method for tagging phenyldiazirine photophores. *J Am Chem Soc* **2006,** *128* (47), 15092-15093.

32.	Sadakane, Y.; Hatanaka, Y., Photochemical fishing approaches for identifying target proteins and elucidating the structure of a ligand-binding region using carbene-generating photoreactive probes. *Anal Sci* **2006,** *22* (2), 209-218.

33.	Dorman, G.; Prestwich, G. D., Benzophenone Photophores in Biochemistry. *Biochemistry-Us* **1994,** *33* (19), 5661-5673.

34.	Fleming, S. A., Chemical Reagents in Photoaffinity-Labeling. *Tetrahedron* **1995,** *51* (46), 12479-12520.

35.   Prestwich, G. D.; Dorman, G.; Elliott, J. T.; Marecak, D. M.; Chaudhary, A., Benzophenone photoprobes for phosphoinositides, peptides and drugs. *Photochem Photobiol* **1997,** *65* (2), 222-234.

36.   Fancy, D. A.; Denison, C.; Kim, K.; Xie, Y. Q.; Holdeman, T.; Amini, F.; Kodadek, T., Scope, limitations and mechanistic aspects of the photo-induced cross-linking of proteins by water-soluble metal complexes. *Chemistry & Biology* **2000,** *7* (9), 697-708.

37.   Colca, J. R.; Harrigan, G. G., Photo-affinity labeling strategies in identifying the protein ligands of bioactive small molecules: Examples of targeted synthesis of drug analog photoprobes. *Comb Chem High T Scr* **2004,** *7* (7), 699-704.

38.   Kluger, R.; Alagic, A., Chemical cross-linking and protein-protein interactions - a review with illustrative protocols. *Bioorg Chem* **2004,** *32* (6), 451-472.

39.   Gomez, G. E.; Cauerhff, A.; Craig, P. O.; Goldbaum, F. A.; Delfino, J. M., Exploring protein interfaces with a general photochemical reagent. *Protein Sci* **2006,** *15* (4), 744-752.

40.   Karabats.Gj; Taller, R. A., Structural Studies by Nuclear Magnetic Resonance .15. Conformations and Configurations of Oximes. *Tetrahedron* **1968,** *24* (8), 3347-&.

41.   Kanemasa, S.; Nishiuchi, M.; Kamimura, A.; Hori, K., 1st Successful Metal Coordination Control in 1,3-Dipolar Cycloadditions - High-Rate Acceleration and Regiocontrol and Stereocontrol of Nitrile Oxide Cycloadditions to the Magnesium Alkoxides of Allylic and Homoallylic Alcohols. *J Am Chem Soc* **1994,** *116* (6), 2324-2339.

42.   Bode, J. W.; Fraefel, N.; Muri, D.; Carreira, E. M., A general solution to the modular synthesis of polyketide building blocks by Kanemasa hydroxy-directed nitrile oxide cycloadditions. *Angewandte Chemie-International Edition* **2001,** *40* (11), 2082-2085.

43.   Liu, B.; Alluri, P. G.; Yu, P.; Kodadek, T., A potent transactivation domain mimic with activity in living cells. *J Am Chem Soc* **2005,** *127* (23), 8254-8255.

44.   Yu, P.; Liu, B.; Kodadek, T. J., Transcription activation by a synthetic molecule in living mammalian cells. *Abstr Pap Am Chem S* **2005,** *229*, U197-U197.

45.   Casey, R. J.; Desaulniers, J. P.; Hojfeldt, J. W.; Mapp, A. K., Expanding the repertoire of small molecule transcriptional activation domains. *Bioorgan Med Chem* **2009,** *17* (3), 1034-1043.

46.   Buhrlage, S., Unpublished results.

47.   Chrivia, J. C.; Kwok, R. P. S.; Lamb, N.; Hagiwara, M.; Montminy, M. R.; Goodman, R. H., Phosphorylated Creb Binds Specifically to the Nuclear-Protein Cbp. *Nature* **1993,** *365* (6449), 855-859.

48.   Bannister, A. J.; Kouzarides, T., The CBP co-activator is a histone acetyltransferase. *Nature* **1996,** *384* (6610), 641-643.

49.   Giles, R. H.; Peters, D. J. M.; Breuning, M. H., Conjunction dysfunction: CBP/p300 in human disease. *Trends in Genetics* **1998,** *14* (5), 178-183.

50.   Ito, M.; Yuan, C. X.; Malik, S.; Gu, W.; Fondell, J. D.; Yamamura, S.; Fu, Z. Y.; Zhang, X. L.; Qin, J.; Roeder, R. G., Identity between TRAP and SMCC complexes indicates novel pathways for the function of nuclear receptors and diverse mammalian activators. *Mol Cell* **1999,** *3* (3), 361-370.

51.   Fleischer, T. C.; Yun, U. J.; Ayer, D. E., Identification and characterization of three new components of the mSin3A corepressor complex. *Mol Cell Biol* **2003,** *23* (10), 3456-3467.

52.   Grozinger, C. M.; Hassig, C. A.; Schreiber, S. L., Three proteins define a class of human histone deacetylases related to yeast Hda1p. *P Natl Acad Sci USA* **1999,** *96* (9), 4868-4873.

53.   Kornberg, R. D., Mediator and the mechanism of transcriptional activation. *Trends Biochem Sci* **2005,** *30* (5), 235-239.

54.   Kornberg, R. D., The molecular basis of eukaryotic transcription. *P Natl Acad Sci USA* **2007,** *104* (32), 12955-12961.

55.   Lee, S. H.; McCormick, F., p97/DAP5 is a ribosome-associated factor that facilitates protein synthesis and cell proliferation by modulating the synthesis of cell cycle proteins. *Embo J* **2006,** *25* (17), 4008-4019.

56.   Gmachl, M.; Gieffers, C.; Podtelejnikov, A. V.; Mann, M.; Peters, J. M., The RING-H2 finger protein APC11 and the E2 enzyme UBC4 are sufficient to ubiquitinate substrates of the anaphase-promoting complex. *P Natl Acad Sci USA* **2000,** *97* (16), 8973-8978.

57.   Hogenesch, J. B.; Gu, Y. Z.; Moran, S. M.; Shimomura, K.; Radcliffe, L. A.; Takahashi, J. S.; Bradfield, C. A., The basic helix-loop-helix-PAS protein MOP9 is a brain-specific heterodimeric partner of circadian and hypoxia factors. *J Neurosci* **2000,** *20* (13), art. no.-RC83.

58.   Bannister, A. J.; Kouzarides, T., Cbp-Induced Stimulation of C-Fos Activity Is Abrogated by E1a. *Embo J* **1995,** *14* (19), 4758-4762.

59.   Petrij, F.; Giles, R. H.; Dauwerse, H. G.; Saris, J. J.; Hennekam, R. C. M.; Masuno, M.; Tommerup, N.; Vanommen, G. J. B.; Goodman, R. H.; Peters, D. J. M.; Breuning, M. H., Rubinstein-Taybi Syndrome Caused by Mutations in the Transcriptional Coactivator Cbp. *Nature* **1995,** *376* (6538), 348-351.

60.   Arany, Z.; Huang, L. E.; Eckner, R.; Bhattacharya, S.; Jiang, C.; Goldberg, M. A.; Bunn, H. F.; Livingston, D. M., An essential role for p300/CBP in the cellular response to hypoxia. *P Natl Acad Sci USA* **1996,** *93* (23), 12969-12973.

61.   Chakravarti, D.; LaMorte, V. J.; Nelson, M. C.; Nakajima, T.; Schulman, I. G.; Juguilon, H.; Montminy, M.; Evans, R. M., Role of CBP/P300 in nuclear receptor signalling. *Nature* **1996,** *383* (6595), 99-103.

62.   Eckner, R., p300 and CBP as Transcriptional Regulators and Targets of Oncogenic Events. *Biological Chemistry* **1996,** *377*, 4.

63.   Ogryzko, V. V.; Schiltz, R. L.; Russanova, V.; Howard, B. H.; Nakatani, Y., The transcriptional coactivators p300 and CBP are histone acetyltransferases. *Cell* **1996,** *87* (5), 953-959.

64.   Oliner, J. D.; Andresen, J. M.; Hansen, S. K.; Zhou, S. L.; Tjian, R., SREBP transcriptional activity is mediated through an interaction with the CREB-binding protein. *Gene Dev* **1996,** *10* (22), 2903-2911.

65.   Chen, H. W.; Lin, R. J.; Schiltz, R. L.; Chakravarti, D.; Nash, A.; Nagy, L.; Privalsky, M. L.; Nakatani, Y.; Evans, R. M., Nuclear receptor coactivator ACTR is a novel histone acetyltransferase and forms a multimeric activation complex with P/CAF and CBP/p300. *Cell* **1997,** *90* (3), 569-580.

66.   Horvai, A. E.; Xu, L.; Korzus, E.; Brard, G.; Kalafus, D.; Mullen, T. M.; Rose, D. W.; Rosenfeld, M. G.; Glass, C. K., Nuclear integration of JAK/STAT and Ras/AP-1 signaling by CBP and p300. *P Natl Acad Sci USA* **1997,** *94* (4), 1074-1079.

67.   Tanaka, Y.; Naruse, I.; Maekawa, T.; Masuya, H.; Shiroishi, T.; Ishii, S., Abnormal skeletal patterning in embryos lacking a single Cbp allele: A partial similarity with Rubinstein-Taybi syndrome. *P Natl Acad Sci USA* **1997,** *94* (19), 10215-10220.

68.   Ghee, M.; Baker, H.; Miller, J. C.; Ziff, E. B., AP-1, CREB and CBP transcription factors differentially regulate the tyrosine hydroxylase gene. *Molecular Brain Research* **1998,** *55* (1), 101-114.

69.   Marian A. Martinez-Balbas, A. J. B., Klaus Martin, Phillip Haus-Seuffert, Michael Meisterernst, Tony Kouzarides, The acetyltransferase activity of CBP stimulates transcription. *The EMBO Journal* **1998,** *17* (10), 6.

70.   Marzio, G.; Tyagi, M.; Gutierrez, M. I.; Giacca, M., HIV-1 Tat transactivator recruits p300 and CREB-binding protein histone acetyltransferases to the viral promoter. *P Natl Acad Sci USA* **1998,** *95* (23), 13519-13524.

71.   Snowden, A. W.; Perkins, N. D., Cell cycle regulation of the transcriptional coactivators p300 and CREB binding protein. *Biochem Pharmacol* **1998,** *55* (12), 1947-1954.

72.   Giordano, A.; Avantaggiati, M. L., p300 and CBP: Partners for life and death. *Journal of Cellular Physiology* **1999,** *181* (2), 218-230.

73.   Goodman, R. H.; Smolik, S., CBP/p300 in cell growth, transformation, and development. *Genes Dev* **2000,** *14* (13), 1553-77.

74.   Kung, A. L.; Rebel, V. I.; Bronson, R. T.; Ch'ng, L. E.; Sieff, C. A.; Livingston, D. M.; Yao, T. P., Gene dose-dependent control of hematopoiesis and hematologic tumor suppression by CBP. *Gene Dev* **2000,** *14* (3), 272-277.

75.   Tanaka, Y.; Naruse, I.; Hongo, T.; Xu, M. J.; Nakahata, T.; Maekawa, T.; Ishii, S., Extensive brain hemorrhage and embryonic lethality in a mouse null mutant of CREB-binding protein. *Mechanisms of Development* **2000,** *95* (1-2), 133-145.

76.   Chan, H. M.; La Thangue, N. B., p300/CBP proteins: HATs for transcriptional bridges and scaffolds. *Journal of Cell Science* **2001,** *114* (13), 2363-2373.

77.   Mayr, B. M.; Canettieri, G.; Montminy, M. R., Distinct effects of cAMP and mitogenic signals on CREB-binding protein recruitment impart specficity to target gene activation via CREB. *P Natl Acad Sci USA* **2001,** *98* (19), 10936-10941.

78.   Vo, N.; Goodman, R. H., CREB-binding protein and p300 in transcriptional regulation. *J Biol Chem* **2001,** *276* (17), 13505-13508.

79.   Chao-Zhong Song, K. K., Yangchao Chen, Ken Murata, George Stamatoyannopoulos, Transcription Coactivator CBP has direct DNA binding activity and stimulates transcription factor DNA binding through small domains. *Biochem Bioph Res Co* **2002,** *296*, 7.

80.   Janknecht, R., The versatile functions of the transcriptional coactivators p300 and CBP and their roles in disease. *Histology and Histopathology* **2002,** *17* (2), 657-668.

81.   Caroline Rouaux, J.-P. L., Anne-Laurence Boutillier, Targeting CREB-binding protein (CBP) loss of function as a therapeutic strategy in neurological disorders. *Biochem Pharmacol* **2004,** *68*, 8.

82.   Iyer, N. G.; Ozdag, H.; Caldas, C., p300/CBP and cancer. *Oncogene* **2004,** *23* (24), 4225-4231.

83.   Hallam, T. M.; Bourtchouladze, R., Rubinstein-Taybi syndrome: molecular findings and therapeutic approaches to improve cognitive dysfunction. *Cellular and Molecular Life Sciences* **2006,** *63* (15), 1725-1735.

84.   Ramirez, J. A.; Nyborg, J. K., Molecular characterization of HTLV-1 Tax interaction with the KIX domain of CBP/p300. *J Mol Biol* **2007,** *372* (4), 958-69.

85.   Nettles, K. W.; Gil, G.; Nowak, J.; Metivier, R.; Sharma, V. B.; Greene, G. L., CBP is a dosage-dependent regulator of nuclear factor-kappa B suppression by the estrogen receptor. *Mol Endocrinol* **2008,** *22* (2), 263-272.

86.   Naidu, S. R.; Love, I. M.; Imbalzano, A. N.; Grossman, S. R.; Androphy, E. J., The SWI/SNF chromatin remodeling subunit BRG1 is a critical regulator of p53 necessary for proliferation of malignant cells. *Oncogene* **2009,** *28* (27), 2492-2501.

87.   Samuelson, A. V.; Lowe, S. W., Selective induction of p53 and chemosensitivity in RB-deficient cells by E1A mutants unable to bind the RB-related proteins. *P Natl Acad Sci USA* **1997,** *94* (22), 12094-12099.

88.   Radhakrishnan, I.; Perez-Alvarado, G. C.; Parker, D.; Dyson, H. J.; Montminy, M. R.; Wright, P. E., Solution structure of the KIX domain of CBP bound to the transactivation domain of CREB: a model for activator:coactivator interactions. *Cell* **1997,** *91* (6), 741-52.

89.   Schanda, P.; Brutscher, B.; Konrat, R.; Tollinger, M., Folding of the KIX domain: Characterization of the equilibrium analog of a folding intermediate using N-15/C-13 relaxation dispersion and fast H-1/H-2 amide exchange NMR spectroscopy. *Journal of Molecular Biology* **2008,** *380* (4), 726-741.

90.   Zor, T.; De Guzman, R. N.; Dyson, H. J.; Wright, P. E., Solution structure of the KIX domain of CBP bound to the transactivation domain of c-Myb. *J Mol Biol* **2004,** *337* (3), 521-34.

91.   Vendel, A. C.; McBryant, S. J.; Lumb, K. J., KIX-mediated assembly of the CBP-CREB-HTLV-1 tax coactivator-activator complex. *Biochemistry-Us* **2003,** *42* (43), 12481-7.

92.   Ernst, P.; Wang, J.; Huang, M.; Goodman, R. H.; Korsmeyer, S. J., MLL and CREB bind cooperatively to the nuclear coactivator CREB-binding protein. *Mol Cell Biol* **2001,** *21* (7), 2249-2258.

93.   Best, J. L.; Amezcua, C. A.; Mayr, B.; Flechner, L.; Murawsky, C. M.; Emerson, B.; Zor, T.; Gardner, K. H.; Montminy, M., Identification of small-molecule antagonists that inhibit an activator: coactivator interaction. *Proc Natl Acad Sci U S A* **2004,** *101* (51), 17622-7.

94.   Pangborn, A. B.; Giardello, M. A.; Grubbs, R. H.; Rosen, R. K.; Timmers, F. J., Safe and convenient procedure for solvent purification. *Organometallics* **1996,** *15* (5), 1518-1520.

95.   Still, W. C.; Kahn, M.; Mitra, A., Rapid Chromatographic Technique for Preparative Separations with Moderate Resolution. *J Org Chem* **1978,** *43* (14), 2923-2925.

96.   Buhrlage, S. J.; Brennan, B. B.; Minter, A. R.; Mapp, A. K., Stereochemical promiscuity in artificial transcriptional activators. *J Am Chem Soc* **2005,** *127* (36), 12456-12457.